

# A review of boiling heat transfer characteristics in binary mixtures

Xu, Jian; Wang, Yi; Yang, Ren; Liu, Wanlong; Wu, Hongwei; Ding, Yulong; Li, Yongliang

DOI:

[10.1016/j.ijheatmasstransfer.2020.120570](https://doi.org/10.1016/j.ijheatmasstransfer.2020.120570)

License:

Creative Commons: Attribution-NonCommercial-NoDerivs (CC BY-NC-ND)

*Document Version*

Peer reviewed version

*Citation for published version (Harvard):*

Xu, J, Wang, Y, Yang, R, Liu, W, Wu, H, Ding, Y & Li, Y 2021, 'A review of boiling heat transfer characteristics in binary mixtures', *International Journal of Heat and Mass Transfer*, vol. 164, 120570.  
<https://doi.org/10.1016/j.ijheatmasstransfer.2020.120570>

[Link to publication on Research at Birmingham portal](#)

## General rights

Unless a licence is specified above, all rights (including copyright and moral rights) in this document are retained by the authors and/or the copyright holders. The express permission of the copyright holder must be obtained for any use of this material other than for purposes permitted by law.

- Users may freely distribute the URL that is used to identify this publication.
- Users may download and/or print one copy of the publication from the University of Birmingham research portal for the purpose of private study or non-commercial research.
- User may use extracts from the document in line with the concept of 'fair dealing' under the Copyright, Designs and Patents Act 1988 (?)
- Users may not further distribute the material nor use it for the purposes of commercial gain.

Where a licence is displayed above, please note the terms and conditions of the licence govern your use of this document.

When citing, please reference the published version.

## Take down policy

While the University of Birmingham exercises care and attention in making items available there are rare occasions when an item has been uploaded in error or has been deemed to be commercially or otherwise sensitive.

If you believe that this is the case for this document, please contact [UBIRA@lists.bham.ac.uk](mailto:UBIRA@lists.bham.ac.uk) providing details and we will remove access to the work immediately and investigate.

# A Review of Boiling Heat Transfer Characteristics in Binary Mixtures

Jian Xu <sup>a,c,§</sup>, Yi Wang <sup>a,§</sup>, Ren Yang <sup>a</sup>, Wanlong Liu <sup>a,c</sup>, Hongwei Wu <sup>b</sup>,  
Yulong Ding <sup>a,\*</sup>, Yongliang Li <sup>a,\*</sup>

<sup>a</sup> School of Chemical Engineering, University of Birmingham, Birmingham, B15 2TT, UK

<sup>b</sup> School of Engineering and Computer Science, University of Hertfordshire, Hatfield, AL10 9AB, UK

<sup>c</sup> Beijing Institute of Aerospace Testing Technology, Beijing, 100074, China

§ The two first authors have equal contributions to the manuscript

\* Corresponding authors. Email: [y.ding@bham.ac.uk](mailto:y.ding@bham.ac.uk) (YD); [y.li.1@bham.ac.uk](mailto:y.li.1@bham.ac.uk) (YL); Tel. +44 (0) 121 414 5135

## Abstract

This paper reviews the state-of-the-art knowledge of boiling heat transfer in binary mixtures with special emphasis placed on the heating and cooling industry. The advantage of using refrigerant mixtures over pure refrigerants include the enhancement of system coefficient of performance (COP), better match with the desired thermal load and being safer, more environmental-friendly refrigerants. In other words, the concept of using mixtures enables more flexible selection of suitable working fluids in particular thermal applications. The purpose of this review article aims to summarize the important published articles on boiling heat transfer in binary mixtures, as well as to identify limitations to existing studies, hereby providing guidelines, directing future studies and invoking further innovations of this well-established but still promising thermal management technique. The present article reviews straightforward on both pool boiling and flow boiling of binary mixtures in a systematic and comprehensive way. Specifically, in addition to the effects of fluid composition, heat flux, mass flux, pressure and heater surface condition, this article also reviews the effects of mass diffusion, heats from dilution and dissolution on pool boiling heat transfer of binary mixtures, along with the effects of flow orientation, flow regime and flow instability on flow boiling heat transfer of binary mixtures. Many papers reviewed herein relate to the heat transfer correlations towards boiling of binary mixtures.

**Keywords:** binary mixtures; pool boiling; flow boiling; heat transfer correlation; heat transfer coefficient; mass diffusion resistance

## 1 Introduction

With the growing demands for the capacity of heat dissipation in many practical applications, including advanced electronics, high power systems and miniature energy transport systems, it is imperative to find a more effective thermal management technique through better

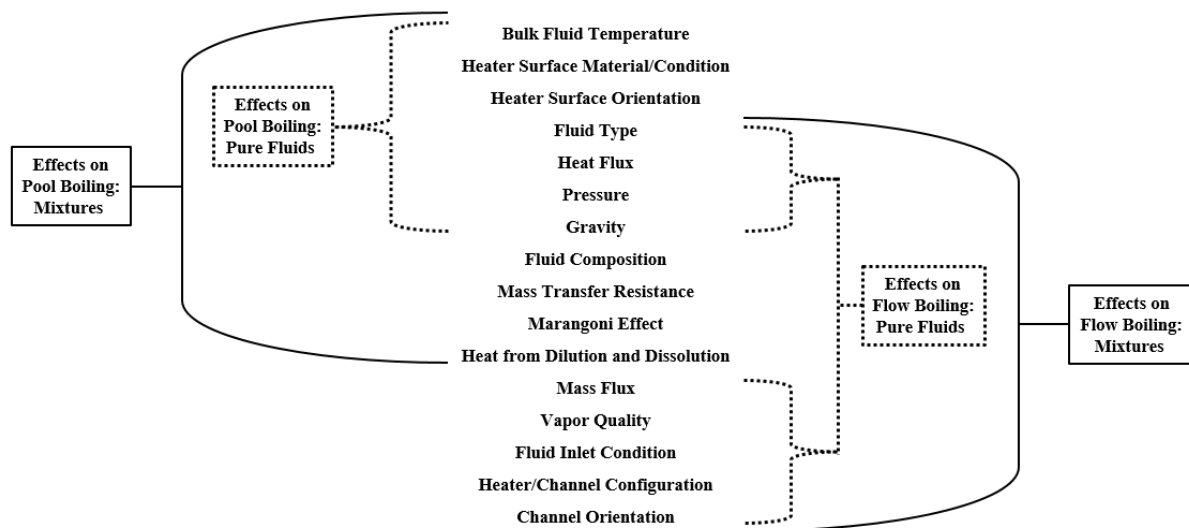
39 understanding its fundamental heat transfer mechanisms. In many power and thermal related  
40 systems, such as high power density electronic chips and lithium battery systems in electric  
41 vehicles, both excessive heat flux and temperature nonuniformity can result in rapid  
42 performance degradation and system failure. It is recognized that the impingement of liquid jet  
43 or spray cooling may satisfy the cooling requirements. However, they are difficult to be  
44 incorporated into a closed loop system and limited by the necessities of complex fluid handling  
45 and reconditioning equipment as well. On the other hand, boiling heat transfer offers superior  
46 heat dissipation rate (e.g.  $\sim 10\text{-}100\text{ W/cm}^2\text{-K}$ ) which can lead to a dramatic decrease in targeting  
47 temperature while maintaining uniform temperature distribution, even during substantial  
48 fluctuations in system heat flux. Boiling heat transfer occurs when the hot surface temperature  
49 exceeds the boiling point of the working fluid and then vapour bubbles start to form. The  
50 cooling effectiveness can thus be significantly improved due to not only the growth and  
51 departure of vapour bubbles drawing bulk liquid towards the hot surface at high frequency, but  
52 also the associated latent heat during the phase change process of the fluid would allow a great  
53 amount of heat dissipation with only a modest increase in fluid temperature.

54

55 Among all the boiling heat transfer techniques, boiling of binary and multicomponent mixtures  
56 has been widely used in thermal management systems [1, 2]. A significant advantage of  
57 multicomponent solution is that the chemical and thermo-physical properties of the overall  
58 mixture can be intentionally tweaked by both choosing the type and arranging the concentration  
59 of each mixture component. For example, the phase change temperature of a mixture can be  
60 deliberately and flexibly controlled at a constant pressure (i.e. a wider range of boiling  
61 temperature at a given pressure). In some applications using pure solutions as the working fluid,  
62 however, the operating pressure of the pure fluids need to be adjusted accordingly to fulfil the  
63 desired phase change conditions [3]. Another more specific example is that, by adaptably  
64 tailoring the thermo-physical properties of multicomponent solutions, binary mixture heat  
65 transfer fluids can be used to reduce the thermodynamic irreversibility in counter-flow heat  
66 exchangers, resulting in an increase of heat exchanger efficiency [4]. Yet a drawback for  
67 boiling heat transfer of binary mixtures, which has been studied by many researchers, is its  
68 lower heat transfer coefficient compared with pure fluids having the same physical properties  
69 [4, 5, 6, 122, 132]. However, the heat transfer coefficient in the flow boiling of binary solutions  
70 has been shown to be at least comparable to that for pure fluids and much higher than that for  
71 single-phase fluid flows [1, 2, 7, 8].

72

73 Although the boiling heat transfer of binary or multicomponent mixtures have been extensively  
 74 investigated from many aspects throughout the years, the authors believe the comprehension  
 75 of the boiling heat transfer mechanisms has been far from complete and there is still much room  
 76 to be enhanced in this area. The major effects that have been studied towards pool and flow  
 77 boiling of pure fluids and binary/multicomponent mixtures is summarized, as shown in Fig.1.  
 78 Correspondingly, selective effects have been reviewed and discussed in details under this  
 79 review article focusing on the effects which are more relevant to binary/multicomponent  
 80 mixtures, such as mass transfer resistance, Marangoni effect and heat from dilution and  
 81 dissolution. More importantly, review articles under the same topic have been rarely seen since  
 82 20 years ago [119-121]. Therefore, considering the advantages and importance of using binary  
 83 mixtures in the concerned field of boiling heat transfer, an updated review with more accurate  
 84 information and thorough interpretation is required to facilitate the wider use and improving  
 85 the performance of binary mixtures as a more efficient boiling heat transfer media. This paper  
 86 does not and cannot review all the interesting and important progress related to binary mixture  
 87 boiling heat transfer, but tries to summarize and discuss about the important published results  
 88 in the related field of boiling heat transfer characteristics of binary mixtures.  
 89



90  
 91 **Fig. 1 Summary of major effects on pool and flow boiling of either pure fluids or binary/multicomponent mixtures**  
 92

93 **2 Pool boiling heat transfer of binary mixtures**  
 94

95 For the practical applications of pool boiling, it is ideal to operate within the nucleate boiling  
 96 regime to utilise the high heat removal rate at low surface temperature. Boiling site density and  
 97 heat transfer coefficient (HTC) have been normally used to evaluate the nucleate boiling

98 process of binary mixtures. Furthermore, among the substantial amount of studies on pool  
99 boiling of mixtures over the past decades, many efforts have been devoted to study the  
100 deterioration of pool boiling HTC in mixtures. Correspondingly, various theoretical  
101 explanations have been proposed to account for the gaps in boiling heat transfer performance  
102 between pure liquids and their corresponding mixtures [9-16].

103

### 104 *2.1 Nucleate pool boiling and critical heat flux (CHF)*

105

106 The nucleate pool boiling HTC for a binary mixture can be considerably lower than the molar  
107 average of the nucleate pool boiling HTC for the pure component in the mixture. The authors  
108 argue that the main reasons for this heat transfer deterioration in mixtures are as follows: (a)  
109 concentration fluctuation effect for non-azeotropic mixtures. That is, when a bubble is  
110 generated in the binary liquid mixture, the concentration of the low boiling point component  
111 should be higher than that of the dew point component [5]; (b) mass transfer resistance for non-  
112 azeotropic mixtures, the more rapid evaporation of the more volatile component would result  
113 in elevating mass transfer resistance for the more volatile component at the gas-liquid interface  
114 (i.e. higher vapour mass of the more volatile component but lower in liquid mass). The heat  
115 transfer from liquid to bubble is controlled not only by heat diffusion but also by mass  
116 diffusion, and the mass diffusivity for the more volatile component in the mixture would be  
117 generally an order of magnitude smaller than the thermal diffusivity due to the increased mass  
118 transfer resistance [5, 18]; (c) Marangoni effect, the additional liquid redistributing force due  
119 to the surface tension gradient induced by the unequalled evaporation rates between mixture  
120 components would remarkably affect the pool boiling performance of binary mixtures [13, 17].  
121 According to previous studies, the raised mass transfer resistance and the loss of effective  
122 superheat are the main reasons of the performance degradation for binary mixtures in nucleate  
123 boiling [19, 20].

124

125 Furthermore, in boiling heat transfer, it is also important to be able to predict the critical heat  
126 flux (CHF), which is the critical point between nucleate boiling and film boiling regimes. The  
127 occurrence of CHF is usually accompanied by an inordinate increase in the surface temperature  
128 for a surface heat flux controlled system while an inordinate decrease of the heat transfer rate  
129 occurs for a surface temperature controlled system. It is known that the presence of dry spots  
130 at heated surfaces with high heat flux is a typical characteristic of nucleate boiling for a surface  
131 heat flux controlled system. The dry spots would even grow larger in near-critical regimes and

132 the heat flux per dry spot area would eventually be comparable with the average heat flux  
133 provided to the heated wall. The equality of these two heat fluxes, which is the point of boiling  
134 crisis, defines the onset of irreversible growth of the dry spot area [21]. Hence, in order to  
135 improve pool boiling heat transfer performance, research studies have been conducted focusing  
136 on not only the HTC but also the CHF of pool boiling heat transfer in binary mixtures.

137

138 Fujita et al. [22] evaluated the CHF over various component concentrations for the nucleate  
139 pool boiling of binary mixtures in a horizontal platinum tube. Seven different types of mixtures  
140 were studied with saturated state at atmospheric pressure. They found that aqueous mixtures of  
141 methanol and ethanol demonstrated a considerable increase in CHF compared to either the  
142 CHF linearly interpolated between pure components or the CHF predicted from a correlation  
143 using mixture properties. The CHF of three organic mixtures were as same as the interpolated  
144 CHF, whereas the remaining methanol/benzene and water/ethylene glycol showed 20% and  
145 50% reduced CHFs, respectively. A new empirical CHF correlation was proposed with the  
146 incorporation of a Marangoni number that took into account the surface tension gradient in the  
147 mixture between the dew and vapour points. It was indicated that the thinner the liquid  
148 microlayer, the higher evaporation rate of the more volatile component of a binary mixture. A  
149 difference in concentration (either in vapour phase or liquid phase) of each mixture component  
150 (due to their unmatched volatility) and consequently a gradient of surface tension were believed  
151 to cause the formation of the wedge-shaped liquid microlayer. If the surface tension of the more  
152 volatile component was weaker than that of the less volatile component, the surface tension  
153 gradient was directed to the thinner part of the microlayer avoiding the increase of dry spot. In  
154 that case, the CHF of the binary mixture would be higher than that of the pure components.  
155 Conversely, if the surface tension of the more volatile component was stronger than that of the  
156 less volatile component, the surface tension gradient would be directed from the dry spot  
157 boundary to the thicker part of the liquid microlayer facilitating the enlargement of the dry  
158 spot. As a result, the CHF in the binary mixture would be smaller than that in the pure  
159 components.

160

161 Furthermore, McGillis and Carey [23] suggested that the surface tension gradient caused by  
162 phase concentration difference of one mixture component might exist at the surfaces of vapour  
163 jets near the heated wall. This surface tension gradient would provide an additional  
164 hydrodynamic restoring force (either positive or negative) to affect the CHF conditions. In  
165 addition, they proposed an empirical correlation capable of predicting CHF in pool boiling heat

166 transfer of several binary mixtures. Yagov [21] also indicated that liquid flow rate to  
167 evaporation-intensive zone near the dry spot boundary might be controlled by the capillary  
168 pressure gradient. It was found that a correlated CHF model, which considered the effect of  
169 surface tension gradient, could well predict the CHF in pool boiling of binary mixtures under  
170 different pressure conditions.

171

## 172 *2.2 Effect of multicomponent mass diffusion on pool boiling of binary mixtures*

173

174 In the boiling of multi-component mixtures, component concentration gradient occurs due to  
175 the difference in volatility among the components. The concentration gradient exists in both  
176 liquid and vapour flows which is caused by the superior evaporation of the more volatile  
177 component even when local component balance is achieved. As this process goes along, the  
178 liquid phase of the less volatile component would become richer and the temperature of fluid  
179 saturation would get increased [24]. The boiling heat transfer in binary mixtures is inherently  
180 influenced by the concentration variation of different components and its associated effects on  
181 heat diffusion, mass diffusion and nucleation mechanism. Therefore, the authors argue that  
182 discovering optimum combinations of mixture component type and concentration thereby  
183 making best use of the component concentration gradient and surface tension gradient in binary  
184 mixtures is the key for improving their boiling heat transfer performance.

185

### 186 *2.2.1 Effect of component concentration*

187

188 He et al. [5] pointed out that a reduction in boiling site density of binary mixtures caused by  
189 the concentration fluctuation effect could be a main reason for the deterioration in heat transfer  
190 performance. The boiling site densities of R134a/R32 and i-butane/propane mixtures were  
191 experimentally investigated under pressures in the range of 0.25-1 MPa and wall superheats in  
192 the range of 3-25 °C. They concluded that the boiling site density of both binary mixtures  
193 decreased initially and then increased with the concentration of the high boiling point  
194 component. Furthermore, it was evident that the evaporation rate would control the depletion  
195 of the liquid phase of the more volatile component into the liquid layer close to the heated  
196 surface. Accordingly, there exists an upper limit to the increase in local saturation temperature  
197 for the nucleate pool boiling of binary mixtures, at when the more volatile component has all  
198 transformed to vapour phase. Boiling range is defined as a range of temperatures across which  
199 the components in a mixture boil. Therefore, it can be seen that the boiling range for binary

200 mixtures is between the saturation temperatures of the more and the less volatile components.  
201 Considering the saturation temperature of a mixture is a function of mixture composition,  
202 Thome [10] proposed a new method for predicting the variation of nucleate pool boiling HTC  
203 based on component compositions. Under low heat fluxes well below the CHF, the developed  
204 new equation that considered the boiling range could accurately predict the boiling HTCs for  
205 six binary mixtures: ethanol/water, acetone/water, ethanol/benzene, nitrogen/argon,  
206 nitrogen/oxygen, and nitrogen/methane. Zhang et al. [25] characterized nucleate pool boiling  
207 heat transfer on a smooth flat surface for HC600a/HFC134a, HC600a/HC290, and  
208 HC600a/HFC23. The influence of boiling range on the pool-boiling heat transfer performance  
209 was investigated experimentally. They stated that the HC600a/HFC23 mixture with a wide  
210 boiling range presented lower HTCs than the mixtures with a narrow boiling range such as  
211 HC600a/HFC134a and HC600a/HC290.

212

### 213 *2.2.2 Effect of mass transfer resistance*

214

215 Celata et al. [18] considered that heat transfer from liquid to vapour bubble in boiling of binary  
216 mixtures was regulated not only by heat diffusion but also by mass diffusion, while the mass  
217 diffusivity for the more volatile component was generally an order of magnitude smaller than  
218 the thermal diffusivity. Alpay and Balkan [6] experimentally studied nucleate pool boiling heat  
219 transfer for acetone-ethanol and methylene chloride-ethanol binary mixtures at pressures from  
220 0.2 to 0.5 MPa and heat fluxes from 10 to 40 kW/m<sup>2</sup>. Their results demonstrated that the  
221 greatest deterioration of heat transfer was observed at the maximum difference between liquid  
222 and vapour mole fractions of the more volatile component (largest mass transfer resistance for  
223 the more volatile component), and it suggested that the mass transfer resistance of the more  
224 volatile component was mainly responsible for the attenuation of boiling heat transfer in binary  
225 mixtures.

226

227 Hui et al. [9] investigated the boiling site density and HTC of ethanol/water and  
228 ethanol/benzene mixtures on a heated vertical brass disk at atmospheric pressure. It was  
229 indicated that the composition of the mixtures had a strong effect on the boiling site density  
230 which could be mostly attributed to the mass diffusion effect. Benjamin et al. [26] looked into  
231 the nucleation site density of acetone/carbon tetrachloride and n-hexane/carbon tetrachloride  
232 mixtures under atmospheric pressure. It was found that the mass diffusion effect could be the  
233 main reason in decreasing boiling nucleation site density of the mixtures. In their study, a



234 greater wall superheat had to be employed as the driving force to alleviate the unfavourable  
235 effect of mass diffusion resistance on boiling heat transfer. Thome and Davey [27] evaluated  
236 the effects of liquid mixture composition and vapour/liquid mole fraction difference of the  
237 more volatile component on bubble growth rate of nitrogen/argon mixtures at pressure of 0.13  
238 MPa. One of the key findings was that the growth rate of mixture bubble was linearly  
239 proportional to the difference of mole fraction between liquid and vapour phase of the more  
240 volatile component. The growth rate of mixture bubble decreased as the ratio between vapour  
241 and liquid phase of the more volatile component increased.

242

### 243 *2.2.3 Marangoni effect*

244

245 Binary mixture systems can be categorized into three groups: positive when the high-boiling  
246 point component of the mixture has a greater surface tension effect, negative when the high-  
247 boiling point component of the mixture has a lower surface tension effect, and neutral when  
248 both components of the mixture have equivalent surface tension effects [28, 29]. For example,  
249 ammonia/water has been proven to be a positive mixture since ammonia has a weaker surface  
250 tension and lower saturation temperature than water [30]. 2-propanol/water has been observed  
251 to be a positive mixture and the surface tension gradient resulting from preferential evaporation  
252 of the more volatile component at heated surface served to promote liquid motion towards the  
253 surface [31]. On the other hand, ethylene glycol/water has been demonstrated as a negative  
254 mixture where the gradient of surface tension worked for suppressing the fluid movement  
255 towards the heated surface [23].

256

257 The Marangoni effect is the mass transfer occurs at the interface between two fluids or phases  
258 driven by the gradient of surface tension. McGillis and Carey [23] realized that the variation of  
259 CHF in boiling of mixtures was closely connected with the component concentration in the  
260 mixtures which was predominantly affected by the surface tension gradient and Marangoni  
261 effect. Ohta et al. [32] argued that self-wetting characteristics of binary mixtures could lead to  
262 boiling heat transfer enhancement, though most other relevant studies showed otherwise. In  
263 their study, binary mixtures with superior self-wetting characteristics were selected as the  
264 working fluid. It was discovered that a surface tension gradient was generated along the surface  
265 of liquid microlayer beneath bubbles owing to the concentration and temperature gradients.  
266 The surface tension variation pushed liquid phases towards the three-phase interline and  
267 prevented further expansion of dry patches, as known as the "Marangoni effect".

268 Correspondingly, heat transfer enhancement was observed in low concentration alcohol  
269 aqueous solution (positive mixture) at relatively lower alcohol concentrations.

270

271 It should be noted that boiling process is highly dependent on buoyancy force introduced by  
272 considerable difference in density between the liquid and vapour phases. In certain  
273 circumstances, interactions among gravity, buoyancy force, surface tension (including  
274 Marangoni effect) are the dominant factors for boiling heat transfer performance in binary  
275 mixtures. Hence, the authors urge that future research and development of binary mixtures  
276 boiling should start with focusing more on tackling the force balance during boiling of binary  
277 mixtures. Ahmed and Carey [31] pointed out that when boiling under microgravity conditions,  
278 buoyancy force would fail to drive vapour phase away from and draw liquid phase towards the  
279 heated surface. As vapour bubbles accumulate, a vapour film would gradually cover the heated  
280 surface, delaying the vaporization process, resulting in surface dry out and dramatically  
281 diminishing the quality of heat transfer. Consequently, they conducted an experiment with  
282 water/2-propanol solution, a positive binary mixture, at three different gravities (i.e. reduced  
283 gravity, normal gravity and high gravity) to explore interactions between Marangoni effect and  
284 gravitational effect in pool boiling of binary mixtures. It was learned through comparing  
285 boiling curves of the same binary mixture under different gravitational environments that, in  
286 these mixtures, the boiling process was almost independent of gravity due to the prevalence of  
287 Marangoni effect. Meanwhile, under reduced gravity conditions, it was shown that the  
288 Marangoni effect was strong enough to offset adverse momentum effects and favour more  
289 stable nucleate boiling. Chai et al. [14] conducted a combined experimental and theoretical  
290 studies on the effect of interfacial behaviours on nucleate boiling heat transfer of ethanol/water,  
291 methanol/water, methanol/n-pentane, ethanol/n-pentane and methanol/ethanol binary  
292 mixtures. It was evident that vapour-liquid interfacial behaviours in binary mixtures essentially  
293 affected boiling dynamics such as bubble detachment, flow movement and heat transfer in the  
294 fluid microlayer, and microlayer stability. In addition, their experimental results could not be  
295 well correlated with theoretical predictions when not taking the Marangoni effect into account.

296

### 297 *2.3 Effect of surface condition on pool boiling of binary mixtures*

298

299 Besides improving pool boiling of binary mixture from the working fluid side, surface  
300 modification is another method to consider for enhancing pool boiling heat transfer  
301 performance and therefore has been frequently discussed in recent years. Both HTC and CHF

302 can be boosted by introducing porous structures, fins, hydrophilic surface condition, and hybrid  
303 surface patterns on the heated surface [33]. Surface modification usually starts from changing  
304 the wettability of the surface. One of the most recognizable surface wettability studies is to  
305 measure the contact angle (CA), which indicates the degree of wetting when a solid and liquid  
306 interact. A low CA ( $<90^\circ$ ) corresponds to high wettability (hydrophilic surface), and fluid will  
307 spread over a large area of the surface. A high CA ( $>90^\circ$ ) corresponds to low wettability  
308 (hydrophobic surface), and contact will be minimized between the fluid and the surface with a  
309 compact liquid droplet formed. When  $CA > 150^\circ$ , this depicts a minimal contact between the  
310 liquid droplet and the surface and corresponds to a super-hydrophobic surface condition [34].

311

312 By far, most of the studies regarding pool boiling on enhanced surfaces have aimed at pure  
313 fluids and investigations of the effect of surface modifications on pool boiling of binary  
314 mixtures are quite limited. Sahu et al. [35] studied the pool boiling of binary mixtures on nano-  
315 textured surfaces (e.g. surfaces coated with copper plated nanofibers). It was observed that the  
316 pool boiling curve of binary mixtures on the nano-textured surfaces considerably deviated from  
317 the standard boiling curve seen on plain surfaces. In particular, the HTC was found to be  
318 significantly higher at low surface superheat conditions since the liquid temperature around  
319 bubbles in nano-cavities was remarkably increased. It was also found that the nanostructures  
320 could prevent bubble merging and transition to film boiling. Kandlikar and Alves [36]  
321 performed an experimental study on pool boiling heat transfer of dilute aqueous solutions of  
322 ethylene glycol. The surface tension and mass diffusion effects were found to be insignificant  
323 on the pool boiling heat transfer performance of the aqueous solutions with low ethylene glycol  
324 concentrations. Future research direction was suggested by Kandlikar and Alves to consider  
325 the possibility of changing contact angles and wetting characteristics on heating surface. Thus,  
326 the authors of this review recommend, in future studies, to improve the pool boiling heat  
327 transfer of binary mixtures by positively capitalizing the effects of surface tension, gravity and  
328 buoyancy with the help of heater surface modifications.

329

#### 330 *2.4 Effect of heats from dilution and dissolution on pool boiling of binary mixtures*

331

332 Inoue and Monde [37] evaluated the enhancement of nucleate pool boiling heat transfer with  
333 the addition of a surface-active agent to binary mixture. It was indicated that heats from  
334 dissolution and dilution were generated near the vapour-liquid interface when vapours were  
335 dissolved in bulk liquid and when condensed liquid was diluted out of the bulk liquid. And the

336 heats of dilution and dissolution impacted on the pressure and temperature of the mixtures,  
337 thereby affecting the pool boiling heat transfer process [15]. Sarafraz et al. [38] experimentally  
338 studied the nucleate pool boiling heat transfer in binary mixtures accompanied with additional  
339 endothermic chemical reactions around a smoothed horizontal cylinder. Ammonium salts were  
340 selected as the dissolving salt considering its higher endothermic enthalpies. It was concluded  
341 that the temperature of the heating surface was locally dropped and the local HTC increased  
342 due to the absorbed heats by the chemical reactions taken place around the heated cylinder  
343 surface. However, at higher heat fluxes, the effect of endothermic reactions was insignificant  
344 in comparison with the exposed higher heat fluxes. In summary, the authors think the heats  
345 from dilution and dissolution are equivalent to an increase in effective specific heat and heat  
346 capacity of binary mixtures and they could be beneficial to the boiling heat transfer  
347 performance of binary mixtures if being controlled properly. But at the current stage, our  
348 mastery of the effect of heats from dilution and dissolution on pool boiling for binary solutions  
349 has far from complete and more attentions should be drawn to this area in the future.

350

### 351 *2.5 Correlations for pool boiling of binary mixtures*

352

353 The boiling behaviour of binary mixtures is more complicating than that of single-component  
354 liquids, as it contains multiple components with various properties and different liquid-vapour  
355 equilibrium schemes. Besides theoretical studies given theoretical limits of pool boiling in  
356 binary mixtures [39, 40], a substantial amount of efforts have been made via using empirical  
357 predictions [4, 10, 18, 39, 40-54] to better understand the real physical mechanisms of boiling  
358 in binary mixtures. It is evident from the literature that pool boiling heat transfer with binary  
359 mixtures is not as good as the respective mole or mass fraction averaged value of their  
360 counterpart pure fluids. Therefore, Inoue et al. [41] proposed a formula to estimate the  
361 deterioration in HTC in pool boiling of binary mixtures and expressed as follows:

362

$$F = f(y_1 - x_1, \Delta T_{bp}, \Delta T_l, D_L, \alpha_L, q) \quad (1)$$

363

364 where  $x_1$  and  $y_1$  are liquid and vapour mass of the more volatile component, respectively,  $\Delta T_{bp}$   
365 is boiling range,  $\Delta T_l$  is the ideal wall superheat,  $D_L$  is mass diffusivity of liquid phase,  $\alpha_L$  is  
366 thermal diffusivity of liquid phase,  $q$  is heat flux.

367

368 To quantitatively characterize pool boiling heat transfer performance of binary mixtures and

369 its difference from pure fluids, plenty of efforts have been devoted to modify and improve Eq.  
 370 (1) with different expressions of  $F$  detailed in Table 1 following by corresponding experimental  
 371 conditions for each study listed in Table 2. The boiling HTC of binary mixtures could then be  
 372 evaluated using Eq. (2) as a function of  $F$ , as follows:

$$\frac{h}{h_1} = \frac{1}{1 + F} \quad (2)$$

374 where  $h_1$  is the ideal HTC calculated using mixture properties for boiling heat transfer of pure  
 375 fluids.  
 376

377 **Table 1** Existing correlations for pool boiling HTC suppression function  $F$  of binary mixtures  
 378

Authors and Year	Expression of $F$	
Stralen [39] (1966)	$x_1 \{(x_{1,\text{local}} - y_{1,\text{local}})/x_{1,\text{local}}\} \sqrt{\alpha_L/D_L} (dT/dx_{1,\text{local}})_{x_{1,\text{local}}=x_1}$	(3)
Stephan and Körner [42] (1969)	$A_0  \tilde{y}_1 - \tilde{x}_1  (0.88 + 0.12p[\text{bar}]), A_0 = 1.53$	(4)
Calus and Rice [43] (1972)	$[1 +  y_1 - x_1  \sqrt{\alpha_L/D_L}]^{0.7} - 1$	(5)
Calus and Leonidopoulos [40] (1974)	$(x_1 - y_1) \sqrt{\alpha_L/D_L} (dT/dx_1) (C_p/H_{LG})$	(6)
Jungnickel et al. [44] (1980)	$A_0  \tilde{y}_1 - \tilde{x}_1  (\rho_V/\rho_L) q^{0.48+0.1\tilde{x}_1}$	(7)
Schlünder [45] (1983)	$\frac{h_1}{q} (T_{s2} - T_{s1}) (\tilde{y}_1 - \tilde{x}_1) \left[ 1 - \exp\left(\frac{-B_o q}{\rho_L H_{LG} \beta_L}\right) \right], B_o = 1, \beta_L = 0.0002$	(8)
Thome [10] (1983)	$k \frac{\Delta T_{\text{bp}}}{\Delta T_1}, k = 1$	(9)
Thome and Shakir [46] (1987)	$\frac{h_1}{q} \Delta T_{\text{bp}} \left[ 1 - \exp\left(\frac{-B_o q}{\rho_L H_{LG} \beta_L}\right) \right], B_o = 1, \beta_L = 0.0003$	(10)
Fujita and Tsutsui [4] (1994)	$k \frac{\Delta T_{\text{bp}}}{\Delta T_1}, k = \left[ 1 - 0.8 \exp\left(-\frac{q}{10^5}\right) \right]$	(11)
Inoue and Monde [53] (1994)	$k \frac{\Delta T_{\text{bp}}}{\Delta T_1}, k = \left[ 1 - 0.75 \exp\left(-\frac{0.75q}{10^5}\right) \right]$	(12)
Fujita and Tsutsui [47] (1997)	$k \frac{\Delta T_{\text{bp}}}{\Delta T_1}, k = \left[ 1 - \exp\left(\frac{-60q}{\rho_L H_{LG}} \left\{ \frac{\rho_V^2}{\sigma g (\rho_L - \rho_V)} \right\}^{1/4}\right) \right]$	(13)
Inoue et al. [41] (1998)	$k \frac{\Delta T_{\text{bp}}}{\Delta T_1}, k = \frac{T_{\text{local}} - T_{\text{bulk}}}{T_{\text{local, max}} - T_{\text{bulk}}} = f(q) \leq 1$	(14)
Rao and Balakrishnan [48] (2004)	$\left[ ( \tilde{y}_1 - \tilde{x}_1  \sqrt{D_L/\alpha_L})^{0.5} \right]^{-1} - 1$	(15)

$$(i) K_{st}A_0(y_1 - x_1)(0.88 + 0.12p[\text{bar}])$$

$$\text{Inoue and Monde [49] (2009)} \quad (ii) \left\{ K_i k \Delta T_{bp} + K_{sh}(y_1 - x_1) \left[ 1 - \exp\left(\frac{-B_0 q}{\rho_L H_{LG} D_L}\right) \right] (T_{s2} - T_{s1}) \right\} / \Delta T_1 \quad (16)$$

$$k = \left[ 1 - 0.75 \exp\left(-\frac{0.75q}{10^5}\right) \right]$$

379  
380

**Table 2** Operating conditions of correlations for pool boiling HTC of binary mixtures

Authors and Year	Fluids Compositions	Operating Conditions for Pool Boiling HTC Correlations for Fluid Mixtures
Stralen [39] (1966)	Water/Methylethylketone (4.1 wt.%) Water/1-Butanol (1.5, 6.0 wt.%)	Heating surface: 200 μm diameter platinum wire Heat flux: 4.5×10 <sup>5</sup> W/m <sup>2</sup> Pressure: 1 atmospheric
Stephan and Körner [42] (1969)	17 binary mixtures considered from literature	Pressure: 1-10 bar
Calus and Rice [43] (1972)	Water/Isopropanol (9 concentrations, 0 to 100 wt.% of the lighter component) Water/Acetone (9 concentrations, 0 to 100 wt.% of the lighter component)	Heating surface: Nickel/Aluminium alloy wire (wire 200 and wire 24) Heat flux in nucleate boiling: 9.4×10 <sup>3</sup> to 1.9×10 <sup>6</sup> W/m <sup>2</sup> Range of boiling point: 80.4-100 °C for Water/Isopropanol, 56.5-89.6 °C for Water/Acetone Range of ΔT: 6.8-51.7 °C for Water/Isopropanol, 10.3-57.2 °C for Water/Acetone Pressure: 1 atmospheric
Calus and Leonidopoulos [40] (1974)	Water/n-Propanol (11 n-Propanol concentrations from 9.0 wt.% to 93.0 wt. %)	Heating surface: Nickel/Aluminium alloy wire (0.03 cm diameter, 7.26 cm long) Heat flux: 1 and 4×10 <sup>5</sup> W/m <sup>2</sup> Pressure: 1 atmospheric
Jungnickel et al. [44] (1980)	R12/R113, R22/R12, R13/R22, R23/R13	Heating surface: copper plate (3 cm <sup>2</sup> ) Heat flux: 4×10 <sup>3</sup> to 4×10 <sup>5</sup> W/m <sup>2</sup> Pressure: 0.1 to 2 MPa Temperature range: -75 to 60 °C
Thome [10] (1983)	6 binary mixture systems including Ethanol/Water, Acetone/Water, Ethanol/Benzene, Nitrogen/Argon, Nitrogen/Oxygen, Nitrogen/Methane	Refer to [10] for more details (based on 13 studies from literature)
Fujita and Tsutsui [4] (1994) Fujita and Tsutsui [47] (1997)	Methanol/Water, Ethanol/Water, Methanol/Ethanol, Ethanol/n-Butanol, Methanol/Benzene (various concentrations tested from 0-100 mole% of the more evaporative component)	Heating surface: copper plate (12.6 cm <sup>2</sup> ) Heat flux: 4 to 610 kW/m <sup>2</sup> Pressure: 1 atmospheric Temperature condition: saturated
Inoue and Monde [53] (1994)	R12/R113, R134a/R113, R22/R113, R22/R11	Heating surface: platinum wire 2 (0.3 mm diameter, 8.8 cm long) Heat flux: less than 10 <sup>5</sup> W/m <sup>2</sup> Pressure: 0.25 to 0.7 MPa
Inoue et al. [41] (1998)	R12/R113, R134a/R113, R22/R113, R22/R11	Heating surface: platinum wire 2 (0.3 mm diameter, 8.8 cm long) Heat flux: up to CHF (greater than 10 <sup>5</sup> W/m <sup>2</sup> ) Pressure: 0.4 and 0.7 MPa
Rao and Balakrishnan [48] (2004)	Isopropanol/ Water and MEK/Water (50 mole%), and ternary mixtures with Acetone mole% from 10% to 90%	Heating surface: copper plate (7 cm <sup>2</sup> ) Heat flux: up to 200 kW/m <sup>2</sup> Pressure: 1 atmospheric

---

Inoue and Monde [49]  
(2009)

Ammonia Water  
(0-100 % concentration)

*Heating surface:* platinum wire 2 (0.3 mm  
diameter, 8.8 cm long)  
*Heat flux:* below 1000 kW/m<sup>2</sup>  
*Pressure:* 0.4 MPa

---

381  
382 As shown in Tables 1 and 2, in Stralen's expression of suppression factor F proposed as early  
383 as in 1966 [39], a bubble growth factor was introduced to determine the actual growth rate of  
384 bubbles boiling on a platinum heating wire surface. It was implied that the bubble growth  
385 equation for pure liquid boiling was also valid for binary mixtures after taking into account the  
386 concentration of the more volatile component in growth factor. Stephan and Körner [42]  
387 noticed that concentration difference of the more volatile component in vapour and liquid had  
388 a crucial impact on degradation of boiling heat transfer in binary mixtures. It was emphasized  
389 that a maximum value of the concentration difference led to a minimum value of the HTC  
390 under a constant heat flux condition. An empirical constant and a pressure correction factor  
391 were added to their correlation for the purpose of better prediction of the HTC. In 1972, Calus  
392 and Rice [43] developed an empirical HTC correlation based on the bubble growth theories  
393 originated from Stralen [39]. It was suggested in their study that the degradation of boiling heat  
394 transfer of binary mixtures was caused by bubble growth reduction in binary systems. Heat and  
395 mass transfer correction factors were brought into the correlation facilitating the prediction of  
396 pool boiling parameters in binary mixtures. Calus continued his work on boiling of binary  
397 mixtures and created an empirical HTC model with Leonidopoulos [40] based on theoretical  
398 studies. There were no empirical constants in the correlation while information of boiling  
399 curves of pure liquids was incorporated to obtain the HTC value and therefore a lower mean  
400 error could be achieved comparing with the correlations from Stephan and Körner [42] and  
401 Calus and Rice [43]. Jungnickel et al. [44] modified the correlation from Stephan and Körner  
402 [42] by additionally adopting a heat flux multiplier in year 1980. The modified correlation also  
403 included a mixture-dependent constant, which was to be determined at an arbitrary pressure in  
404 advance. The results showed that the difference between measured and computed HTC values  
405 was less than 15% for all cases. Schlünder [45] mentioned that saturation temperature  
406 difference among each component in mixture should be considered as an important parameter  
407 in boiling HTC correlation. And a correction factor taking into account the mass transfer  
408 coefficient was adopted in Schlünder's correlation to improve the correlation from Stephan and  
409 Körner [42].

410

411 Furthermore, in 1983, Thome [10] recognized reduction in effective wall superheat as a major  
412 factor of the boiling heat transfer attenuation in binary mixtures. It was also the first time that

413 boiling range (range between the upper and lower saturation temperature limit of a mixture),  
414 determined solely from the phase diagram, was considered as a decisive parameter for mixture  
415 boiling heat transfer performance. Then in 1987, Thome and Shakir [46] echoed the concept of  
416 boiling range by suggesting that, at peak nucleate heat flux, there existed an maximum boiling  
417 point of the liquid adjacent to the heated surface due to the preferential evaporation of the more  
418 volatile component. Accordingly, it can be observed from Table 1 that the boiling range  $\Delta T_{bp}$   
419 was a key parameter in the HTC correlations of Thome [10] and Thome and Shakir [46]. In  
420 1994, the correlation of Thome [10] was further modified by Fujita and Tsutsui [4] by replacing  
421 the mass transfer term with a term determined as a function of heat flux, so that took into  
422 account the effect of heat flux on the heat transfer reduction instead of mass transfer and  
423 mixture properties. Inoue and Monde [53] kept the basic form of the Fujita and Tsutsui  
424 correlation [4] but further corrected the empirical constants. The improved correlation was  
425 shown to be able to predict the HTCs for binary mixtures within an accuracy of  $\pm 25\%$ . To  
426 continue improving the correlation of Thome [10], Fujita and Tsutsui [47] considered the effect  
427 of heat flux in a dimensionless form to make the correlation simpler and more applicable. Later,  
428 Inoue et al. [41] interpreted the coefficient “k” in Thome correlation [10] from the point of  
429 view of local surface temperature rather than heat flux. It was pointed out that the local surface  
430 temperature during boiling of binary mixtures should be mainly affected by component  
431 concentration fluctuation due to the preferential evaporation of the more volatile liquid. As the  
432 development of surface technology, in 2004, Rao and Balakrishnan [48] produced a correlation  
433 to estimate the ideal boiling HTC of binary mixtures taking into account the influence of  
434 surface-liquid interaction and surface roughness. It was indicated that the newly proposed  
435 correlation could predict the experimental data in a satisfactory manner. In 2009, the correlation  
436 provided by Inoue and Monde [49] confirmed that the HTCs of binary mixtures were regulated  
437 by both boiling range and concentration difference of the more volatile component in liquid  
438 and vapour phase. It was pointed out that the HTCs for different binary mixtures could be well  
439 predicted when appropriate values of empirical factors were applied.

440

441 Besides, Kandlikar [50] developed a theoretical model to evaluate pool boiling heat transfer of  
442 binary mixtures through establishing a pseudo-single component HTC  $h_{psc}$  and a mass  
443 diffusion related suppression factor  $F_D$ . The effects of liquid composition and interface  
444 temperature of growing bubble on heat transfer performance of binary mixtures were  
445 analytically estimated. The proposed HTC model is as follows,



446

$$h = h_{psc} F_D \quad (17)$$

447

448 where,  $F_D$  is diffusion-induced suppression factor to account for the reduction in HTC due to449 mass diffusion effects.  $F_D$  can be calculated as follows:

450

$$F_D = 0.678 \cdot \left( \frac{1}{1 + (C_p/H_{LG})(\alpha_L/D_L)^{1/2}(\Delta T_s/g)} \right), \quad v > 0.005 \quad (18)$$

$$F_D = 1 - 64v, \quad 0 < v \leq 0.005 \quad (19)$$

451

452 where  $C_p$  is specific heat,  $H_{LG}$  is latent heat of evaporation,  $\Delta T_s$  is wall superheat,  $g$  is gravity453 acceleration,  $v$  is volatility parameter and it was obtained through:

454

$$v = |(y_1 - x_1) (dT/dx_1)| \sqrt{\alpha_L/D_L} (C_p/H_{LG}) \quad (20)$$

455

456 The above HTC model was compared with the theoretical model from Calus and

457 Leonidopoulos [40], and two other empirical correlations from Calus and Rice [43] and Fujita

458 and Tsutsui [47]. It was shown that the model from Kandlikar [50] was capable of predicting

459 the HTCs of azeotropic mixtures (benzene/methanol, R-23/R-13 and R-22/R-12) as well as

460 other mixtures with varying boiling points. Armijo and Carey [17] employed a similar

461 philosophy when constructing their HTC correlation substituting the ideal HTC with an

462 average pseudo-single component HTC. The corrected correlation was proven to be more

463 efficient in predicting the Marangoni effect in mixtures under sub-atmospheric conditions.

464

465 Scriven [55] first proposed that variation in relative HTC in boiling of binary mixtures should

466 be determined by two additional similarity numbers: Lewis number (Le) and Kutateladze

467 number (Ku), defined as below in Eq. (22). As it can be noticed, Le is a ratio between mass

468 diffusivity and thermal diffusivity, Ku represents an energy ratio related to evaporation process.

469 Gogonin [56] continued to point out that the function of wall superheat in boiling of binary

470 mixtures could be considered as same as that in boiling of homogeneous liquids, which could

471 be described by certain similarity numbers such as Le and Ku. In Gogonin's work, the HTC

472 correlation was simplified to highlight the effects of mass and thermal diffusion and wall

473 superheat change during evaporation of the more volatile component, as expressed in the

474 following equations:

475

$$\frac{h}{h_1} = \frac{Nu}{Nu_1} = f\left(\frac{\rho_V^2}{Le Ku^2}\right) = f\left(\frac{\Delta T_s \lambda C_p \rho_V^2}{D_L H_{LG} \rho_L (\rho_L - \rho_V)^2}\right) \quad (21)$$

$$Le = D_L / \alpha_L, \quad Ku = \frac{H_{LG}}{\Delta T_s C_p} \quad (22)$$

476 where  $h_1$  is the ideal HTC,  $Nu_1$  is ideal Nusselt number,  $v$  is volatility parameter,  $\lambda$  is thermal  
 477 conductivity,  $\rho_L$  and  $\rho_V$  are density of liquid and vapor phase, respectively.

478

479 The HTC correlations discussed above were tested against experimental results by succeeding  
 480 researchers. Wu et al. [57] measured the HTCs for nucleate boiling on a smooth flat copper  
 481 surface in a binary mixture of tetrafluoromethane (FC14) and methane (HC50) under a  
 482 saturated pressure of 0.3 MPa at a wide range of heat fluxes (30-150 kW/m<sup>2</sup>) and mixture  
 483 concentrations. The experimental data was compared with existing HTC correlations for  
 484 boiling of binary mixtures [4, 41, 46]. It was found that the correlation from Fujita-Tsutsui [4]  
 485 exhibited a good agreement with Wu et al.'s results within an average deviation of 9.5%.  
 486 Sathyabhama and Babu [12] experimentally studied the nucleate pool boiling HTC of  
 487 ammonia/water mixture at a low ammonia mass fraction of  $0 < x_{NH_3} < 0.3$ . The obtained HTC  
 488 was compared with the correlations from Calus and Rice [43], Stephan and Körner [42] and  
 489 Inoue and Monde [49] for ammonia water mixtures, respectively. Results showed that the  
 490 empirical constants and indexes of the first two correlations (see [42] and [43] in Table 1) had  
 491 to be modified using the least mean square method, to minimize errors between the predicted  
 492 values and Sathyabhama and Babu's experimental data. The exponential constant that best  
 493 fitted the experimental data was 0.67 instead of 0.7 in Table 1 for Calus and Rice's correlation  
 494 while the most fitted constant  $A_0$  of Stephan and Körner's correlation was 1.6631. The  
 495 modified correlations were demonstrated to be good at predicting Sathyabhama and Babu's  
 496 experimental data with an accuracy of  $\pm 18\%$  and  $\pm 16\%$ , respectively. Therefore, the authors  
 497 of this review urge more future studies, either experimental, numerical or theoretical, on  
 498 validating and thereby continuing to improve the existing HTC correlations of binary mixture  
 499 pool boiling until the appearance of ultimate correlations.

500

501 To summarize, pool boiling of binary mixtures is a very complicating problem. Despite of the  
 502 fact that researchers have spent plenty of efforts to develop HTC correlations trying to  
 503 quantitatively characterize this boiling phenomenon since 1960s, there is still not a particular  
 504 outstanding correlation that can outperform all the others by comprehensively considering all

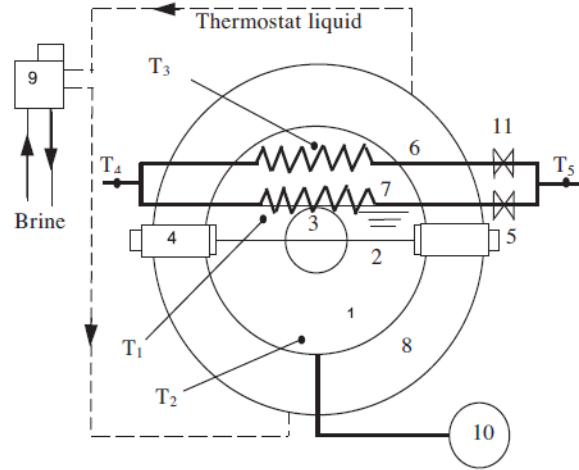
505 the relevant effects that affect the pool boiling of binary mixtures such as the heat exchanges  
506 from dilution and dissolution. More importantly, as shown in Tables 1 and 2, most of the  
507 proposed correlations were generated under different experimental circumstances (i.e. type of  
508 mixture component, component concentration, boundary condition) and will probably not work  
509 well when being applied to a different mixture and different experimental conditions [48, 49,  
510 122, 124], the same problems exist in pool boiling of pure fluids as well [125, 126]. However,  
511 the work related to building empirical correlation through experimental results is still  
512 meaningful and unfinished, because it will continuously complement the database of pool  
513 boiling of binary mixtures and persistently train empirical correlations preparing for an  
514 ultimately generalized theoretical equation for pool boiling of binary mixtures, probably  
515 similar to the Navier-Stokes equations for fluid flows.

516

#### 517 *2.6 Examples of experimental apparatus for pool boiling in binary mixtures*

518

519 To investigate the pool boiling heat transfer with dilute binary mixtures, Kandlikar and Alves  
520 [36] built an experimental system similar to the one used by Fujita et al. [22]. The newly built  
521 system could be able to heat a pool of quiescent liquid to its saturation temperature at  
522 atmospheric pressure while enabling the observation of bubble dynamics on a tubular heating  
523 element. Inoue and Monde [37] studied the nucleate pool boiling of ammonia/water mixtures  
524 by modifying the experimental apparatus from Kandlikar and Alves [36] and Fujita et al. [22],  
525 as shown in Fig. 2. The cooling process in the system was further improved to be more efficient  
526 so that the mixing heat could be removed for more accurate boiling heat transfer data. In the  
527 pressure vessel, a platinum wire, served as the heating surface, was placed horizontally and  
528 heated by direct electric current. Due to the demand of thermal isolation, the vessel was  
529 immersed in a thermostat bath and the temperature in the vessel was kept constant by a pumped  
530 thermostat. Generated vapour was condensed by a condenser and then being forced back to the  
531 bulk liquid for the sake of saving working fluid. Heat of dissolution produced at the vapour-  
532 liquid interface was removed by a cooling pipe.



533  
 534 **Fig. 2** Schematic of the pool boiling test apparatus for binary mixtures in Inoue and Monde's study [37]  
 535 (1. pressure vessel. 2. heated wire. 3. viewing window. 4. insulator. 5. electrode. 6. condenser. 7. cooling pipe. 8. thermostat  
 536 bath. 9. thermostat with pump. 10. pressure gauge. 11. valves. T1, T2, T3, T4, T5 are thermocouples.)  
 537

538 Nemade and Khandekar [58] conducted an experiment on pool boiling heat transfer of ethanol-  
 539 water mixture on a flat surface of aluminium with a diameter of 30 mm. The surface was placed  
 540 in a cylindrical heater block assembly in which heat was conducted to the surface from four  
 541 cartridge heaters (150 W each) in a heater block. The entire heater block and test surface were  
 542 enclosed by Teflon insulation ( $k = 0.25 \text{ W/m}\cdot\text{K}$ ) to prevent heat loss. As shown in Fig. 3, five  
 543 thermocouples were arranged 0.8 mm below the testing surface – one at the centre and the other  
 544 four were evenly spread along a horizontal contour line of the circular heater block. Each  
 545 thermocouple was used for estimation of bulk liquid pool and vapour temperature. In addition,  
 546 a thermocouple was installed at the base of the heater block to monitor the maximum safety  
 547 temperature of the system and to approximate heat flux transmitted to the testing surface.  
 548 Hence, if  $T_{\text{ave}}$  was the average thermocouple reading then the actual surface temperature  $T_{\text{surf}}$   
 549 was estimated as follows:

550

$$T_{\text{surf}} = T_{\text{ave}} - \frac{q\delta}{\lambda} \quad (23)$$

551  
 552 where  $q$  is calculated heat flux,  $\lambda$  is thermal conductivity of the heater block, and  $\delta$  is the  
 553 distance to the targeting surface.  
 554

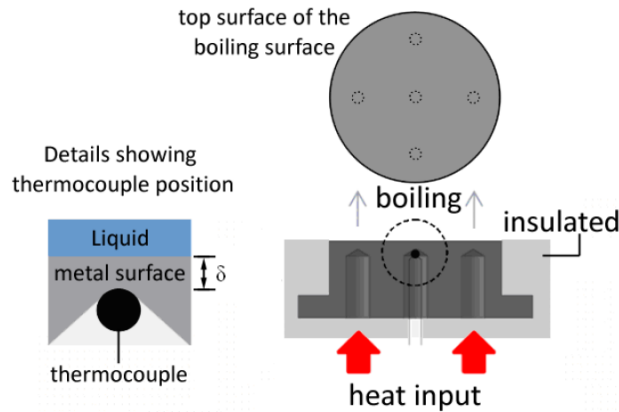


**Fig. 3** Schematic of the boiling test surface and positions of the embedded thermocouples in Nemade and Khandekar's study [58]

555  
556  
557  
558

559 In summary, it is not difficult to see that the way of setting up pool boiling experiments for  
560 binary mixtures is similar to those of pure working fluids. However, pool boiling of binary  
561 mixtures is more complex with effects such as component concentration, surface tension  
562 gradient and heat associated with dilution and dissolution and therefore should be addressed  
563 through smarter designs of experimental measurements (e.g. temperature, pressure and  
564 visualization) and analysing methodologies (e.g. how to quantitatively express the effects of  
565 surface tension and heat from dilution and dissolution using experimentally measured  
566 parameters).

567

568 *2.7 Issues of experimental uncertainties and result inconsistencies for pool boiling in binary*  
569 *mixtures*

570

571 As it is known, substantial efforts are needed to construct, characterize pool boiling  
572 experiments and the phenomena are difficult to analyse. Moreover, the pool boiling studies in  
573 literature have been conducted in different experimental apparatuses under various  
574 experimental conditions. Consequently, inconsistencies are sometimes found among pool  
575 boiling results. More importantly, these conundrums have created numerous obstacles for  
576 succeeding researchers to validate their results with previous references and justify  
577 corresponding boiling-related phenomena. Hence, results of selective effects on pool boiling  
578 heat transfer performance of binary mixtures have been summarized and listed in Tables 3-6  
579 for the effects of fluid composition, heat flux, pressure and heater surface condition,  
580 respectively, aiming to create a reference to be used by other researchers for comparisons and  
581 understandings of pool boiling-related observations.

582

**Table 3** The effect of fluid composition on pool boiling heat transfer performance of binary mixtures

Authors and Year	Fluids Compositions	Operating Conditions	Effects of Fluid Composition on Pool Boiling Heat Transfer
Fujita and Tsutsui [4] (1994)	Methanol/Water, Ethanol/Water, Methanol/Ethanol, Ethanol/n-Butanol, Methanol/Benzene (various concentrations tested from 0-100 mole% of the more evaporative component)	Heating surface: copper plate (12.6 cm <sup>2</sup> ) Heat flux: 4 to 610 kW/m <sup>2</sup> Pressure: 1 atmospheric Temperature condition: saturated	HTC of mixture was reduced below the interpolated values between their pure components, or between one of their pure components. A distinct min in HTC was observed at an intermediate concentration.
Fujita and Bai [22] (1997)	Methanol/Water, Ethanol/Water, Methanol/Ethanol, Ethanol/n-Butanol, Methanol/Benzene, Benzene/N-heptane and Water/Ethylene glycol (75 concentrations tested from 0-100 mole% of the more evaporative component)	Heating surface: 0.5 mm horizontal platinum wire Heat flux: up to CHF Pressure: 1 atmospheric Temperature condition: saturated	CHF first ↑ as mole fraction of the more volatile component ↑, then ↓ for methanol/water and ethanol/water while the effect of concentration on CHF was relatively insignificant for other mixtures.
Inoue et al. [41] (1998)	R12/R113, R134a/R113, R22/R113, R22/R11	Heating surface: platinum wire 2 (0.3 mm diameter, 8.8 cm long) Heat flux: up to CHF (greater than 10 <sup>5</sup> W/m <sup>2</sup> ) Pressure: 0.25-0.7 MPa	HTC ↓ when adding a second mixture component, reaching to lowest values in the mass concentration range of 0.3-0.7.
Kandlikar and Alves [36] (1999)	Water/Ethylene glycol (1-10 wt.% Ethylene glycol)	Heating surface: 3.08 mm OD, 2.05 mm ID, 42.4 mm long horizontal stainless steel tube Heat flux: 10-100 kW/m <sup>2</sup> Pressure: 1 atmospheric Temperature condition: saturated	In low concentration region, the binary diffusion effects insignificant for water/ethylene glycol and a slight improvement in HTC over pure water.
Rao and Balakrishnan [48] (2004)	Acetone–isopropanol–water and acetone–MEK (methyl ethyl ketone)–water (acetone mole fraction 0.1-0.9 as the more volatile component while the mole fractions of other two components kept equal)	Heating surface: 29.8 mm diameter aluminium circular plate Heat flux: < 120 kW/m <sup>2</sup> Pressure: 1 atmospheric	HTC for a given heat flux ↓ and then ↑ with ↑ in the concentration of acetone.
Zhang et al. [25] (2007)	HC600a/HFC134a, HC600a/HC290, and HC600a/HFC23 (various mass fraction ratios from 0 to 1)	Heating surface: 25 mm diameter copper circular plate Heat flux: 10-300 kW/m <sup>2</sup> Pressure: 0.5 MPa Temperature condition: boiling range from 50 to 150 K	HTC ↓ first and reached and maintained at its minimum value, and then ↑ with the concentration of the more volatile component.
Sathyabhama and Babu [12] (2011)	Ammonia water (0-30 wt.% NH <sub>3</sub> )	Heating surface: 6 mm diameter, 20 mm long cylindrical stainless steel rod Heat flux: 360-2000 kW/m <sup>2</sup> Pressure: 4-8 bar	HTC in the mixture ↓ with ↑ in ammonia mass fraction.
Wu et al. [57] (2012)	Pure tetrafluoromethane (FC14), methane (HC50) and their binary mixtures	Heating surface: 30 mm diameter copper circular plate Heat flux: 30-150 kW/m <sup>2</sup> Pressure: 0.3 MPa Temperature condition: boiling range from 80 to 300 K	HTC ↓ first and reached its minimum value, and then ↑ with FC14 concentration.

Sarafraz [122] (2012)	Citric acid/water (mass fraction 0.15-0.61)	Heating surface: 21 mm diameter, 105 mm long cylindrical stainless steel rod Heat flux: < 113 kW/m <sup>2</sup> Pressure: 0.3 MPa Temperature condition: Saturated	HTCs of the mixtures were remarkably less than those in single component substances and dramatically deteriorated in the vicinity of both single component substances (concentration of one component close to 0). HTC ↓ with mass fraction of citric acid within the tested range.
Gong et al. [16] (2013)	Ethane, isobutane and their binary mixtures (whole concentration range from 0 to 1)	Heating surface: 30 mm diameter copper circular plate Heat flux: 20-150 kW/m <sup>2</sup> Pressure: 0.3 MPa Temperature condition: boiling range from 0 to 50 K	HTC ↓ first and reached and maintained at its minimum value, and then ↑ with the concentration of the more volatile component.
Hamzekhani [11] (2014)	Ethanol/water (0, 1, 0.04-0.723 wt.% Ethanol), NaCl/water (50-300 kg/m <sup>3</sup> NaCl) and Na <sub>2</sub> SO <sub>4</sub> /water (50-300 kg/m <sup>3</sup> Na <sub>2</sub> SO <sub>4</sub> )	Heating surface: 20 mm diameter stainless steel rod Heat flux: 5-105 kW/m <sup>2</sup> Pressure: 1 atmospheric Temperature condition: saturated	Bubble detachment diameter ↑ with ↑ electrolyte concentration and ↓ with ↑ ethanol mass fraction.

**Table 4** The effect of heat flux on pool boiling heat transfer performance of binary mixtures

Authors and Year	Fluids Compositions	Operating Conditions	Effects of Heat Flux on Pool Boiling Heat Transfer
Alpay and Balkan [6] (1989)	Acetone-ethanol and methylene chloride-ethanol (full concentration range covered from 0 to 1)	Heating surface: 4.8 mm diameter copper tube Heat flux: 10 to 40 kW/m <sup>2</sup> Pressure: 2.0-5.0 bar Temperature condition: saturated nucleate boiling	Boiling HTCs of either the pure liquids or the binary mixtures ↑ with ↑ heat flux. HTC deteriorations were observed for mixtures compared with pure fluids and the deterioration ↓ as heat flux ↑.
Fujita and Tsutsui [4] (1994)	Methanol/Water, Ethanol/Water, Methanol/Ethanol, Ethanol/n-Butanol, Methanol/Benzene (various concentrations tested from 0-100 mole% of the more evaporative component)	Heating surface: copper plate (12.6 cm <sup>2</sup> ) Heat flux: 4 to 610 kW/m <sup>2</sup> Pressure: 1 atmospheric Temperature condition: saturated	HTC of mixtures ↓ below the interpolated values between pure components, or between one of their pure components and the azeotrope in case of azeotrope-forming mixtures. A distinct min in HTC was observed at an intermediate concentration. Heat flux ↑, the HTC reduction ↑ and the minima ↑ at higher heat fluxes.
Inoue et al. [41] (1998)	R12/R113, R134a/R113, R22/R113, R22/R11	Heating surface: platinum wire 2 (0.3 mm diameter, 8.8 cm long) Heat flux: up to critical heat flux (greater than 10 <sup>5</sup> W/m <sup>2</sup> ) Pressure: 0.25-0.7 MPa	Nucleation site density, bubble size and frequency of bubble emission ↑ with ↑ in heat flux. ↑ of vapour with ↑ heat flux would make concentration at an equilibrium state shift toward ↓ liquid concentration in the mixtures. This situation was ↑ by ↑ the heat flux. ↑ in the amount of evaporation with ↑ heat flux resulted in ↑ in temperature along the bubble point curve.

Kandlikar and Alves [36] (1999)	Water/Ethylene glycol (1-10 wt.% Ethylene glycol)	Heating surface: 3.08 mm OD, 2.05 mm ID, 42.4 mm long horizontal stainless steel tube Heat flux: 10-100 kW/m <sup>2</sup> Pressure: 1 atmospheric Temperature condition: saturated	HTC of water/ethylene glycol at a given concentration ↑ with ↑ in heat flux.
Zhang et al. [25] (2007)	HC600a/HFC134a, HC600a/HC290, and HC600a/HFC23 (various mass fraction ratios from 0 to 1)	Heating surface: 25 mm diameter copper circular plate Heat flux: 10-300 kW/m <sup>2</sup> Pressure: 0.5 MPa Temperature condition: boiling range from 50 to 150 K	Reduction in HTC was found in mixtures compared with those of pure fluids. For a given mixture composition, HTC reduction was not uniform with heat flux variations. ↑ reductions occurred at ↑ heat fluxes.
Sathyabhama and Babu [12] (2011)	Ammonia water (0-30 wt.% NH <sub>3</sub> )	Heating surface: 6 mm diameter, 20 mm long cylindrical stainless steel rod Heat flux: 360-2000 kW/m <sup>2</sup> Pressure: 4-8 bar	HTC in the mixture ↑ with ↑ in heat flux
Wu et al. [57] (2012)	Pure tetrafluoromethane (FC14), methane (HC50) and their binary mixtures	Heating surface: 30 mm diameter copper circular plate Heat flux: 30-150 kW/m <sup>2</sup> Pressure: 0.3 MPa Temperature condition: boiling range from 80 to 300 K	HTCs of mixtures ↑ with ↑ in heat flux. The HTCs of mixtures were significantly lower than that of their pure components, and the reduction become ↑ with ↑ heat flux.
Sarafraz et al. [38] (2012)	Water/glycerol, water/MEG (Mono-ethylene glycol) and water/DEG (di-ethylene glycol) with volumetric concentrations of 1%-5% and 100 g of Ammonium nitrate, ammonium perborate and Ammonium sulfate were dissolved into mixtures as additives for endothermic chemical reactions	Heating surface: 21 mm diameter, 150 mm long cylindrical stainless steel rod Heat flux: < 90 kW/m <sup>2</sup> Temperature condition: Saturated	↑ of HTC with ↓ in concentration of the more volatile component was observed particularly at higher heat fluxes. HTCs of mixtures ↑ with ↑ in heat flux.
Gong et al. [16] (2013)	Ethane, isobutane and their binary mixtures (whole concentration range from 0 to 1)	Heating surface: 30 mm diameter copper circular plate Heat flux: 20-150 kW/m <sup>2</sup> Pressure: 0.3 MPa Temperature condition: boiling range from 0 to 50 K	↑ heat flux can obviously ↑ the bubble departure diameter and frequency for both pure refrigerants and mixtures.
Hamzekhani [11] (2014)	Ethanol/water (0, 1, 0.04-0.723 wt.% Ethanol), NaCl/water (50-300 kg/m <sup>3</sup> NaCl) and Na <sub>2</sub> SO <sub>4</sub> /water (50-300 kg/m <sup>3</sup> Na <sub>2</sub> SO <sub>4</sub> )	Heating surface: 20 mm diameter stainless steel rod Heat flux: 5-105 kW/m <sup>2</sup> Pressure: 1 atmospheric Temperature condition: saturated	Bubble diameter ↑ with ↑ heat flux. For pure fluids of water and ethanol, HTC ↑ with ↑ heat flux.
Dang et al. [13] (2018)	R134a/R245fa pure fluids and mixtures (10/90, 30/70, 50/50, 70/30 and 90/10 by wt%)	Heating surface: 10 mm×10 mm horizontal plain copper surface Heat flux: 1.2-360 kW/m <sup>2</sup> Temperature condition: same evaporating temperature of 26 °C	The boiling HTC of zeotropic mixtures, although ↑ with ↑ of heat flux, was degraded compared to the corresponding ideal HTCs, except for some specific cases with high heat flux.

**Table 5** The effect of pressure on pool boiling heat transfer performance of binary mixtures

Authors and Year	Fluids Compositions	Operating Conditions	Effects of Pressure on Pool Boiling Heat Transfer
Alpay and Balkan [6]	Acetone-ethanol and methylene chloride-ethanol	Heating surface: 4.8 mm diameter copper tube	HTCs of either the pure liquids or the binary



(1989)	(full concentration range covered from 0 to 1)	<i>Heat flux:</i> 10 to 40 kW/m <sup>2</sup> <i>Pressure:</i> 2.0-5.0 bar <i>Temperature condition:</i> saturated nucleate boiling	mixtures ↑ with ↑ pressure. Both heat flux and HTC showed a linear relationship in log-log coordinates. The slopes of the lines ↓ as pressure ↑.
Inoue et al. [41] (1998)	R12/R113, R134a/R113, R22/R113, R22/R11	<i>Heating surface:</i> platinum wire 2 (0.3 mm diameter, 8.8 cm long) <i>Heat flux:</i> up to critical heat flux (greater than 10 <sup>5</sup> W/m <sup>2</sup> ) <i>Pressure:</i> 0.25-0.7 MPa	The effect of pressure on HTC was not significant and smaller in the mixtures than in the single component substances.
Sathyabhama and Babu [12] (2011)	Ammonia water (0-30 wt.% NH <sub>3</sub> )	<i>Heating surface:</i> 6 mm diameter, 20 mm long cylindrical stainless steel rod <i>Heat flux:</i> 360-2000 kW/m <sup>2</sup> <i>Pressure:</i> 4-8 bar	HTC in the mixture ↑ with ↑ in system pressure.
Gong et al. [16] (2013)	Ethane, isobutane and their binary mixtures (whole concentration range from 0 to 1)	<i>Heating surface:</i> 30 mm diameter copper circular plate <i>Heat flux:</i> 20-150 kW/m <sup>2</sup> <i>Pressure:</i> 0.1-0.5 MPa <i>Temperature condition:</i> boiling range from 0 to 50 K	HTC ↑ with system saturation pressures for both ethane and isobutene pure fluids.
Nemade and Khandekar [58] (2013)	2.0%, 25.0% and 80.0% molar ethanol-water mixtures, and 100% pure forms of both the liquids	<i>Heating surface:</i> 30 mm diameter circular aluminium surface <i>Heat flux:</i> 10-150 kW/m <sup>2</sup> <i>Pressure:</i> 1 atmospheric <i>Temperature condition:</i> boiling range from 30 °C to 70 °C	significant ↓ in HTC for the mixture compared to pure water even for very low concentration of ethanol. This phenomenon was observed at all operating pressures. At higher concentrations, HTC first ↓ to a minimum, then a maximum, close to the azeotropic composition. The varying behaviour of HTC was intensified with ↑ in operating vapor pressure.

586  
587

**Table 6** The effect of surface condition on pool boiling heat transfer performance of binary mixtures

<b>Authors and Year</b>	<b>Fluids Compositions</b>	<b>Operating Conditions</b>	<b>Effects of Heater Surface Condition on Pool Boiling Heat Transfer</b>
Calus and Leonidopoulos [40] (1974)	Water/n-Propanol (11 n-Propanol concentrations from 9.0 wt.% to 93.0 wt. %)	<i>Heating surface:</i> Nickel/Aluminium alloy “wire 200” vs. Nickel/Aluminium alloy “wire 24” (0.03 cm diameter, 7.26 cm long) <i>Heat flux:</i> 1 and 4×10 <sup>5</sup> W/m <sup>2</sup> <i>Pressure:</i> 1 atmospheric	In pool boiling of binary mixtures, the “liquid-surface combination factor” is determined mainly by the nature and structure of the heat transfer surface. The contribution of the liquid to this factor is very small.
Bajorek and Lloyd [123] (1989)	Binary and ternary mixtures based on acetone, methanol, ethanol, ethyl acetate, 2-propanol, 2-butanone (entire mole fraction range covered from 0 to 1)	<i>Heating surface:</i> 22.2 mm diameter copper tube with a smooth surface rubbed with 400 grade emery paper for a finish similar to drawn tubing vs. 16 mm root diameter copper tube with 750 fin/m and fin diameter was 19.07 mm. <i>Heat flux:</i> 10-300 kW/m <sup>2</sup> <i>Pressure:</i> 1 atmospheric <i>Temperature condition:</i> Saturated	The multicomponent HTCs were found to be significantly lower than those estimated by a linear combination of the HTCs in the pure components. Significant degradation in HTCs was also found to occur on the finned tube.

Benjamin and Balakrishnan [26] (1997)	Distilled water, carbon tetrachloride, n-hexane, and acetone	<i>Heating surface:</i> 25 mm diameter circular aluminium and stainless steel surfaces, copper surface RA of 0.52, 0.89, 1.17 $\mu\text{m}$ , stainless steel surface RA of 0.2 $\mu\text{m}$ . <i>Heat flux:</i> up to 100 $\text{kW}/\text{m}^2$ <i>Pressure:</i> 1 atmospheric <i>Temperature condition:</i> Saturated	Average surface roughness (RA) was first time defined. The nucleation site density depended on the surface micro-roughness. A dimensionless surface roughness parameter has been proposed in a new nucleation site density correlation.
Nemade and Khandekar [58] (2013)	2.0%, 25.0% and 80.0% molar ethanol-water mixtures, and 100% pure forms of both the liquids	<i>Heating surface:</i> 30 mm diameter circular aluminium surface, average surface roughness number (RA) 0.8 $\mu\text{m}$ vs. 20 $\mu\text{m}$ <i>Heat flux:</i> 10-150 $\text{kW}/\text{m}^2$ <i>Pressure:</i> 1 atmospheric <i>Temperature condition:</i> boiling range from 30 $^{\circ}\text{C}$ to 70 $^{\circ}\text{C}$	HTCs $\uparrow$ with $\uparrow$ in average surface roughness number
Sahu et al. [35] (2015)	Ethanol, water and their mixtures (volumetric ratios 3:1, 1:3, 1:1)	<i>Heating surface:</i> circular copper plate (1.5 in $\times$ 0.315 in) with/without nanofiber mat, RA of bare copper plate was 5 $\mu\text{m}$ , nanofiber diameter in the range of 100-200 nm, thickness 5-10 $\mu\text{m}$ . <i>Heat flux:</i> < 25 $\text{W}/\text{cm}^2$ <i>Temperature condition:</i> saturated	The pool boiling data on the nano-textured surfaces did not follow the standard boiling curve and showed a sharp deviation. In particular, the heat flux and accordingly, the HTC on nanostructured surfaces were found to be significantly higher at low surface superheats.

588

589 Agreed across the boiling research community, experimental uncertainties have been a long-  
590 existed and thorny issue for boiling experiments not only for pure fluids but also for binary  
591 mixtures due to their complexities and thereby difficulties of setting up optimum experimental  
592 measurements as well as quantifying the corresponding measurement errors. As a result, most  
593 of the data have been obtained from different experimental systems and methods with various  
594 measurement errors. In pool boiling experiments, there are three major measurements, heater  
595 surface and bulk fluid temperatures, supplied heat flux that essentially affect the uncertainties  
596 of experimental results such as the boiling curves. Considering the chaotic nature of boiling  
597 phenomena and not to interfere bubble dynamics on heater surfaces, most of heater surface  
598 temperatures in pool boiling experiments have been estimated by indirect measurements such  
599 as infrared (IR) camera [127, 128] and inserting thermocouples a few distances apart from the  
600 heater surfaces [13, 37, 38, 58]. In addition, those indirect temperature measuring methods  
601 have their own intrinsic problems that may cause more inaccurate results later on. For example,  
602 it is difficult to select a proper emissivity setting for IR camera to illustrate accurate heater  
603 surface temperature while avoiding all sorts of environmental interferences either from the  
604 fluids or the experimental apparatuses. The temperature readings obtained from the  
605 thermocouples below heater surfaces are not the actual surface temperatures though the final

606 surface temperatures will be approximated accordingly based on the temperature reading, heat  
607 flux and thermal conductance resistance between the thermocouples and the heater surface.  
608 Also, in this way, more uncertainty parameters are introduced into the overall uncertainty  
609 equation of the measured heater surface temperature. Thus, extreme cautions have to be taken  
610 analysing experimental uncertainties when indirect surface temperature measurements are  
611 employed in pool boiling experiments. With the further development of manufacturing  
612 technology, one feasible solution to improve the accuracies of heater surface temperature  
613 measurements is to measure temperature directly on the surface, for example, by manufacturing  
614 surface mounted thin film thermocouples [129, 130]. In pool boiling experiments, heat is  
615 usually supplied to horizontal heater surfaces via a metal block and embedded electrical heaters  
616 while via direct voltage-current electrical heating to wire heaters. Regardless horizontal flat or  
617 wire heaters, one of the priorities is to minimize heat losses and properly account for the amount  
618 of heat losses in corresponding heat transfer calculations. For example, air/Teflon insulation  
619 layers and vacuum chambers have been employed to reduce heat losses and facilitate oriented  
620 heat transfer in pool boiling experiments [13, 16, 26, 48, 57, 58]. Heat flux calibration  
621 experiments or heat loss estimations have been carried out for both horizontal and wire heaters,  
622 whose results were applied in heat transfer calculations to account for the heat losses during  
623 pool boiling experiments [11, 20, 23]. On the other hand, measuring bulk fluid temperature  
624 during pool boiling experiments is relatively straightforward. The bulk fluid temperature can  
625 be obtained by immersing thermocouples into the bulk fluid but their interferences on pool  
626 boiling heat transfer should be deliberately minimized. In particular for pool boiling of binary  
627 mixtures, multiple immersion thermocouples have to be used to monitor the bulk fluid  
628 temperature of the mixture considering local saturation temperature varies and is a function of  
629 local concentration of the more volatile mixture component [13, 20, 57, 122, 124].

630

### 631 **3 Flow boiling heat transfer in binary mixtures**

632

633 Comparing to pool boiling, flow boiling has superior advantages in heat transfer performance  
634 due to its convective cooling nature and has been widely and irreplaceably used in fields related  
635 to high power densities. However, one of the main challenging issues of flow boiling is its high  
636 complexity due to the varying properties of heat transfer media (e.g. transient axial quality).  
637 The complexity gets furthered for flow boiling of binary mixtures due to complicating  
638 interactions among multiple components in the mixture and close coupling between heat and  
639 mass transfer at vapor/liquid interfaces [60]. Wang and Chato [61] completed a good summary

640 indicating that there were still issues to be further investigated in flow boiling of binary  
641 mixtures, such as: (1) the degradation of HTC with flow boiling of binary mixtures; (2) the  
642 suppression of nucleate boiling with mixtures compared to their pure components; (3) the  
643 influence of Prandtl number on both mixtures and their pure components; (4) the effects of heat  
644 flux, mass flux, quality and pressure on flow boiling with mixtures; (5) the similarity of  
645 circumferential boiling behavior between mixtures and pure components. In terms of HTC in  
646 flow boiling of binary mixtures, researchers have suggested mass flux as an essential factor  
647 affecting the HTC. Studies also showed that departed vapour bubbles were affected by  
648 interfacial mass transfer resistance. Reattachment has been observed at a condition of high  
649 Reynolds number, which is believed to benefit heat transfer rate since bubbles would again  
650 contact with the heated surface and continue to grow. Similar to pool boiling, CHF is a very  
651 important factor in the study of flow boiling, which generally occurs after the formation of a  
652 thin liquid film and the appearance of dry patches. The authors think fully understanding the  
653 physics of dry-patch is the key to explain the CHF phenomena in flow boiling of binary  
654 mixtures.

655

### 656 *3.1 Major heat transfer mechanisms in flow boiling of binary mixtures*

657

658 Flow boiling of binary mixtures mainly involves two main schemes, nucleate boiling and  
659 convective boiling so that mastering the balance between them is the key to comprehensively  
660 characterize flow boiling of binary mixtures. Under most of the experimental conditions in  
661 Kærn et al.'s study [52], it was shown that nucleate boiling had little effect on the overall flow  
662 boiling. But the contribution of nucleate boiling became considerable for ammonia/water  
663 mixtures at low mass fluxes, low vapor qualities and high heat fluxes. He et al. [63] indicated  
664 that there must be a maximum HTC value considering the coupled effects of forced convection  
665 and nucleate boiling when heat flux remained as constant. Furthermore, Kandlikar and Bulut  
666 [62] implied that the convection in flow boiling can be approximated through well-established  
667 pure component correlations substituting with mixture properties because of the comparability  
668 between the two mechanisms. However, it needs to be noted that the nucleate boiling part of  
669 flow boiling is mainly governed by the nucleation and growth of bubbles in the binary mixtures.  
670 The suppression in nucleate boiling in binary mixtures is caused by the heat transfer resistance  
671 (i.e. mass transfer resistance) introduced by the component concentration difference in liquid  
672 and vapor phase depending on the vapour-liquid equilibrium curves (dew point and bubble  
673 point) for binary mixtures. Moreover, Wettermann and Steiner [64] measured the HTC in

674 horizontal tube with a binary mixture of  $C_2F_6/C_2H_2F_4$  and ternary mixture of  $C_2F_6/SF_6/C_2H_2F_4$ .  
675 It was shown that the experimental results could be best predicted by determining the mixture  
676 properties using a pure component correlation within the forced convective region, whereas in  
677 the nucleate flow boiling region, a HTC degradation existed and had to be predicted with an  
678 ideal mass transfer-based HTC model.

679

680 According to the work of Kandlikar et al. [65], flow boiling for binary mixtures could be  
681 divided into three regions, near-azeotropic region, moderate diffusion-induced suppression  
682 region and severe diffusion-induced suppression region. The severe diffusion-induced region  
683 was dominated by convective effects. The nucleate boiling contribution in this region should  
684 be further reduced due to the large difference in compositions between liquid and vapor phases,  
685 and the resulted high mass diffusion resistance at the liquid-vapour interface of a growing  
686 bubble. Li et al. [66] investigated the flow boiling heat transfer performance of refrigerant  
687 mixtures of HFO-1234yf and R32 in a smooth horizontal tube with an inner diameter of 2 mm.  
688 For refrigerant mixture of HFO-1234yf and R32 (80/20 by mass %), the nucleate boiling heat  
689 transfer was noticeably suppressed at low vapour quality for small boiling numbers, whereas  
690 the forced convective heat transfer was remarkably restrained at high vapour quality for large  
691 boiling numbers. Boiling number is a dimensionless group representing a ratio between the  
692 mass of vapour generated at the heat transfer surface and mass flow rate per flow cross sectional  
693 area. In a following study, Li et al. [67] specified that mass diffusion resistance and temperature  
694 gradient within the binary mixture were among the most dominant factors for its flow boiling  
695 heat transfer performance. In addition, Azzolin et al. [68] evaluated the heat transfer  
696 performance of non-azeotropic binary and ternary low-GWP (global warming potential)  
697 mixtures. The tested mixtures were R455A, a ternary blend of R32, R1234yf and  $CO_2$   
698 (21.5/75.5/3.0 by mass composition percentage) and a blend of R32 and R1234ze (E) at 50/50  
699 by mass composition. Although the HTC increased with the applied heat flux for both mixtures,  
700 at a certain heat flux, R455A displayed lower HTCs compared to that of R32/R1234ze (E). The  
701 main reason was attributed to the different scenarios of composition and temperature gradient  
702 in R455A and the mixture of R32 and R1234ze (E) during flow boiling. Accordingly, it was  
703 mentioned in their study that a smaller temperature gradient was associated with a lower mass  
704 transfer resistance during flow boiling of the mixtures. Therefore, similar to pool boiling of  
705 binary mixtures, lower mass transfer resistance is still favored in flow boiling of binary  
706 mixtures for better heat transfer performance.

707

### 708 3.1.1 Nucleate boiling heat transfer in flow boiling of binary mixtures

709

710 Bertsch et al. [69] investigated flow boiling heat transfer with refrigerants R-134a and R-245a  
711 in cold plate evaporators with copper microchannels. Their results showed that nucleate boiling  
712 dominated the heat transfer of flow boiling. In addition, it was observed that heat flux and vapor  
713 quality significantly affected the HTC but the effects of saturation pressure and mass flux were  
714 limited. In the study of Yu et al. [70], it was found that the nucleate-boiling HTC, up to the  
715 transition-boiling region, was a function of heat flux but not a function of mass flux or inlet  
716 subcooling. Similar to Bertsch's study, the nucleate heat transfer mechanism dominated over  
717 flow convection for a large mass flux and inlet subcooling range. Moreover, the study of Kim  
718 et al. [71] pointed out that dry patch formation and rewetting momentum would be good aspects  
719 to explore for the CHF mechanisms departing from nucleate boiling. From their visualization  
720 study, it was revealed that elongated massive bubble was a key factor in the dry patch growth.  
721 The appearance of an irreversible dry patch was observed after several successive reversible  
722 dry patches as heat flux increased. Additionally, Peng et al. [72] experimentally examined  
723 subcooled flow boiling heat transfer characteristics of binary mixtures in microchannel plates.  
724 It was proposed that there existed an optimum concentration that could lead to a maximum  
725 HTC. The HTC at the onset of flow boiling and in the partial nucleate boiling region were  
726 substantially affected by liquid concentration, microchannel and plate configuration, flow  
727 velocity and the amount of subcooling. However, these factors had little effects on the HTC in  
728 fully nucleate boiling regime.

729

730 For the practical applications of binary mixture flow boiling, Kondou et al. [73] concluded  
731 from several previous flow boiling studies that the use of zeotropic mixtures was able to  
732 minimize energy losses in heat exchangers. Bamorovat Abadi et al. [74] proposed that  
733 incorporating with organic Rankine cycles could make the temperature gradient of zeotropic  
734 mixtures become an advantage in heat transfer systems. It was believed that those organic  
735 mixtures associated with attenuated temperature fluctuations, featuring a more stable heat  
736 transfer process and less possibility to wall dry-out. Vasileiadou et al. [75] investigated the  
737 two-phase flow heat transfer for ethanol/water mixture. It was shown that the heat transfer  
738 performance was improved by adding small amount of ethanol into water (5% v/v  
739 ethanol/water mixture), as shown in Fig. 4. It was also suggested the ethanol/water mixture,  
740 which had less wall temperature fluctuations, could prevent the wall dry-out and a potential  
741 critical failure in cooling system.

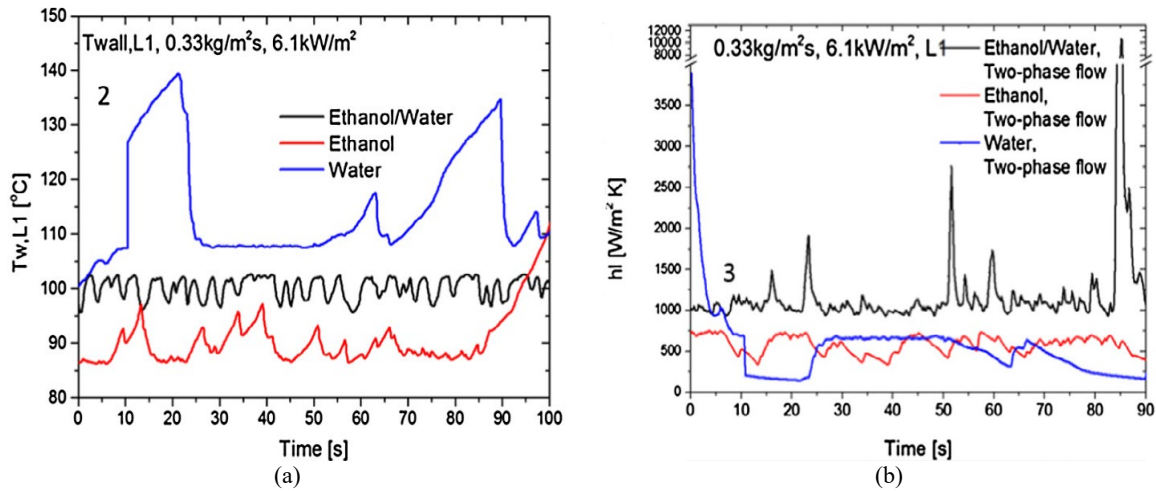


Fig. 4 (a) Channel wall temperature fluctuation and (b) Local heat transfer coefficient over time of 5% v/v ethanol/water mixture, water and ethanol ( $G = 0.33 \text{ kg/m}^2 \cdot \text{s}$ ,  $q'' = 2.8 \text{ kW/m}^2$ ) [75]

### 3.1.2 Convective heat transfer in flow boiling of binary mixtures

As discussed earlier, flow boiling of binary mixtures is similar with that of pure fluids, which is all about nucleate boiling, convective boiling and balance between nucleation and convection. But the effects of component type and concentration, surface tension and mass transfer resistance have to be figured out for tackling the further improvement of binary mixture flow boiling performance. Suhas and Sathyabhama [76] indicated that in convective heat transfer of flow boiling, a concentration gradient layer would appear not only at the surface of a bubble but also at the liquid–vapour interface at the bottom wall. Because the less volatile component in the bulk flow had to go through the diffusion layer before getting to the interface for evaporation, the HTC of mixtures could be inhibited by the mass diffusion during a subcooled flow boiling process. Thus, for the convective heat transfer part of flow boiling in a binary mixture, it can be seen that the mass transfer resistance inside the diffusion layer has a remarkable influence on the overall HTC [77]. Moreover, Sarafraz and Hormozi [60] pointed out that for the forced convective region, with an increase of heat flux, a slight increase in HTC could be observed, while in the nucleate boiling region, HTC increased significantly. The slight increase of HTC was attributed to the bubble formation and the turbulence introduced by bubble interactions. It was also noticed in their study that with an increase of fluid flow rate, the flow boiling HTC increased dramatically in both convective and nucleate boiling regions. The reason might be that the elevating flow rate could lead to not only stronger convection but also faster removal of bubbles. Furthermore, Yu et al. [70] studied the forced convective boiling heat transfer of distilled water and ethylene glycol/water mixtures in both horizontal and

768 vertical flow. It was indicated that in the convection-dominant boiling region, heat flux was  
769 relatively independent of wall superheat and flow pattern was more like a single-phase rather  
770 than two-phase flow. In addition, Kim et al. [80] experimentally investigated the effect of oil  
771 on convective boiling of R-123 in an enhanced tube bundle at saturation temperature. It was  
772 noticed that the oil-rich layer near heating surface significantly reduced the boiling HTC, but  
773 two-phase convection in the bundle was believed to be able to remove or at least reduce the  
774 thermal degradation caused by oil.

775

### 776 *3.2 Effects of Reynolds number and flow regimes on flow boiling of binary mixtures*

777

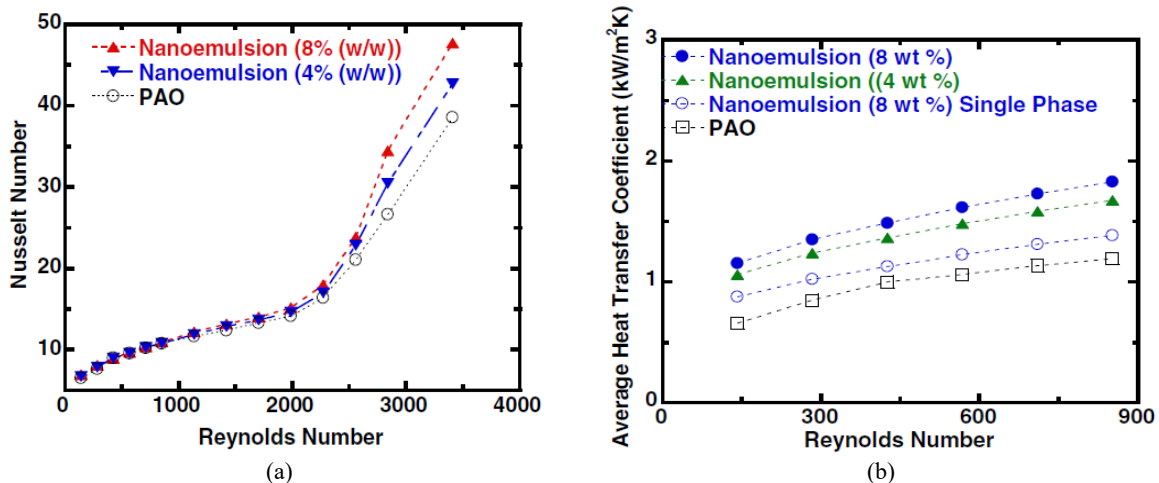
778 As it can be deduced, both pool boiling and flow boiling of binary mixtures start from  
779 nucleation and nucleate boiling while the effects of flowing related features such as Reynolds  
780 number and flow regime differentiate binary mixture flow boiling from pool boiling. For  
781 example, Yuan et al. [81] carried out a visualization study to investigate the bubble behaviour  
782 including growth, sliding and coalescence of subcooled flow boiling in a narrow channel. It  
783 was found that the sliding process of bubbles was more likely to enhance heat transfer than that  
784 of stationary bubbles in pool boiling process. The experimental study of Sinha et al. [82]  
785 revealed that, at a high Reynolds number ( $\sim 7200$ ), vapor bubbles reattached back to a heated  
786 surface after lift-off. The reattachment led to a further growth of the bubble by absorbing  
787 additional heats from the heated wall. At low Reynolds number ( $\sim 3600$ ), bubbles tended to  
788 collapse in the bulk flow after lift-off due to the dominant forces on the bubble normal to the  
789 heated surface and the effect of condensing when vapor bubbles entering the subcooled bulk  
790 flow. Therefore, it can be seen that the fact of getting the fluid to flow could positively affect  
791 bubble dynamics and so overall boiling heat transfer performance.

792

793 Furthermore, Sun et al. [83] conducted an experimental investigation on the flow boiling of  
794 refrigerants R134A and R410A inside a smooth tube and two newly developed surface-  
795 enhanced tubes. Improved heat transfer performance was observed in the enhanced tubes and  
796 the HTC was about 1.15-1.66 times of that in the smooth tubes. It was argued that the modified  
797 surface structure was beneficial in enhancing turbulence mixing (effective Reynolds number),  
798 increasing active heat transfer area and providing more nucleate sites. Trinh and Xu [85]  
799 specified in their experimental study of ethanol/polyalphaolefin nano-emulsion flowing  
800 through circular mini-channels that the ethanol nano-droplets formed through the nano-  
801 emulsion process could significantly enhance the HTC compared to the base fluid. It was



802 suggested that the phase change process of ethanol nano-droplets under flow boiling condition  
 803 absorbed a relatively large amount of latent heat, which could be one of the reasons for the heat  
 804 transfer enhancement. Another possible reason could be the sufficient mixing and mass  
 805 transport at transitional and turbulent flow regimes, which resulted in improved heat transfer  
 806 between surfactant molecules and the base fluid. Fig. 5 (a) compared the measured average  
 807 Nusselt number for nano-emulsion fluids and the base fluid over the experimental Reynolds  
 808 number range in single phase heat transfer. It can be observed that the effect of nano-emulsion  
 809 on convective heat transfer was little in laminar flow but significant in transitional and the early  
 810 stage of turbulent flow. The average HTC was calculated and plotted as a function of Reynolds  
 811 number for flow boiling of nano-emulsion fluids, as shown in Fig. 5 (b). It can be observed that  
 812 the ethanol/PAO nano-emulsion fluids had slightly higher HTCs compared to pure PAO in  
 813 single phase flow while the HTCs got considerably enhanced as the fluid underwent convective  
 814 boiling. Kim and Mudawar [88] developed a theoretical model for boiling heat transfer based  
 815 on the assumptions of smooth interface between the annular liquid film and vapour core, and  
 816 uniform film thickness around the channel's circumference. The model took into account the  
 817 interfacial suppression of turbulent eddies due to surface tension. The results showed that the  
 818 transition from laminar to turbulent film flow might occur at small film Reynolds numbers for  
 819 shear-driven films. It was also pointed out that turbulent effects should be considered when  
 820 modelling the transport behaviour of annular film. As shown in Fig. 6 (a) and (b), the annular  
 821 model with turbulent liquid film showed higher HTC values than that with the laminar liquid  
 822 film for water and R32, respectively.



823  
 824 **Fig. 5** (a) Average Nusselt number versus Reynolds number (single phase flow, nano-emulsion and pure PAO), (b) Average  
 825 heat transfer coefficient with/without phase change versus Reynolds number in laminar flow region [85]  
 826

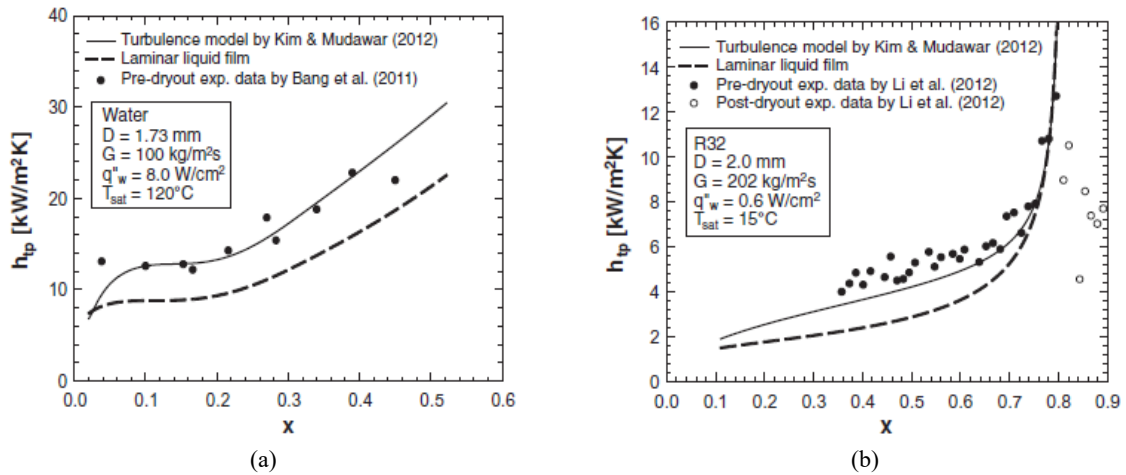


Fig. 6 Local two-phase heat transfer coefficient conditions of (a) water flow with  $D = 1.73$  mm,  $G = 100$  kg/m<sup>2</sup>·s,  $q_w'' = 8.0$  W/cm<sup>2</sup> and  $T_{sat} = 120$  °C, (b) R32 flow with  $D = 2.0$  mm,  $G = 202$  kg/m<sup>2</sup>·s,  $q_w'' = 0.6$  W/cm<sup>2</sup> and  $T_{sat} = 15$  °C [88]

827  
828  
829  
830

831 In general, Kandlikar and Balasubramanian [84] summarized and plotted the information of  
832 typical Reynolds number and system dimension being studied across the flow boiling  
833 community in Fig. 7. The figure shows that the studied Reynolds number fell into the laminar  
834 flow region as the relevant hydraulic diameter became smaller. It can also be seen from Fig. 7  
835 that for hydraulic diameters & below 1 mm, the flow boiling was mostly in the laminar region  
836 while turbulent region started to get involved beyond 1mm tube diameter. One of the main  
837 reasons, in the opinion of the authors of this review, should be the tremendously raised flow  
838 resistance for the experimental configurations with hydraulic diameter below 1 mm.

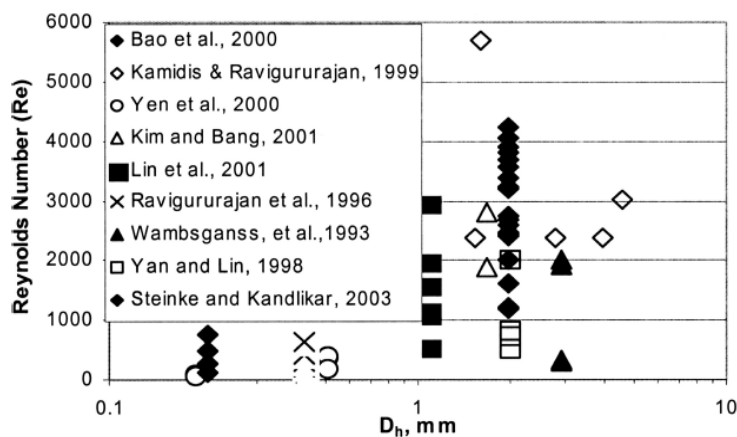
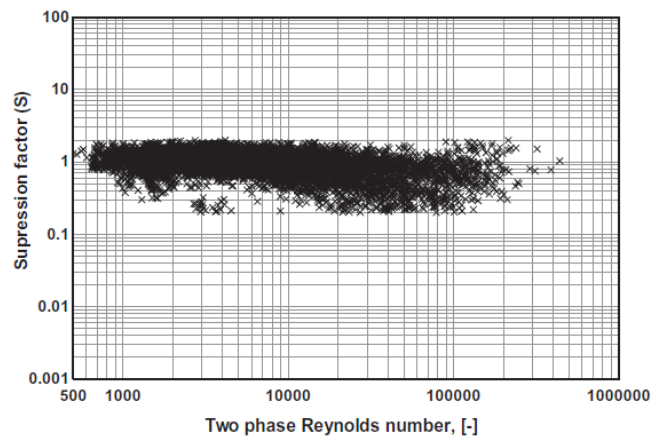


Fig. 7 Ranges of Reynolds Number employed in various experimental investigations on flow boiling [84]

839  
840  
841

842 Moreover, Mahmoud and Karayiannis [86] assessed the existing macro and microscale heat  
843 transfer models and correlations for flow boiling in small tubes. A new HTC correlation for  
844 flow boiling heat transfer in small tubes was developed based on the superposition model from  
845 Chen et al. [78] (Eq. 24) for better predictions of existing experimental results. Accordingly, a  
846 modified suppression factor  $S$ , which accounts for the effects of mixture microscopic heat

847 transfer on overall flow boiling heat transfer, was featured in the new correlation. The newly  
848 proposed suppression factor was defined as a function of two phase Reynolds number. Almost  
849 all the data in Mahmoud and Karayiannis's data bank was correlated using the new HTC  
850 correlation and the corresponding experimental suppression factor for each experimental case  
851 was calculated. Fig. 8 shows the calculated experimental suppression factors for HTC  
852 correlations of flow boiling in small tubes versus the two-phase Reynolds number. It was  
853 indicated that, in general, the coefficient for microscopic heat transfer (i.e. suppression factor)  
854 gradually decreased as the two phase Reynolds number increased. This makes sense since that  
855 macroscopic heat transfer would dominate over microscopic heat transfer at certain two phase  
856 Reynolds number and continue to dominate more at higher two phase Reynolds numbers. It is  
857 also worth noting that the coefficient of microscopic heat transfer approximately approached  
858 to unity one at extremely low two phase Reynolds numbers, as shown in Fig. 8. In Chen et al.'s  
859 correlation [78] (Eq. 24), macroscopic heat transfer is associated with the bulk movement of  
860 the vapor and liquid, whereas microscopic heat transfer is associated with the turbulence  
861 induced by the conception, growth and departure of vapor bubbles.  
862



863  
864  
865  
866

Fig. 8 Experimental suppression factor versus two-phase Reynolds number for flow boiling in small to micro tubes [86]

867 In addition, as bulk flow Reynolds number, channel hydraulic diameter and heat flux were  
868 considered to be the determining factors for flow boiling in laminar flow to turbulent transition,  
869 Kandlikar and Steinke [87] constructed a flow boiling correlation map based on the available  
870 literature, as shown in Fig. 9, presenting the respective hydraulic diameter and corresponding  
871 Reynolds number used among different flow boiling correlations in the literature.  
872

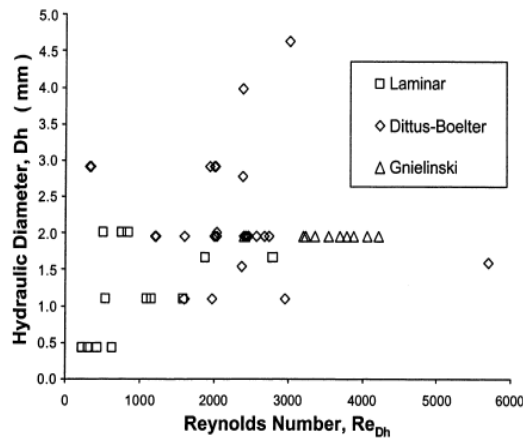


Fig. 9 Flow boiling correlation map [87]

873  
874  
875

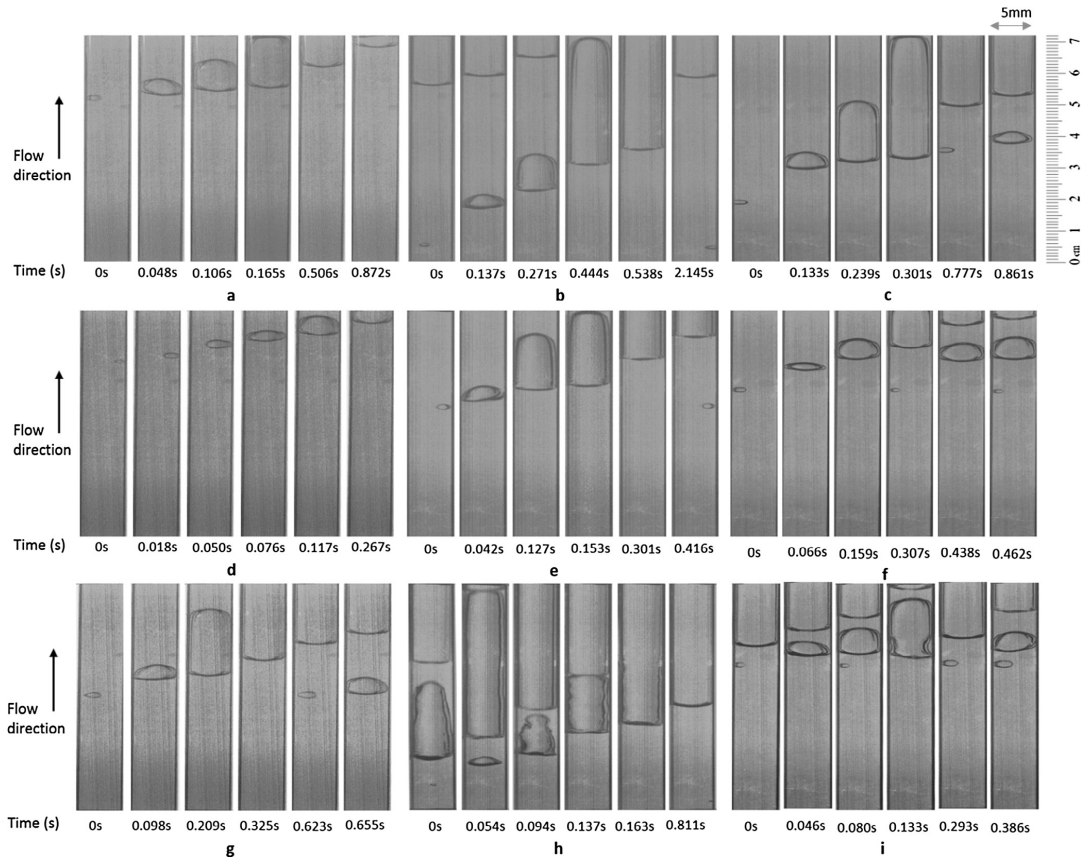
### 876 3.3 The effect of flow orientation in flow boiling of binary mixtures

877

878 As it is known, flow boiling of binary mixtures should be governed by energy and momentum  
879 equations. Therefore, the effect of flow orientation has to be considered because it affects the  
880 force terms in the momentum equation such as gravity and buoyancy.

881

882 For vertical flow, Abadi et al. [74] visualized the flow boiling of a mixture of R134a and R25fa  
883 in a circular glass vertical tube with 3 mm in inner diameter and 200 mm in length. The mass  
884 flux and heat flux in the experiment were set in wide ranges of 300-800 kg/m<sup>2</sup>-s and 1-69  
885 kW/m<sup>2</sup>, respectively. Different flow regimes were visibly investigated such as bubbly flow,  
886 slug flow, and annular flow. It was discovered that the throat-annular flow appeared in limited  
887 cases but not in all mixtures. Furthermore, Vasileiadou et al. [75] conducted an experimental  
888 study on the flow boiling heat transfer of ethanol/water binary mixture in a vertical oriented  
889 square channel. Although the flow characteristics varied under different operating conditions,  
890 the main flow pattern was recorded, as shown in Fig. 10. It was found that small bubbles tended  
891 to grow rapidly into slug/annular flow and the fast expansion of bubbles would instantly block  
892 the channel which might result in an increase of pressure drop and then prevent a refilling of  
893 the liquids. It was claimed that the heat transfer mechanism of two-phase flow was based on  
894 repeatable cycles of bubble recoil, dewetting, rewetting and ebullition. It was also discovered  
895 through Fig. 11 that increased mass flux could delay the start of nucleate boiling as enhanced  
896 convective heat transfer would diminish wall superheat. On the other hand, it can be observed  
897 that increased heat flux promoted the onset of nucleation by activating more nucleation sites  
898 due to a lifted wall superheat.



899  
900  
901  
902  
903  
904

**Fig. 10** Flow regimes of flow boiling at  $G = 0.33 \text{ kg/m}^2\text{-s}$  and  $q=4.2 \text{ kW/m}^2$  for (a) water, (b) ethanol and (c) 5% v/v ethanol/water mixture and at  $G = 0.66 \text{ kg/m}^2\text{-s}$  and  $q=4.2 \text{ kW/m}^2$  for (d) water, (e) ethanol and (f) 5% v/v ethanol/water mixture, and at  $G = 0.66 \text{ kg/m}^2\text{-s}$  and  $6.1 \text{ kW/m}^2$  for (g) water, (h) ethanol and (i) 5% v/v ethanol/water mixture [75]

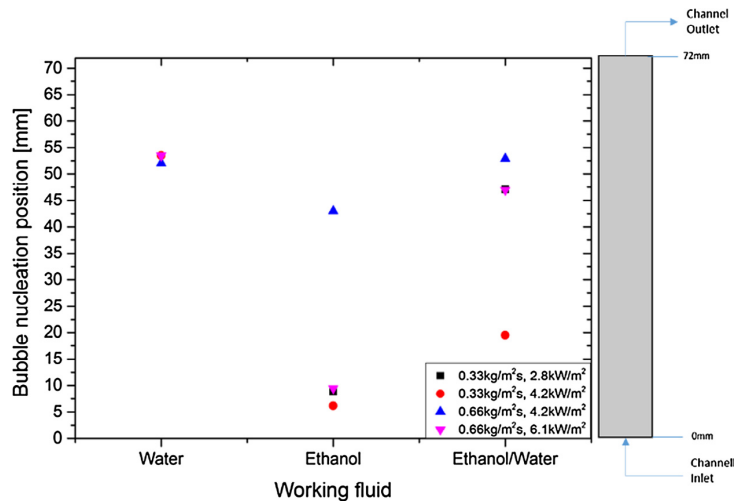
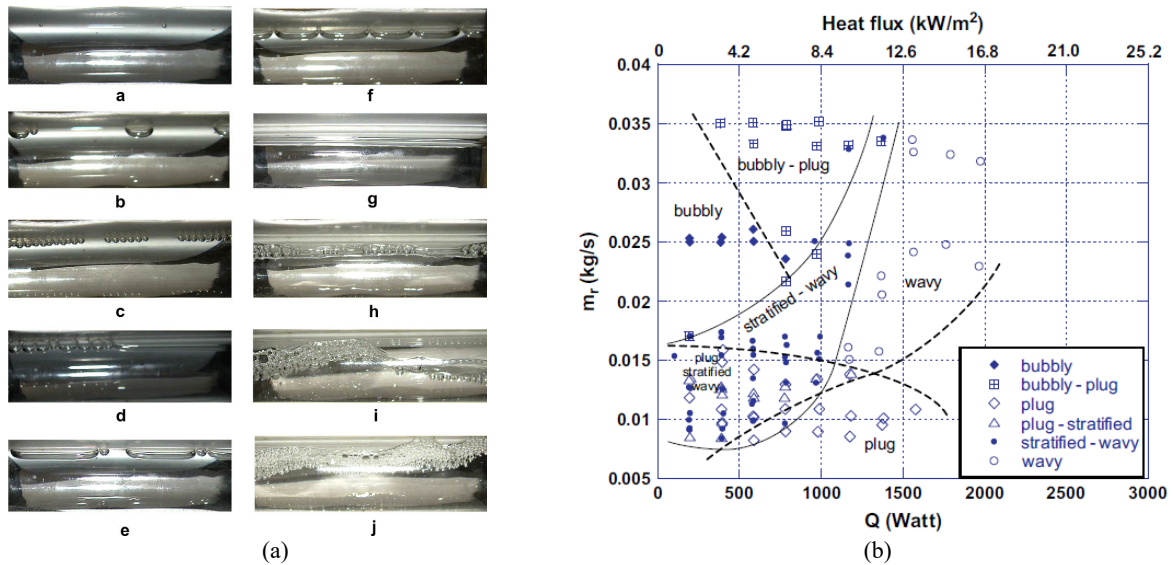


**Fig. 11** Nucleation onset positions at different mass and heat fluxes [75]

905  
906  
907  
908

909 For horizontal flow, Orian et al. [91] experimentally tested the flow boiling of a binary organic  
910 mixture of miscible fluids chlorodifluoromethane (R22)–dimethylacetamide (DMAC) in a  
911 horizontal tube. As shown in Fig. 12 (a), different flow patterns such as bubbly, plug, stratified,  
912 stratified-wavy and wavy flows were visibly captured in the test tube. A flow pattern map was

913 generated based on their experimental data which would allow the prediction of flow pattern  
 914 for a specific working fluid under a certain operating condition, as shown in Fig. 12 (b). The  
 915 boundaries between two different flow patterns were difficult to be identified since mixed flow  
 916 patterns could exist under certain conditions. It was asserted that with knowing the heat input  
 917 and the inlet flow conditions, namely, the nominal volumetric flow rate and weight fraction,  
 918 the refrigerant mass flow rate could be calculated and the flow pattern could be predicted by  
 919 this map.



920  
 921 **Fig. 12** (a) Flow patterns that were observed during flow boiling experiment in a binary mixture: a–c: bubbly, d: bubbly-  
 922 plug, e–f: plug, g: stratified, h: stratified-wavy, i: wavy, j: wavy-slug (b) Flow pattern map [91]  
 923

924 Moreover, Guo et al. [89] experimentally explored flow boiling using ORC related working  
 925 fluid such as R134a/R245fa with 0.82/0.18 (mass fraction) in smooth horizontal tube. The flow  
 926 boiling HTC and pressure drop were measured under different testing conditions. It was shown  
 927 that the HTCs increased with the increase of mass flux, heat flux and evaporating pressure.  
 928 Especially, lower pressure drops and higher HTCs were obtained for the mixture of  
 929 R134a/R245fa with 0.82/0.18 than that of its pure fluid. Grauso et al. [90] carried out an  
 930 experimental study on the flow boiling of CO<sub>2</sub> and propane mixtures (with 83.2/16.8 % and  
 931 70.0/30.0 % in mass concentrations) in a smooth horizontal tube with a 6 mm internal diameter.  
 932 The HTCs obtained in their study were remarkably degraded compared with the ideal HTCs.  
 933 In addition, it was indicated that the HTCs were dominantly controlled by heat flux and slightly  
 934 affected by mass flux and working temperature. He et al. [64] looked into the flow boiling heat  
 935 transfer performance of a near azeotropic refrigerant mixture R290/R32 inside different  
 936 horizontal tubes including 5 mm smooth and micro-fined tubes, 7 mm smooth and micro-fined  
 937 tubes and 9.52 mm micro-fined tube. The variations of flow boiling HTCs with different

938 evaporation temperatures and tube inner diameters were comprehensively studied. It was found  
939 that the heat transfer tubes with small diameter were able to reduce the required amount of  
940 refrigerant in the refrigeration system with flammable working fluids.

941

### 942 *3.4 The effects of fluid viscosity and pressure drop in flow boiling of binary mixtures*

943

#### 944 *3.4.1 Effect of viscosity*

945

946 To apply binary mixture as a flow boiling heat transfer fluid, both heat transfer performance  
947 and flow resistance have to be taken into consideration so do the mixture viscosity and pressure  
948 drop. According to our literature search, flow boiling of low viscosity fluid in heated tubes has  
949 been thoroughly investigated, but there was quite few research on highly viscous pseudo-plastic  
950 fluids, which are summarized and discussed below. Wienecke et al. [92] conducted  
951 experiments to examine the heat transfer process in a boiling system consisting of very high  
952 viscosity silicone oil in pentane solvent. Their experimental results were validated against  
953 established flow boiling HTC models. Results showed that the tested correlations had poor  
954 capabilities predicting the flow boiling HTCs for highly viscous fluids. Moreover, Hu et al.  
955 [93] stated that, under the actual conditions of a compression air-conditioning system, some  
956 quantity of oil would eventually circulate with the refrigerant and have a considerable impact  
957 on the refrigerant evaporation heat transfer, as oil would change the refrigerant thermal and  
958 transport properties such as density, viscosity and thermal conductivity. Furthermore, the  
959 higher viscosity oil was shown leading to more degree of heat transfer deterioration than the  
960 lower viscosity oil. Liu et al. [96] evaluated the heat transfer of a highly viscous pseudo-plastic  
961 liquid in a vertical tube under constant heat flux. A HTC correlation was established which  
962 took into account the effect of liquid viscosity on the heat transfer of flow boiling. The results  
963 revealed that the HTC of a highly viscous fluid was less than that of a low viscosity one. Liu  
964 et al. also visually characterized the flow patterns of highly viscous pseudo-plastic fluid under  
965 flow boiling in a vertical glass tube. A new type flow pattern of flash flow was observed, which  
966 appeared only in a highly viscous fluid. They pointed out that in the highly viscous fluid, it was  
967 easy to reach a high local liquid superheat and vapour bubbles were covered with heavy fluid.  
968 Bubbles rapidly expanded when superheat was beyond a certain point, then exploded, and the  
969 flash flow happened. Consequently, CHF could appear at low heat flux in a highly viscous  
970 fluid. The possible explanations would be: (1) liquid film was easily removed from the wall  
971 due to elevating local wall superheat, resulting in a local unstable film surface boiling, leading

972 to a poor heat transfer; (2) the evaporative component inhabited on a portion of the heating  
973 surface forming a vapour layer leading to heat transfer reduction.

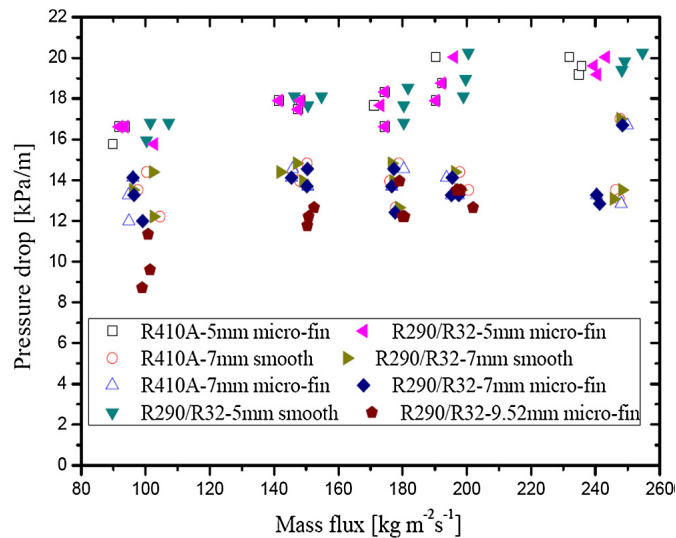
974

### 975 3.4.2 Effect of pressure drop

976

977 McAssey and Kandlikar et al. [94] carried out an investigation on the HTC under flow boiling  
978 conditions for mixtures of water with ethylene glycol and propylene glycol. A constant  
979 volumetric flow rate was set for all operating conditions. It was found that since most of the  
980 pressure drop occurred through a control valve, changes in pressure drop due to heating had a  
981 minor impact on the flow rate and heat transfer in the test section. Furthermore, He et al. [64]  
982 experimentally reported that the flow boiling pressure drop of R32/R290 mixture under typical  
983 working conditions was relatively moderate. The flow boiling pressure drops of R32/R290  
984 mixture were in the range of 16-20 kPa in small diameter tubes, which was similar to that of  
985 R410A. The experimental pressure drop results of R32/R290 mixture and R410A were shown  
986 in Fig. 13.

987



988  
989  
990  
991

**Fig. 13** Pressure drop results of R32/R290 mixture and R410A in the experiments conducted by He et al. [64]

992 In order to examine the connection between the effects of heat transfer and pressure drop in  
993 flow boiling, Vasileiadou et al. [75] explored the pressure drop for two-phase flow heat transfer  
994 with 5% v/v ethanol/water. The pressure drop was observed to fluctuate over time while boiling  
995 was prevalent in the flow, and the variations of pressure changed in magnitude and frequency  
996 for different fluids and operating conditions. During bubble nucleation and particularly when  
997 vapour expansion occurred, there was an increase in pressure drop in the channel. The



998 expansion of a bubble would make the liquid flow to be blocked leading to the highest pressure  
999 drop. Their results demonstrated two types of fluctuations in pressure drop: low amplitude,  
1000 high frequency and high amplitude, low frequency fluctuations. For cases of higher heat fluxes  
1001 and smaller mass fluxes, where boiling was more intensive and vapour expansion was more  
1002 rigorous, the second type of fluctuations was more prevailing. Due to the motions and collisions  
1003 of bubbles, the peaks in pressure drop were believed to be caused by the sudden expansion of  
1004 vapour while the smaller amplitude oscillations were postulated to be the result of bubble flows.  
1005 Therefore, for the optimisation of systems, the correct use of frictional pressure drop  
1006 correlations for zeotropic refrigerants under these operating conditions was essential. The  
1007 authors of this review also urge that same level of understandings about the pressure drop in  
1008 binary mixture flow boiling should be acknowledged as the heat transfer performance and  
1009 always consider heat transfer performance and pressure drop penalty at the same time when  
1010 dealing with flowing heat transfer fluid.

1011

1012 In addition, Barraza et al. [95] presented experimental results for the frictional pressure drop  
1013 along with its sensitivity for a number of zeotropic multi-component mixtures boiling in  
1014 smaller channels. The measured data was compared with several well-established pressure drop  
1015 correlations in the literature. It was shown that their experimental set-up was capable of  
1016 measuring the frictional pressure drop with an uncertainty of less than 20%. Liu and Garimella  
1017 [97] experimentally studied flow boiling of water, which is an extreme special case of binary  
1018 mixture in microchannels. The relevant microchannel dimensions were  $275 \times 636$  and  
1019  $406 \times 1063 \mu\text{m}^2$ . The experiments were conducted at inlet water temperatures in the range of  
1020  $67\text{-}95$  °C and mass fluxes of  $221\text{-}1283 \text{ kg/m}^2\text{-s}$ . The maximum heat flux investigated in the  
1021 tests was  $129 \text{ W/cm}^2$  and the maximum exit quality is 0.2. The measured pressure  
1022 drop was shown in Fig. 14 as the flow transiting from single-phase to two-phase flow across  
1023 the microchannel. The pressure drop was evaluated between the two manifolds upstream and  
1024 downstream and the inlet/exit losses were adjusted as well. As it can be observed from Fig. 14,  
1025 the pressure drop slightly decreased in the single-phase region as the heat flux increased due to  
1026 reduced viscosity of water at higher temperatures. It can also be seen that the pressure drop  
1027 increased dramatically after the onset of nucleate boiling when the accelerating effect  
1028 of vapour content was predominant.

1029

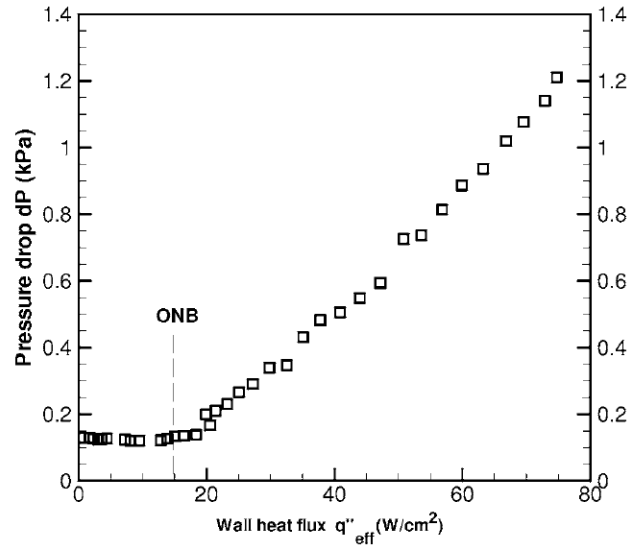


Fig. 14 Pressure drop during transition from single-phase to two-phase flow across the microchannel heat sink,  $G=324 \text{ kg/m}^2\cdot\text{s}$ ,  $T_{f,in}=66.6 \text{ }^\circ\text{C}$  [95]

1030  
1031  
1032  
1033

### 3.5 Correlations for flow boiling of binary mixtures

1034

1035  
1036 Comparing to the number of existed correlations for pool boiling, there are quite few well-  
1037 established correlations for flow boiling of binary mixtures in the literature, which were mostly  
1038 derived from the HTC correlations for the forced convective boiling of pure fluids. The first  
1039 common form of the correlations was based on Chen et al.'s correlation [78], shown as follows:

1040

$$h_{mix} = h_{mac} \cdot F_{mix} + h_{mic} \cdot S_{mix} \quad (24)$$

1041

1042 where  $h_{mac}$  is the macroscopic heat transfer associated with the bulk movement of vapor and  
1043 liquid,  $h_{mic}$  is the microscopic heat transfer associated with the turbulence induced by the  
1044 conception, growth and departure of vapor bubbles.  $F_{mix}$  and  $S_{mix}$  are the correction factors  
1045 for synchronizing two separate heat transfer mechanisms towards the overall flow boiling heat  
1046 transfer of fluid mixtures.

1047

1048 Another basic form of the correlations was originated from Mishra et al. [98], shown as follows:

1049

$$\frac{h}{h_L} = A \cdot \left(\frac{1}{X_{tt}}\right)^m \cdot Bo^n \quad (25)$$

1050

1051 where  $h_L$  is the non-boiling coefficient for total liquid flow calculated from the Dittus-Boelter  
1052 equation [99],  $X_{tt}$  is the Lockhart-Martinelli parameter [100] defined as

1053  $(\rho_V/\rho_L)^{0.5} \cdot (\mu_L/\mu_V)^{0.1} \cdot ((1-\chi)/\chi)^{0.9}$  which expresses the liquid fraction of a flowing fluid,  $A$ ,  $m$ ,  $n$   
1054 are empirical constants, respectively.

1055

1056 The available correlations for flow boiling of binary mixtures in the literature are summarized  
1057 in Table 3 followed by detailed experimental conditions for each study in Table 4. Bennett and  
1058 Chen [101] extended Chen et al.'s correlation [78] to binary mixtures. In their correlation, the  
1059  $h_{mic}$  (microscopic heat transfer associated with the turbulence induced by the conception,  
1060 growth and departure of vapor bubbles) was derived from an expression proposed by Forster  
1061 and Zuber [110] for pool boiling, which was modified by Bennett and Chen to address the  
1062 greater thermal gradient in the vapour generating region near the hot wall due to forced  
1063 convection. Accordingly, a suppression factor, as a function of the two-phase Reynolds  
1064 number, was defined for the  $h_{mic}$ . In addition, while the  $h_{mac}$  (macroscopic heat transfer  
1065 associated with the bulk movement of vapor and liquid) was originated from the Dittus-Boelter  
1066 correlation, which was the same as in Chen et al.'s correlation, Bennett and Chen further  
1067 established a new correction factor for  $h_{mac}$  to include the effect of mass transfer on the thermal  
1068 driving force. Mishra et al. [98] adapted equation (25) to R12/R22 mixtures and identified the  
1069 associated coefficient values (i.e.  $A$ ,  $m$ ,  $n$ ) for different mixture compositions. Later, Jung et  
1070 al. [103] experimentally investigated azeotropic (e.g. R12/R152a) and non-azeotropic (e.g.  
1071 R22/R114) refrigerant mixtures and generated correlations for flow boiling heat transfer with  
1072 refrigerant mixtures based on the supposition of Chen et al.'s correlation. Furthermore, the  
1073 correlation of Ünal [111] for nucleate boiling HTC was employed in Jung et al.'s correlations.  
1074 One advantageous feature of the correlation is that it could be applied to both pure/azeotropic  
1075 refrigerants and non-azeotropic refrigerants by applying the correct coefficient factors.

1076

1077 Starting 1990s, Granryd [105] theoretically achieved a correlation for convective boiling of  
1078 non-azeotropic mixtures based on two phase heat transfer in evaporation within an annular  
1079 flow under similar gas phase resistance assumptions with the studies of Silver [112] and Bell-  
1080 Ghaly [113]. Based on the correlations of Silver and Bell-Ghaly using the annular flow model,  
1081 Little [107] produced a HTC correlation for flow boiling of zeotropic mixtures in horizontal  
1082 tubes, in which a liquid film flew along the tube wall and vapour flew in the centre of the tube  
1083 surrounding by the liquid film. In addition, Rammohan et al. [102] constructed a HTC  
1084 correlation according to the flow boiling studies of subcooled glycerol/water and  
1085 isopropanol/water mixtures. An effective HTC was developed from the HTC of single phase

1086 flow taking into account the two phase interactions in a flowing mixture. Sivagnanam and  
1087 Varma [104] proposed a flow boiling HTC correlation regarding acetone/water,  
1088 isopropanol/water and butanol/water mixtures by modifying the correlation from Moles and  
1089 Shaw [109], given for subcooled boiling of pure liquids. Heat and mass transfer correction  
1090 factors were introduced to account for the concentration of the more volatile component of the  
1091 mixture. Wenzel and Steinhagen [106] modified Chen et al.'s correlation [78] by taking into  
1092 consideration the balance between enhanced convective cooling of the colder mixture  
1093 component due to increased subcooling and corresponding attenuated boiling of the more  
1094 volatile mixture component.

1095

1096 Recently, Li et al. [67] proposed a semi-empirical correlation for the flow boiling heat transfer  
1097 of HFO1234yf, HFC32, and their refrigerant mixtures. The correlation was also in the form of  
1098 Chen et al.'s correlation superposing the contributions from nucleate boiling ( $h_{mic}$ ) and  
1099 convection ( $h_{mac}$ ), as shown in Table 3. Besides, two new correction factors ( $F_{Li}$ ,  $S_{Li}$ ) were  
1100 introduced to Chen et al.'s correlation to account for the effects of convection on two-phase  
1101 flow and nucleate boiling. Moreover, Ardhapurkar et al. [108] adapted the correction factors  
1102 regarding the mixture effect to the calculation of two-phase HTCs for multi-component  
1103 mixtures of nitrogen–hydrocarbons. The performance of three modified correlations (i.e.  
1104 Gungor–Winterton correlation [115], Silver-Bell-Ghaly correlation [112, 113] and Granryd  
1105 correlation [105]) were modified and trained accordingly against their experimental data. The  
1106 results showed that the modified Silver-Bell-Ghaly correlation and modified Granryd  
1107 correlation were in good agreements with the experimental data and could be used in the future  
1108 to predict two-phase HTCs for multi-component mixtures of nitrogen–hydrocarbons. Dang et  
1109 al. [116] experimentally studied the flow boiling characteristics of R134a/R245fa zeotropic  
1110 mixtures in a single rectangular micro-channel. To take into account the Marangoni and  
1111 capillary effects, they extended the flow boiling HTC predicting correlation to micro-scale for  
1112 zeotropic mixtures based on their experimental results and a recent micro-scale correlation  
1113 proposed by Azzolin et al. [117], who discussed about how to extend a flow boiling correlation  
1114 developed for pure fluids to the case of zeotropic mixtures.

1115

1116 As it can be observed from Tables 7 and 8, regardless of the decent number of available  
1117 correlations to elucidate the flow boiling heat transfer of multicomponent mixtures, not any  
1118 two correlations were developed for the same mixture type and concentration and under the  
1119 same experimental conditions. And therefore, extreme cautions have to be taken (i.e. the details

1120 of working fluid and experimental conditions must be critically examined) before applying  
 1121 those heat transfer correlations in future related studies [67, 108, 131, 132]. More importantly,  
 1122 it is imperative to unify and generalize the knowledge of boiling heat transfer correlations, not  
 1123 only flow boiling but also pool boiling for multicomponent mixtures through a benchmark  
 1124 study which should be consented and carried out across the whole boiling community like what  
 1125 has been done in the nanofluid community [118].

1126  
 1127

**Table 7** Established correlations for flow boiling heat transfer coefficient of binary mixtures

Authors and Year	Flow Boiling HTC Correlations for Fluid Mixtures
Bennet and Chen [101] (1980)	$h_{\text{mix}} = h_{\text{mac}} \cdot F_{\text{mix}} + h_{\text{mic}} \cdot S_{\text{mix}}$ $F_{\text{mix}} = F \cdot f(\text{Pr}_L) \cdot \left[ \frac{\Delta T}{\Delta T_S} \right]_{\text{mac}}$ $f(\text{Pr}_L) = \left[ \frac{\text{Pr}_L + 1}{2} \right]^{0.444}$ $\left[ \frac{\Delta T}{\Delta T_S} \right]_{\text{mac}} = 1 - \frac{(1 - y_M) \cdot q}{\rho_L \cdot H_{\text{LG}} \cdot h_m \cdot \Delta T_S} \cdot \left. \frac{dT_S}{dx_M} \right _{P_{\text{bulk}}}$ $h_m = 0.023 \cdot \frac{D}{D_i} \cdot \text{Re}_{\text{tp}}^{0.8} \cdot \text{Sc}^{0.4}$ $S_{\text{mix}} = \frac{S}{1 - \frac{C_{pL} \cdot (y_M - x_M)}{H_{\text{LG}}} \cdot \frac{dT_S}{dx_M} \cdot \left( \frac{\alpha}{D} \right)^{1/2}}$ $S = \frac{1}{1 + 2.53 \cdot 10^{-6} \cdot \text{Re}_{\text{tp}}^{1.17}}$ $\text{Re}_{\text{tp}} = \text{Re}_L \cdot [f(\text{Pr}_L) \cdot F]^{1.25}$
Mishra et al. [98] (1981)	$\frac{h}{h_{\text{nb}}} = A \cdot \left( \frac{1}{X_{\text{tt}}} \right)^m \cdot \text{Bo}^n$ $A = 5.64, m = 0.23, n = 0.05 \begin{cases} R12, 23 - 27\% \\ R22, 77 - 73\% \end{cases}$ $A = 21.75, m = 0.29, n = 0.23 \begin{cases} R12, 41 - 48\% \\ R22, 59 - 52\% \end{cases}$
Rammohan et al. [102] (1981)	$\frac{h_{\text{eff}}}{h_{\text{nb}}} = 34.8 \cdot (1 - 0.73 \cdot \chi^{0.58}) \cdot \left( \frac{C_p \cdot \mu}{\lambda} \right)_L^{0.56} \cdot \left( \frac{q}{H_{\text{LG}} \cdot \rho_V \cdot v} \right)_S^{0.67} \cdot \left( \frac{H_{\text{LG}} \cdot \rho_V}{C_p \cdot \Delta T_{\text{sub}} \cdot \rho_L} \right)_S^{0.6}$
Jung et al. [103] (1989)	$h_{\text{tp}} = \frac{N}{C_{\text{UN}}} \cdot h_{\text{UN}} + C_{\text{me}} \cdot F_p \cdot h_{\text{lo}}$ $F_p = 2.37 \cdot \left( 0.29 + \frac{1}{X_{\text{tt}}} \right)^{0.85}$ $C_{\text{me}} = 1 - 0.35 \cdot  \tilde{y} - \tilde{x} ^{1.56}, 0.9 < C_{\text{me}} \leq 1$ $C_{\text{UN}} = \frac{\Delta T_{\text{mix}}}{\Delta T_1}, \text{ refer to [112] for more details}$ $N = 4048 \cdot X_{\text{tt}}^{1.22} \cdot \text{Bo}^{1.13} \text{ for } X_{\text{tt}} < 1$ $\frac{h_{\text{UN}}}{h_1} = \frac{1}{C_{\text{UN}}}$

$$\frac{1}{h_1} = \frac{\chi_1}{h_1} + \frac{\chi_2}{h_2}$$

Subscripts 1 and 2 refer to component 1 and 2 in the mixture, respectively.

$$\frac{h_{\text{eff}}}{h_{\text{nb}}} = 55 \cdot \left[ 1 + |\bar{y} - \bar{x}| \cdot \left( \frac{\alpha}{D} \right)^{0.5} \right]^{-0.7} \cdot \left[ \frac{T_{\text{ws}}}{T_{\text{is}}} \right]^4 \cdot \left[ \frac{C_p \cdot \mu}{\lambda} \right]_{\text{L}}^{0.5} \cdot \left[ \frac{H_{\text{LG}} \cdot \rho_V}{C_p \cdot \Delta T_{\text{sub}} \cdot S} \right]^{0.76} \cdot \left( \frac{q}{H_{\text{LG}} \cdot \rho_V \cdot v} \right)_S^{0.84} \quad (30)$$

$$h = h_{\text{nb}} \cdot F + h_{\text{b}} \cdot S$$

$$\frac{h_{\text{b}}}{h_1} = 1 + \frac{h_1}{q} \cdot (T_{\text{S1}} - T_{\text{S2}}) \cdot (\bar{y} - \bar{x}) \cdot \left[ 1 - \exp\left( \frac{-q}{10^{-4} \cdot \rho_L \cdot H_{\text{LG}}} \right) \right]$$

$$\frac{1}{h_1} = \frac{\chi_1}{h_1} + \frac{\chi_2}{h_2} \quad (31)$$

Subscripts 1 and 2 refer to water and another mixture component, respectively.

$$\frac{1}{h} = \frac{1}{h_{\text{L, film}}} + \frac{\chi^2 \cdot C_{pV}^2}{\left( (1 - \chi) \cdot C_{pL} + \chi \cdot C_{pV} \right) \cdot \left( \frac{\partial h}{\partial T} \right)_P} + \frac{1}{h_{\text{L, vapor}}} \quad (32)$$

Refer to [115] for expressions of  $h_{\text{L, film}}$  and  $h_{\text{L, vapor}}$

$$h_{\text{mix}} = F_{\text{Li}} \cdot (h_{\text{mac}} \cdot F_{\text{mix}}) + S_{\text{Li}} h_{\text{mic}} \cdot S_{\text{mix}}$$

$$F_{\text{Li}} = \exp\left(-0.027 \cdot (T_{\text{mix},s} - T_{\text{b}})\right)$$

$$S_{\text{Li}} = \frac{\Delta T_{\text{mix}}}{\Delta T_1} = \left[ 1 - (\bar{y} - \bar{x}) \cdot \frac{dT}{d\bar{x}} \cdot \left( \frac{C_{pL}}{\Delta h_V} \right) \cdot \left( \frac{\alpha}{D_m} \right)^{0.5} \right]^{-1} \quad (33)$$

Modified Gungor-Winterton

$$h_{\text{mix}} = h_{\text{lo}} \cdot E_{\text{new}}$$

$$h_{\text{lo}} = 0.023 \cdot \left( \frac{\lambda_L}{D_i} \right) \cdot \left[ (1 - \chi) \cdot \frac{G \cdot D_i}{\mu} \right]^{0.8} \cdot Pr_L^{0.4}$$

$$E_{\text{new}} = 1 + 3000 \cdot (Bo \cdot F_c)^{0.86} + 1.12 \cdot \left( \frac{\chi}{1 - \chi} \right)^{0.75} \cdot \left( \frac{\rho_L}{\rho_V} \right)^{0.41}$$

$$F_c = \frac{h_{\text{mix}}}{h_1}$$

$$\frac{h_{\text{mix}}}{h_1} = \frac{1}{1 + K}$$

$$K = \frac{\Delta T_g}{\Delta T_1} \cdot \left[ 1 - \exp\left( \frac{-Bo \cdot q}{h_m \cdot \rho_L \cdot H_{\text{LG}}} \right) \right]$$

Ardhapurkar et al. [108]  
(2014)

Modified Silver-Bell Ghaly

(34)

$$\frac{1}{h_{\text{mix}}} = \frac{1}{h_c} + \frac{Z_g}{h_g}$$

$$h_c = h_{\text{lo}} \cdot E_{\text{new}}$$

$$E_{\text{new}} = 1 + 3000 \cdot (Bo \cdot F_c)^{0.86} + 1.12 \cdot \left( \frac{\chi}{1 - \chi} \right)^{0.85} \cdot \left( \frac{\rho_L}{\rho_V} \right)^{0.7}$$

Modified Granryd

$$\frac{h_{\text{mix}}}{h_{\text{lo}}} = \frac{F_p}{1 + A} = F_{\text{mix}}$$

$$A = \left( \frac{F_p}{C_{LV}} \right) \cdot \chi^2 \cdot \left[ \left( \frac{1 - \chi}{\chi} \right) \cdot \left( \frac{\mu_V}{\mu_L} \right) \right]^{0.8} \cdot \left( \frac{Pr_L}{Pr_V} \right)^{0.4} \cdot \left( \frac{\lambda_L}{\lambda_V} \right) \cdot \left( \frac{C_{pV}}{C_{pLocal}} \right)$$

$$C_{LV} = 1.4 \text{ if } G > 500 \text{ kg/m}^2\text{-s}$$

$$C_{LV} = 2 \text{ if } G < 300 \text{ kg/m}^2\text{-s}$$

$$h_{tp,l} = \frac{q}{\Delta T_l} = \frac{1}{\varphi \cdot \left(\frac{q}{\Delta T_1}\right)^{-1} + (1-\varphi) \cdot \left(\frac{q}{\Delta T_2}\right)^{-1}} = \left[ \frac{\varphi}{h_{tp,1}} + \frac{1-\varphi}{h_{tp,2}} \right]^{-1}$$

$$Ma = \frac{\Delta \sigma}{\rho_l \cdot v_l^2} \cdot \left[ \frac{\sigma}{g \cdot (\rho_l - \rho_v)} \right]^{0.5} \cdot Pr$$

$$F_{Ma} = 1 + \frac{Ma - Ma_{min}}{Ma_{max} - Ma_{min}}$$

$$F_{Ca} = \frac{G \cdot \mu_l}{(1-\chi) \cdot \rho_l \cdot \sigma}$$

$$F_{mix} = [F_{Ma}^{0.1} \cdot (100 \cdot F_{Ca})^{0.2} \cdot F_a]^{-1}$$

$$F_a = \left( \frac{\varphi \cdot T_{db} \cdot h_{tp,l}}{10 \cdot q_{ref} \cdot P_{cr} \cdot 10^5} \right)^{0.08} \cdot \left( \frac{7 \cdot q_{ref}}{q} \right)^{0.26}$$

$$h_{tp,mix} = h_{tp,l} \cdot \left[ F_{mix} \cdot \left( 0.736 \frac{x}{0.43} + 0.51 \right) \right]^2$$

Dang C. et al. [116]  
(2017)

**Table 8** Operating conditions for established correlations for flow boiling heat transfer coefficient of binary mixtures

Authors and Year	Fluids Compositions	Operating Conditions for Flow Boiling HTC Correlations for Fluid Mixtures
Bennet and Chen [101] (1980)	Ethylene glycol-Water 0 to 99.7% by mass ethylene glycol	Test section: inconel tube (25.4 mm inner diameter, 76 mm long) Mass flux: 0.16 to 1.6×10 <sup>3</sup> kg/m <sup>2</sup> -s Heat flux: 7.0 to 30.0×10 <sup>5</sup> W/m <sup>2</sup> Quality: near 0 to 30% Martinelli parameters: 0.16 to 300 Two phase Reynolds number: 9.5 to 60×10 <sup>5</sup>
Mishra et al. [98] (1981)	Pure R12 R12 (23-27% mass); R22 (77-73%) R12 (41-48% mass); R22 (59-52%)	Test section: stainless steel tube (12.5 mm inner diameter, 15 mm outer diameter, 2.6 m long) Mass flux: 54 to 136 kg/hr Heat flux: 3250 to 15200 W/m <sup>2</sup> Exit evaporating temperature: 5 °C
Rammohan et al. [102] (1981)	Glycerol-Water, Water-Isopropanol 0 to 100% of less volatile component	Test section: perspex tube (3 mm thick wall, 2.4 mm inner diameter, 0.62 m long), platinum heating wire (0.3 mm diameter, 0.315 m long) Subcoolings: 40, 50, 60 and 64 K Velocities: 0.16, 0.32, 0.38, 0.48 and 0.54 m/s Viscosity: 0.005 to 0.1 Pa·s Heat fluxes: 7.86 to 24×10 <sup>5</sup> W/m <sup>2</sup>
Jung et al. [103] (1989)	R12/R152a 0, 21, 60, 89 and 100 mole% R12	Test section: stainless steel tube (9.0 mm inner diameter, 0.25 mm thick wall, 8 m long) Pressure: 300 and 360 kPa for R12 and R152a Mass flux: 250 to 720 kg/m <sup>2</sup> -s Heat flux: 10, 17, 26, 36 and 45 kW/m <sup>2</sup> Quality: up to 95%
Sivagnanam and Varma [104] (1990)	Acetone (5-25% mass)/Water Isopropanol (5-20% mass)/Water Butanol (2-8% mass)/Water	Test section: glass tube (47 mm inner diameter, 0.59 m long), platinum heating wire (0.3 mm diameter, 0.495 m long) Subcoolings: 10 to 40 K Velocities: 0.16 to 1 m/s Heat fluxes: 1.9 to 28×10 <sup>5</sup> W/m <sup>2</sup>
Wenzel and Steinhagen [106] (1991)	Isopropanol (0-67.5% mass)/Water	Test section: stainless steel annular section Subcoolings: 5 to 25 K Velocities: 0.1 to 0.9 m/s Heat fluxes: 1 to 40×10 <sup>4</sup> W/m <sup>2</sup>
Li et al. [67] (2013)	Pure HFO1234yf, Pure HFC32,	Test section: stainless steel tube (2.0 mm inner diameter, 0.7 to 2.3 m long)

1128  
1129  
1130

	HFO1234yf 80%/ HFC32 20% mass HFO1234yf 50%/ HFC32 50% mass	<i>Mass flux:</i> 100, 200 and 400 kg/m <sup>2</sup> -s <i>Heat flux:</i> 6, 12 and 24 kW/m <sup>2</sup> <i>Quality:</i> 20 to 100%
Little [107] (2008) Ardhapurkar et al. [108] (2014)	Various mixture compositions of N <sub>2</sub> /CH <sub>4</sub> /C <sub>2</sub> H <sub>6</sub> /C <sub>3</sub> H <sub>8</sub> /C <sub>4</sub> H <sub>10</sub>	<i>Test section:</i> copper tube (0.835 mm inner diameter, 27 mm long) <i>Pressure:</i> 434 to 1365 kPa <i>Mass flux:</i> 256 to 841 kg/m <sup>2</sup> -s <i>Heat flux:</i> 80 kW/m <sup>2</sup>
Dang C. et al. [116] (2017)	R134a/R245fa (10/90, 30/70 and 70/30 by wt.%)	<i>Test section:</i> single copper micro-channel (1×1 mm, 106 mm long) <i>Mass flux:</i> 60 to 1100 kg/m <sup>2</sup> -s <i>Heat flux:</i> 30 to 120 kW/m <sup>2</sup> <i>Evaporating temperature:</i> 18.5 °C

1131

### 1132 *3.6 Issues of experimental uncertainties and result inconsistencies for flow boiling in binary* 1133 *mixtures*

1134

1135 Similar to pool boiling, experimental uncertainties exist in flow boiling experiments preventing  
1136 the achievements of more accurate and consistent results. The total measurement uncertainty  
1137 in flow boiling of binary mixtures mainly depends on the accuracy of quantifying tube/channel  
1138 inner wall temperature and estimating the local saturation temperature [66, 136, 144]. The  
1139 uncertainty of inner wall temperature is determined from outer wall temperature in comparison  
1140 with heat flux and wall thickness [66, 73, 134, 135, 137]. The uncertainty in saturation  
1141 temperature is related to the uncertainty of heat flux as well since the local saturation  
1142 temperature is usually obtained from the local pressure and local enthalpy of the working fluid  
1143 calculated from the heat flux value [73, 77, 137, 138, 143]. Therefore, the keys to minimize  
1144 experimental uncertainties in flow boiling of binary mixtures are improving the accuracy of  
1145 temperature and pressure sensors via finer installations and calibrations and taking more  
1146 precise heat flux values via avoiding heat losses and carrying out proper heat flux calibrations.  
1147 For example, temperature sensors like thermocouples have to be calibrated under both  
1148 isothermal, heating and cooling conditions and corresponding calibration equations shall be  
1149 implemented for more precise temperature measurements [66, 73, 132, 136, 140, 144].  
1150 Similarly, pressure transducers should be examined under both atmospheric and elevating  
1151 pressure conditions and corresponding calibration equations should eventually be applied to  
1152 the measured values for more accurate pressure readings [77, 134, 143]. Thermal insulation  
1153 such as adding an insulation layer with low thermal conductivity and creating a vacuum  
1154 environment for test sections can be employed to avoid heat losses [77, 134, 141, 142, 145].  
1155 The actual percentage of supplied heat flux being used for heating the working fluid can be  
1156 checked based on energy balance and the enthalpy change of the working fluid going through  
1157 a heated test section [73, 77, 134, 139, 141, 142]. Also, it is important to apply correct values



1158 of thermophysical properties for all fluid components in the mixture during all the calculations  
 1159 for which National Institute of Standards and Technology (NIST) database is a superb reference  
 1160 source [116, 134, 136, 142, 143]. In addition, the measurements can be repeated for several  
 1161 times at different days to check the repeatability and further improve the overall experimental  
 1162 accuracy [143, 144].

1163

1164 Following what have been discussed in the pool boiling section, selective effects on flow  
 1165 boiling heat transfer performance of binary mixtures have been summarized in Tables 9-11 for  
 1166 the effects of fluid composition, heat flux, and flow rate, respectively, aiming to create a  
 1167 reference to be used by other researchers for comparisons and understandings of flow boiling-  
 1168 related observations.

1169  
 1170

**Table 9** The effect of fluid composition on flow boiling heat transfer performance of binary mixtures

Authors and Year	Fluids Compositions	Operating Conditions	Effects of Fluid Composition on Flow Boiling Heat Transfer
Tsutsui et al. [133] (2000)	R134a/R123 (0-0.6 molar fraction)	<i>Channel:</i> horizontal 3 m long stainless steel tube of 10 mm diameter and 1.5 mm wall thickness <i>Heat flux:</i> 10-50 kW/m <sup>2</sup> <i>Mass flux:</i> 150-600 kg/(m <sup>2</sup> ·s) <i>Inlet Pressure:</i> 0.6 MPa	HTCs of mixture were less than the interpolated values between pure fluids both in the low quality region where the nucleate boiling is dominant and in the high quality region where the convective evaporation is dominant.
Zou et al. [134] (2010)	R170/R290 (0-1 molar fraction)	<i>Channel:</i> horizontal copper tube with inner diameter of 8 mm, outer diameter 40 mm and length of 120 mm <i>Heat flux:</i> 13.1-65.5 kW/m <sup>2</sup> <i>Mass flux:</i> 60-103 kg/(m <sup>2</sup> ·s) <i>Saturation Pressure:</i> 0.35-0.57 MPa	HTCs of pure R170 and R290 were higher than that of binary mixture due to the nonlinear mixture property effect and the mass transfer resistance effect.
Li et al. [66] (2012)	R1234yf/R32 (80/20, 50/50 by mass%)	<i>Channel:</i> horizontal stainless steel tube with inner diameter of 2 mm and 0.7-2.3 m length <i>Heat flux:</i> 6-24 kW/m <sup>2</sup> <i>Mass flux:</i> 100-400 kg/(m <sup>2</sup> ·s) <i>Saturation Temperature:</i> 15 °C.	HTCs of mixture with an R32 mass fraction of 20% were 10-30% less than those of pure R1234yf for various mass and heat fluxes. When the mass fraction of R32 ↑ to 50%, the HTCs were 10-20% greater than that of pure R1234yf but about 20-50% less than that of pure R32 under large mass and heat flux conditions.
Sarafraz et al. [132] (2012) [140] (2013)	Ethanol/water (10%-50% by mass) DEG/water (1-5% by volume)	<i>Channel:</i> stainless steel based vertical annular gap with hydraulic diameter of 30 mm and length of 300 mm <i>Heat flux:</i> ~132 kW/m <sup>2</sup> <i>Mass flux:</i> 1.5-3.5 L/min <i>Bulk Temperature:</i> 323-353 K	HTCs of ethanol/water mixtures at any concentrations were less than pure water and were less dependent on the inlet concentration. Differently, little ↑ in HTC was clearly observed when small amount of DEG was added to the mixture.

Kondou et al. [73] (2013)	R32/R1234ze(E) (20/80 and 50/50 by mass%)	<i>Channel:</i> horizontal micro-fin copper tube of 5.21 mm inner diameter and 2216 mm long <i>Heat flux:</i> 10-15 kW/m <sup>2</sup> <i>Mass flux:</i> 150-400 kg/(m <sup>2</sup> ·s) <i>Saturation Temperature:</i> 10 °C	HTC of mixture was lower than that of each pure component, which was minimized at the inlet composition of 0.2/0.8 by mass, where the temperature glide and mass fraction distribution were maximized.
Qiu et al. [135] (2015)	R1234ze(E)/R32 (27/73 by mass%)	<i>Channel:</i> 8 mm inner diameter and 2400 mm long horizontal copper tube <i>Heat flux:</i> 5-10 kW/m <sup>2</sup> <i>Mass flux:</i> 200-400 kg/(m <sup>2</sup> ·s) <i>Saturation Temperature:</i> 20 °C	HTC of R1234ze(E) was 33% less than that of R600a and 18% less than that of mixture.
Vasileiadou et al. [75] (2017)	ethanol/water (5/95 by volume%)	<i>Channel:</i> borosilicate glass based with tantalum surface vertical square channel with 5 mm inner hydraulic diameter, wall thickness 0.7 mm, heated length 72 mm <i>Heat flux:</i> 2.8-6.1 kW/m <sup>2</sup> <i>Mass flux:</i> 0.33-1.0 kg/(m <sup>2</sup> ·s) <i>Saturation Temperature:</i> 40 °C	The addition of ethanol into water (5%v/v) could enhance the HTC compared with that of pure components. For the mixture, the amplitude of heating wall temperature fluctuation is significantly lower than for pure liquids, allowing for a more stable heat transfer process.
Dang et al. [116] (2017)	R134a/R245fa (10/90, 30/70 and 70/30 by mass%)	<i>Channel:</i> aluminium based single rectangular channel with cross-section of 1 mm×1 mm and length of 106 mm <i>Heat flux:</i> 30-120 kW/m <sup>2</sup> <i>Mass flux:</i> 60-1100 kg/(m <sup>2</sup> ·s) <i>Saturation Temperature:</i> 18.5 °C	HTC degradation was a common feature for the mixtures, which was ↑ with temperature glide; The HTC ↑ with the concentration of the more volatile component at the similar temperature glide.
Dang et al. [136] (2018)	R134a/R245fa (10/90, 30/70 and 70/30 by mass%)	<i>Channel:</i> aluminium based seven parallel channels with the length of 110 mm and cross-section of 2 mm×1 mm <i>Heat flux:</i> 20-350 kW/m <sup>2</sup> <i>Mass flux:</i> 300-400 kg/(m <sup>2</sup> ·s) <i>Saturation Temperature:</i> 26 °C	HTC of mixtures was lower than that of pure components in most instances. The small addition of R134a was beneficial for improving the HTC at higher heat flux. The trends of HTC related with heat flux depended on the inlet concatenation of mixture.
Jige et al. [137] (2020)	R1234yf/R32 (79/21 and 47/53 by mass%)	<i>Channel:</i> aluminium based 12 horizontal rectangular channels with hydraulic diameter of 0.82 mm with heating length of 150 mm <i>Heat flux:</i> 5-20 kW/m <sup>2</sup> <i>Mass flux:</i> 50-400 kg/(m <sup>2</sup> ·s)	HTCs of the mixtures were lower than those of pure components under most conditions due to mass diffusion resistance and temperature glide; The HTC for the 47/53 (mass) mixtures were greater than those of the 21/79 (mass) mixtures.
Guo et al. [138] (2020)	R134a/R245fa (33/67 by mass%)	<i>Channel:</i> horizontal copper tube with 10 mm inner diameter and 1 mm tube thickness, total length 2 m, which was divided into 8 sections <i>Heat flux:</i> 6-24 kW/m <sup>2</sup> <i>Mass flux:</i> 100-300 kg/(m <sup>2</sup> ·s) <i>Saturation Temperature:</i> 55-95 °C	HTC of the mixture was much lower than that of pure R134a and was close to that of pure R245fa.

**Table 10** The effect of heat flux on flow boiling heat transfer performance of binary mixtures

Authors and Year	Fluids Compositions	Operating Conditions	Effects of Heat Flux on Flow Boiling Heat Transfer
Tsutsui et al. [133] (2000)	R134a/R123 (0-0.6 molar fraction)	<i>Channel:</i> horizontal 3 m long stainless steel tube of 10 mm diameter and 1.5 mm wall thickness <i>Heat flux:</i> 10-50 kW/m <sup>2</sup> <i>Mass flux:</i> 150-600 kg/(m <sup>2</sup> ·s) <i>Inlet Pressure:</i> 0.6 MPa	The HTC was dependent on heat flux at low vapor quality with higher HTCs at higher heat fluxes.
Zou et al. [134] (2010)	R170/R290 (0-1 molar fraction)	<i>Channel:</i> horizontal copper tube with inner diameter of 8 mm, outer diameter 40 mm and length of 120 mm <i>Heat flux:</i> 13.1-65.5 kW/m <sup>2</sup> <i>Mass flux:</i> 60-103 kg/(m <sup>2</sup> ·s) <i>Saturation Pressure:</i> 0.35-0.57 MPa	HTCs of mixtures were lower than corresponding pure components and this degradation ↑ as ↑ heat flux and ↓ as vapor quality or mass flux ↑.
Li et al. [66] (2012)	R1234yf/R32 (80/20, 50/50 by mass%)	<i>Channel:</i> horizontal stainless steel tube with inner diameter of 2 mm and 0.7-2.3 m length <i>Heat flux:</i> 6-24 kW/m <sup>2</sup> <i>Mass flux:</i> 100-400 kg/(m <sup>2</sup> ·s) <i>Saturation Temperature:</i> 15 °C.	HTCs of pure R1234yf and the mixtures all ↑ with the heat flux. For the mixture with a 20% mass fraction of R32, when the heat flux was large the HTC difference between that of pure R1234yf and the mixture was large at low vapor quality.
Sarafraz et al. [132] (2012) [140] (2013)	Ethanol/water (10%-50% by mass) DEG/water (1-5% by volume)	<i>Channel:</i> stainless steel based vertical annular gap with hydraulic diameter of 30 mm and length of 300 mm <i>Heat flux:</i> ~132 kW/m <sup>2</sup> <i>Mass flux:</i> 1.5-3.5 L/min <i>Bulk Temperature:</i> 323-353 K	The HTC of mixture ↑ by ↑ the heat flux.
Qiu et al. [135] (2015)	R1234ze(E)/R32 (27/73 by mass%)	<i>Channel:</i> 8 mm inner diameter and 2400 mm long horizontal copper tube <i>Heat flux:</i> 5-10 kW/m <sup>2</sup> <i>Mass flux:</i> 200-400 kg/(m <sup>2</sup> ·s) <i>Saturation Temperature:</i> 20 °C	The local HTC slightly ↑ with heat flux.
Dang et al. [136] (2018)	R134a/R245fa (10/90, 30/70 and 70/30 by mass%)	<i>Channel:</i> aluminium based seven parallel channels with the length of 110 mm and cross-section of 2 mm×1 mm <i>Heat flux:</i> 20-350 kW/m <sup>2</sup> <i>Mass flux:</i> 300-400 kg/(m <sup>2</sup> ·s) <i>Saturation Temperature:</i> 26 °C	The HTC of mixture ↑ at higher effective heat flux and the suppression effect gradually ↓ with ↑ heat flux.
Qiu et al. [139] (2018)	R1234ze(E)/R32 (27/73 by mass%)	<i>Channel:</i> horizontal copper tube with 8 mm inner diameter and 2400 mm length <i>Heat flux:</i> 5-10 kW/m <sup>2</sup> <i>Mass flux:</i> 200-500 kg/(m <sup>2</sup> ·s) <i>Saturation Temperature:</i> 10-20 °C.	The ↑ of heat flux led to a slight ↑ of local HTCs in the whole vapor quality.
Jige et al. [137] (2020)	R1234yf/R32 (79/21 and 47/53 by mass%)	<i>Channel:</i> aluminium based 12 horizontal rectangular channels with hydraulic diameter of 0.82 mm with heating length of 150 mm <i>Heat flux:</i> 5-20 kW/m <sup>2</sup>	The HTCs of the mixtures are strongly influenced by mass flux, vapor quality and mass fraction, whereas the influence of heat flux on heat transfer was small.

1174  
1175  
1176

		<i>Mass flux:</i> 50-400 kg/(m <sup>2</sup> ·s)	
Guo et al. [138] (2020)	R134a/R245fa (33/67 by mass%)	<i>Channel:</i> horizontal copper tube with 10 mm inner diameter and 1 mm tube thickness, total length 2 m, which was divided into 8 sections <i>Heat flux:</i> 6-24 kW/m <sup>2</sup> <i>Mass flux:</i> 100-300 kg/(m <sup>2</sup> ·s) <i>Saturation Temperature:</i> 55-95 °C	The HTC ↑ with the heat flux.

**Table 11** The effect of mass flux on flow boiling heat transfer performance of binary mixtures

Authors and Year	Fluids Compositions	Operating Conditions	Effects of Mass Flux on Flow Boiling Heat Transfer
Tsutsui et al. [133] (2000)	R134a/R123 (0-0.6 molar fraction)	<i>Channel:</i> horizontal 3 m long stainless steel tube of 10 mm diameter and 1.5 mm wall thickness <i>Heat flux:</i> 10-50 kW/m <sup>2</sup> <i>Mass flux:</i> 150-600 kg/(m <sup>2</sup> ·s) <i>Inlet Pressure:</i> 0.6 MPa	The HTC ↑ with ↑ in mass flux in the whole vapor quality region.
Zou et al. [134] (2010)	R170/R290 (0-1 molar fraction)	<i>Channel:</i> horizontal copper tube with inner diameter of 8 mm, outer diameter 40 mm and length of 120 mm <i>Heat flux:</i> 13.1-65.5 kW/m <sup>2</sup> <i>Mass flux:</i> 60-103 kg/(m <sup>2</sup> ·s) <i>Saturation Pressure:</i> 0.35-0.57 MPa	The HTC of mixture was significantly affected by mass flux. The larger the mass flux, the higher the HTC was obtained at the same composition.
Li et al. [66] (2012)	R1234yf/R32 (80/20, 50/50 by mass%)	<i>Channel:</i> horizontal stainless steel tube with inner diameter of 2 mm and 0.7-2.3 m length <i>Heat flux:</i> 6-24 kW/m <sup>2</sup> <i>Mass flux:</i> 100-400 kg/(m <sup>2</sup> ·s) <i>Saturation Temperature:</i> 15 °C.	The HTC ↑ with ↑ in mass flux.
Sarafraz et al. [132] (2012) [140] (2013)	Ethanol/water (10%-50% by mass) DEG/water (1-5% by volume)	<i>Channel:</i> stainless steel based vertical annular gap with hydraulic diameter of 30 mm and length of 300 mm <i>Heat flux:</i> ~132 kW/m <sup>2</sup> <i>Mass flux:</i> 1.5-3.5 L/min <i>Bulk Temperature:</i> 323-353 K	The HTC ↑ with ↑ in mass flux.
Qiu et al. [135] (2015)	R1234ze(E)/R32 (27/73 by mass%)	<i>Channel:</i> 8 mm inner diameter and 2400 mm long horizontal copper tube <i>Heat flux:</i> 5-10 kW/m <sup>2</sup> <i>Mass flux:</i> 200-400 kg/(m <sup>2</sup> ·s) <i>Saturation Temperature:</i> 20 °C	The local HTC strongly ↑ with mass flux and slightly ↑ with heat flux.
Qiu et al. [139] (2018)	R1234ze(E)/R32 (27/73 by mass%)	<i>Channel:</i> horizontal copper tube with 8 mm inner diameter and 2400 mm length <i>Heat flux:</i> 5-10 kW/m <sup>2</sup> <i>Mass flux:</i> 200-500 kg/(m <sup>2</sup> ·s) <i>Saturation Temperature:</i> 10-20 °C.	The ↑ of mass flux led to a significant ↑ of HTCs.

Jige et al. [137] (2020)	R1234yf/R32 (79/21 and 47/53 by mass%)	<i>Channel:</i> aluminium based 12 horizontal rectangular channels with hydraulic diameter of 0.82 mm with heating length of 150 mm <i>Heat flux:</i> 5-20 kW/m <sup>2</sup> <i>Mass flux:</i> 50-400 kg/(m <sup>2</sup> ·s)	The HTC of the mixtures were strongly influenced by mass flux, vapor quality and mass fraction, whereas the influence of heat flux on heat transfer was small.
Guo et al. [138] (2020)	R134a/R245fa (33/67 by mass%)	<i>Channel:</i> horizontal copper tube with 10 mm inner diameter and 1 mm tube thickness, total length 2 m, which was divided into 8 sections <i>Heat flux:</i> 6-24 kW/m <sup>2</sup> <i>Mass flux:</i> 100-300 kg/(m <sup>2</sup> ·s) <i>Saturation Temperature:</i> 55- 95 °C	At high saturation temperatures, the mass flux had less influence on the HTC of the mixture at a large heat flux.

1177  
1178

## 1179 5 Conclusions

1180

1181 In this study, recent research developments on boiling heat transfer in binary mixtures have  
1182 been reviewed in a systematic manner. The advantages of mixing various fluid components as  
1183 working fluids include but not limited to better flexibility and compatibility between the  
1184 working fluids and the desired heat transfer applications and enabling the potential replacement  
1185 of environmentally harmful heat transfer fluids. Although the boiling heat transfer of binary or  
1186 multicomponent mixtures have been extensively investigated from many aspects throughout  
1187 the years, the authors believe the comprehension of the boiling heat transfer mechanisms has  
1188 been far from complete and there is still much room to be enhanced in this area.

1189

1190 A lot of the data have been obtained from different experimental systems and methods with  
1191 various measurement errors, which has led to result inconsistencies among studies of boiling  
1192 heat transfer in binary or multicomponent mixtures. Thus, more advanced and accurate  
1193 experimental apparatuses and uncertainty analysis are urgently demanded in future  
1194 investigations. The work to evaluate various effects (e.g. fluid composition, heat flux, pressure)  
1195 on the overall boiling heat transfer performance of binary/multicomponent mixtures and to  
1196 build empirical correlation through experimental results are still unfinished and meaningful  
1197 because it will continuously complement the database of corresponding boiling-related studies.  
1198 As the database unceasingly gets supplemented and the empirical correlation persistently gets  
1199 trained, the ultimate goal is to prepare for a generalized theoretical equation fully capable of  
1200 describing the boiling phenomena of binary/multicomponent mixtures, probably similar to the  
1201 Navier-Stokes equations governing fluid flows.

1202

1203 **Furthermore**, it needs to be stressed here that, though most studies regarding boiling heat  
1204 transfer of binary mixtures showed lower heat transfer coefficients than those in their  
1205 corresponding pure fluids, the boiling heat transfer performance of binary mixtures could be  
1206 improved from the following aspects: (a) adjusting the fluid composition and the associated  
1207 effects on mass diffusion (i.e. Marangoni effect), heat diffusion and nucleation mechanism; (b)  
1208 modifying/enhancing the heater surface characteristics; (c) eliminating the additional heats  
1209 from dissolution and dilution; (d) balancing between the contributions of nucleating boiling  
1210 heat transfer and convective heat transfer to the overall flow boiling heat transfer; (e) promoting  
1211 the overall fluid mixing in flow boiling; (f) minimizing flow instabilities in flow boiling.  
1212 **Therefore, despite the fact that there have been correspondingly several pioneering studies, the**  
1213 **efforts of improving boiling heat transfer performance in binary mixtures, such as discovering**  
1214 **optimum fluid compositions and enhancing heater surfaces, should continue and draw more**  
1215 **attentions in the future, considering the advantages of mixing different fluid components for**  
1216 **desired properties as well as the intrinsic benefits of employing boiling heat transfer as a**  
1217 **thermal management method.**

1218

1219 Among the above potential heat transfer enhancing methods, surface modification has rarely  
1220 been investigated in flow boiling of binary mixtures which requires more attentions in the  
1221 future. Moreover, help is demanded from more advanced and accurate numerical studies for  
1222 better understanding the boiling mechanisms in binary/multicomponent mixtures in spite of  
1223 their great complexities. Furthermore, a more systematic and generalized heat transfer  
1224 correlation is still yet to be constructed for both pool boiling and flow boiling of mixtures,  
1225 built upon the existing correlations available in literature, which have been thoroughly  
1226 reviewed in this paper.

1227 **Highlights**

1228

1229 • The recent developments in pool and flow boiling heat transfer of binary mixtures have  
1230 been reviewed

1231 • The important effects on boiling heat transfer performance of binary mixtures have  
1232 been investigated and summarized

1233 • Established heat transfer correlations for both pool boiling and flow boiling of binary  
1234 mixtures have been evaluated and compared

1235 • Future research requirements on mechanism study and heat transfer enhancement of  
1236 binary mixtures have been highlighted

1237

1238 **Declaration of Conflicting Interests**

1239

1240 The authors declare that there is no conflict of interest.

1241

1242 **Acknowledgement**

1243

1244 The authors would like to acknowledge the financial support of the Engineering and Physical  
1245 Sciences Research Council (EPSRC) of the United Kingdom (EP/N000714/1 and  
1246 EP/N021142/1). Jian Xu and Wanlong Liu also would like to acknowledge the financial  
1247 support from the China Scholarship Council.

1248

1249

1250 **Nomenclature**

$A$	Empirical coefficient
$A_0$	Constant
$B_0$	Boiling number
$C_p$	Specific heat [J/kg·K]
$C_{me}$	Correction factor which considers mass transfer resistance in the convective evaporation region
$C_{UN}$	Ünal's constant to consider mixture effects in nucleate pool boiling [111]
$C_{LV}$	Enhancement factor considering the effects between gas and liquid
$D$	Mass diffusivity [ $\text{m}^2 \text{s}^{-1}$ ]
$D_i$	Inner diameter [m]
$E_{new}$	New two-phase convection multiplier
$F$	Suppression function for heat transfer coefficient of binary mixtures
$F_a$	Apparent impact factor
$F_{Ca}$	Impact factor of capillary effect
$F_D$	Diffusion induced suppression factor
$F_p$	Revised correction factor for macroscopic heat transfer contribution based on data with pure fluids in the evaporative region
$F_{Ma}$	Impact factor of Marangoni effect
$F_{mix}$	Correction factor of macroscopic heat transfer contribution to the overall flow boiling of fluid mixture
$g$	Gravitational acceleration [ $\text{ms}^{-2}$ ]
$G$	Mass flux [ $\text{kg m}^{-2} \text{s}^{-1}$ ]
$H$	Specific enthalpy [ $\text{J kg}^{-1}$ ]
$H_{LG}$	Latent heat of evaporation [ $\text{kJ kg}^{-1}$ ]
$h$	Heat transfer coefficient [ $\text{Wm}^{-2}\text{K}^{-1}$ ]
$h_m$	Mass transfer coefficient [ $\text{m s}^{-1}$ ]
$h_{UN}$	Nucleate pool boiling heat transfer coefficient of a mixture
$h_{L, \text{film}}$	Heat transfer coefficient from bulk liquid to liquid film
$h_{L, \text{vapor}}$	Heat transfer coefficient from bulk liquid to vapor
$k$	Coefficient in heat transfer deterioration function
$K_i, K_{sh}, K_{st}$	Adjustable coefficients
$m$	Empirical power index
$n$	Empirical power index
$N$	Nucleate boiling factor
$p$	Pressure [bar]
$P$	Pressure [Pa]
$Pr$	Prandtl number
$q$	Heat flux [ $\text{Wm}^{-2}$ ]
$q_{ref}$	Reference heat flux [ $\text{Wm}^{-2}$ ]
$S$	Boiling suppression factor
$S_{mix}$	Correction factor of microscopic heat transfer contribution to the overall flow boiling of fluid mixture
$T$	Temperature [K]
$v$	Volatility parameter
$v/v$	Volume to volume ratio
$X_{tt}$	Lockhart-Martinelli parameter
$x, \tilde{x}$	Liquid mass and mole fraction
$x_M$	Liquid composition based on mass of the more volatile component
$y, \tilde{y}$	Vapor mass and mole fraction
$y_M$	Vapour composition based on mass of more volatile component
$Z_g$	Ratio of the sensible cooling of the vapour to the total cooling rate
$CA$	Contact angle



<i>Ma</i>	Marangoni number
<i>Ku</i>	Kutateladze number
<i>Le</i>	Lewis number
<i>Nu</i>	Nusselt number
<i>Sc</i>	Schmidt number
<i>CHF</i>	Critical heat flux
<i>HTC</i>	Heat transfer coefficient

**Greek**

$\alpha$	Thermal diffusivity [ $\text{m}^2\text{s}^{-1}$ ]
$\beta$	Constant
$\lambda$	Thermal conductivity [ $\text{Wm}^{-1}\text{K}^{-1}$ ]
$\delta$	Thickness [m]
$\mu$	Dynamic viscosity [Pa·s]
$\rho$	Density [ $\text{kg m}^{-3}$ ]
$\Delta T_{\text{bp}}$	Boiling range, maximum rise in local saturation temperature [K]
$\Delta T_1$	Ideal wall superheat [K]
$\Delta T_s$	Wall superheat [K]
$\sigma$	Surface tension [ $\text{N m}^{-1}$ ]
$v$	Liquid velocity [ $\text{m s}^{-1}$ ]
$\chi$	Vapor quality
$\varphi$	Mass fraction of the more volatile component

**Subscripts**

<i>b</i>	Boiling
<i>c</i>	Convective
<i>g</i>	Gas
<i>I</i>	Ideal state
<i>L</i>	Liquid
<i>m</i>	Mixture
<i>S</i>	Saturation
<i>V</i>	Vapor
<i>1</i>	More volatile component
<i>2</i>	Less volatile component
<i>cr</i>	Critical point
<i>db</i>	Between dew point and boiling point
<i>Li</i>	Developed by Li et al. [67]
<i>lo</i>	Liquid only
<i>ls</i>	Saturation temperature of pure more volatile component
<i>nb</i>	no boiling
<i>tp</i>	Two-phase
<i>ws</i>	Saturation temperature of water
<i>ave</i>	Average value
<i>eff</i>	Effective
<i>mac</i>	Macroscopic
<i>max</i>	Maximum
<i>mic</i>	Microscopic
<i>min</i>	Minimum
<i>mix</i>	Mixture
<i>psc</i>	Pseudo-single component
<i>sub</i>	Subcooled
<i>surf</i>	Surface value
<i>bulk</i>	Bulk liquid
<i>local</i>	Axial local value

1252 **References**

1253

- 1254 1. Táboas, F., Vallès M., Bourouis M. and Coronas A., Flow boiling heat transfer of  
1255 ammonia/water mixture in a plate heat exchanger, *International Journal of*  
1256 *Refrigeration*, **33-4** (2010) 695-705
- 1257 2. Fu B.R., Tsou M.S., and Pan C., Boiling heat transfer and critical heat flux of  
1258 ethanol–water mixtures flowing through a diverging microchannel with artificial  
1259 cavities, *International Journal of Heat and Mass Transfer*, **55-5** (2012) 1807-1814
- 1260 3. In S., Baek S., Jin L. and Jeong S., Flow boiling heat transfer of R123/R134a mixture  
1261 in a microchannel, *Experimental Thermal and Fluid Science*, **99** (2018) 474-486
- 1262 4. Fujita, Y. and Tsutsui M., Heat transfer in nucleate pool boiling of binary mixtures,  
1263 *International Journal of Heat and Mass Transfer*, **37-1** (1994) 291-302
- 1264 5. He J., Liu J. and Xu X., Analysis and experimental study of nucleation site densities  
1265 in the boiling of mixed refrigerants, *International Journal of Heat and Mass Transfer*,  
1266 **105** (2017) 452-463
- 1267 6. Alpay H.E. and Balkan F., Nucleate pool boiling performance of acetone-ethanol and  
1268 methylene chloride-ethanol binary mixtures, *International Journal of Heat and Mass*  
1269 *Transfer*, **32-12** (1989) 2403-2408
- 1270 7. Choi C., Shin J.S., Yu D.I. and Kim M.H., Flow boiling behaviors in hydrophilic and  
1271 hydrophobic microchannels, *Experimental Thermal and Fluid Science*, **35-5** (2011)  
1272 816-824
- 1273 8. Karayiannis T.G. and Mahmoud M.M., Flow boiling in microchannels: Fundamentals  
1274 and applications, *Applied Thermal Engineering*, **115** (2017) 1372-1397
- 1275 9. Hui T.O. and Thome J.R., A study of binary mixture boiling: boiling site density and  
1276 subcooled heat transfer, *International Journal of Heat and Mass Transfer*, **28-5**  
1277 (1985) 919-928
- 1278 10. Thome J.R., Prediction of binary mixture boiling heat transfer coefficients using only  
1279 phase equilibrium data, *International Journal of Heat and Mass Transfer*, **26-7** (1983)  
1280 965-974
- 1281 11. Hamzekhani S., Falahieh M.M., and Akbari A., Bubble departure diameter in nucleate  
1282 pool boiling at saturation: Pure liquids and binary mixtures, *International Journal of*  
1283 *Refrigeration*, **46** (2014) 50-58
- 1284 12. Sathyabhama A. and Babu T.P.A., Experimental investigation in pool boiling heat  
1285 transfer of ammonia/water mixture and heat transfer correlations, *International*  
1286 *Journal of Heat and Fluid Flow*, **32-3** (2011) 719-729
- 1287 13. Dang C., Jia L., Peng Q., Huang Q. and Zhang X., Experimental and analytical study  
1288 on nucleate pool boiling heat transfer of R134a/R245fa zeotropic mixtures,  
1289 *International Journal of Heat and Mass Transfer*, **119** (2018) 508-522
- 1290 14. Chai L.H., Peng X.F. and Lee D.J., Interfacial effects on nucleate boiling heat transfer  
1291 of binary mixtures, *International Journal of Thermal Sciences*, **40-2** (2001) 125-132
- 1292 15. Inoue T., Monde M. and Teruya Y., Pool boiling heat transfer in binary mixtures of  
1293 ammonia/water, *International Journal of Heat and Mass Transfer*, **45-22** (2002)  
1294 4409-4415
- 1295 16. Gong M., Wu Y., Ding L., Cheng K. and Wu J., Visualization study on nucleate pool  
1296 boiling of ethane, isobutane and their binary mixtures, *Experimental Thermal and*  
1297 *Fluid Science*, **51** (2013) 164-173
- 1298 17. Armijo K.M. and Carey V.P., Prediction of binary mixture boiling heat transfer in  
1299 systems with strong Marangoni effects, *Frontiers in Heat and Mass Transfer*, **1**  
1300 (2010) 023003

- 1301 18. Celata G.P., Cumo M. and Setaro T., A review of pool and forced convective boiling  
1302 of binary mixtures, *Experimental Thermal and Fluid Science*, **9-4** (1994) 367-381
- 1303 19. Deng H., Fernandino M. and Dorao C.A., A numerical investigation of flow boiling  
1304 of non-azeotropic and near-azeotropic binary mixtures, *International Journal of*  
1305 *Refrigeration*, **49** (2015) 99-109
- 1306 20. Fazel S.A.A. and Jamialahmadi M., Semi-empirical modeling of pool boiling heat  
1307 transfer in binary mixtures, *International Journal of Heat and Fluid Flow*, **44** (2013)  
1308 468-477
- 1309 21. Yagov V.V., Critical Heat Flux Prediction for Pool Boiling of Binary Mixtures,  
1310 *Chemical Engineering Research and Design*, **82-4** (2004) 457-461
- 1311 22. Fujita Y. and Bai Q., Critical heat flux of binary mixtures in pool boiling and its  
1312 correlation in terms of Marangoni number, *International Journal of Refrigeration*, **20-**  
1313 **8** (1997) 616-622
- 1314 23. McGillis W.R. and Carey V.P., On the Role of Marangoni Effects on the Critical Heat  
1315 Flux for Pool Boiling of Binary Mixtures, *Journal of Heat Transfer*, **118-1** (1996)  
1316 103-109
- 1317 24. Barbosa J. Jr., Wadekar V. and Hewitt G., A Review of Heat and Mass Transfer in  
1318 Boiling of Binary Mixtures, in *Conference: HTFS Annual Meeting* (1999): Dublin.
- 1319 25. Zhang, L., Gong M., Wu J. and Xu L., Nucleate Pool Boiling Heat Transfer of Binary  
1320 Mixtures with Different Boiling Ranges, *Experimental Heat Transfer*, **20-3** (2007)  
1321 251-260
- 1322 26. Benjamin R.J. and Balakrishnan A.R., Nucleation site density in pool boiling of  
1323 binary mixtures: Effect of surface micro-roughness and surface and liquid physical  
1324 properties, *The Canadian Journal of Chemical Engineering*, **75-6** (1997) 1080-1089
- 1325 27. Thome J.R. and Davey G., Bubble growth rates in liquid nitrogen, argon and their  
1326 mixtures, *International Journal of Heat and Mass Transfer*, **24-1** (1981) 89-97
- 1327 28. Stefanov Z. and Karaivanova M.K., Influence of the Marangoni Effect on the  
1328 Efficiency of Plate Columns for Binary Distillation, *Chemical Engineering &*  
1329 *Technology*, **34-12** (2011) 2029-2032
- 1330 29. Zuiderweg F.J. and Harmens A., The influence of surface phenomena on the  
1331 performance of distillation columns, *Chemical Engineering Science*, **9-2** (1958) 89-  
1332 103
- 1333 30. Hyvärinen A.P., Raatikainen T., Laaksonen A., Viisanen Y. and Lihavainen H.,  
1334 Surface tensions and densities of H<sub>2</sub>SO<sub>4</sub> + NH<sub>3</sub> + water solutions, *Geophysical*  
1335 *Research Letters*, **32-16** (2005) L16806
- 1336 31. Ahmed S. and Carey V.P., Effects of gravity on the boiling of binary fluid mixtures,  
1337 *International Journal of Heat and Mass Transfer*, **41-16** (1998) 2469-2483
- 1338 32. Ohta H., Yamaguchi S., Ito Y., Shinmoto Y. and Abe Y., Nucleate boiling of low-  
1339 concentration alcohol aqueous solutions for the development of thermal management  
1340 systems in space, *Microgravity Science and Technology*, **19-3** (2007) 141-143
- 1341 33. Kumar C.S.S., Kumar G.U., Arenales M.R.M., Hsu C.C. Suresh S. and Chen P.H.,  
1342 Elucidating the mechanisms behind the boiling heat transfer enhancement using nano-  
1343 structured surface coatings, *Applied Thermal Engineering*, **137** (2018) 868-891
- 1344 34. Duta L., Popescu A.C., Zgura I., Preda N. and Mihailescu I.N., Wettability of  
1345 Nanostructured Surfaces, *INTECH*, (2015) 207-252
- 1346 35. Sahu R.P., Sinha-Ray S. and Yarin A.L., Pool boiling on nano-textured surfaces  
1347 comprised of electrically-assisted supersonically solution-blown, copper-plated  
1348 nanofibers: Experiments and theory, *International Journal of Heat and Mass*  
1349 *Transfer*, **87** (2015) 521-535

- 1350 36. Kandlikar S.G. and Alves L., Effects of Surface Tension and Binary Diffusion on  
1351 Pool Boiling of Dilute Solutions: An Experimental Assessment, *Journal of Heat*  
1352 *Transfer*, **121-2** (1999) 488-493
- 1353 37. Inoue T. and Monde M., Enhancement of nucleate pool boiling heat transfer in  
1354 ammonia/water mixtures with a surface-active agent, *International Journal of Heat*  
1355 *and Mass Transfer*, **55-(13-14)** (2012) 3395-3399
- 1356 38. Sarafraz M.M., Peyghambarzadeh S.M. and Alavifazel S.A., Enhancement of  
1357 nucleate pool boiling heat transfer to dilute binary mixtures using endothermic  
1358 chemical reactions around the smoothed horizontal cylinder. *Heat and Mass Transfer*,  
1359 **48-10** (2012) 1755-1765
- 1360 39. Stralen S.J.D.V., The mechanism of nucleate boiling in pure liquids and in binary  
1361 mixtures—part I, *International Journal of Heat and Mass Transfer*, **9-10** (1966) 995-  
1362 1020
- 1363 40. Calus W.F. and Leonidopoulos D.J., Pool boiling—Binary liquid mixtures,  
1364 *International Journal of Heat and Mass Transfer*, **17-2** (1974) 249 - 256
- 1365 41. Inoue T., Kawae N. and Monde M., Characteristics of heat transfer coefficient during  
1366 nucleate pool boiling of binary mixtures, *Heat and Mass Transfer*, **33-4** (1998) 337-  
1367 344
- 1368 42. Stephan K. and Körner M., Berechnung des Wärmeübergangs verdampfender binärer  
1369 Flüssigkeitsgemische, *Chemie Ingenieur Technik*, **41-7** (1969) 409-417
- 1370 43. Calus W.F. and Rice P., Pool boiling-binary liquid mixtures, *Chemical Engineering*  
1371 *Science*, **27-9** (1972) 1687-1697
- 1372 44. Jungnickel H., Wassilew P. and Kraus W.E., Investigations on the heat transfer of  
1373 boiling binary refrigerant mixtures, *International Journal of Refrigeration*, **3-3** (1980)  
1374 129-133.
- 1375 45. Schlunder E.U., Heat transfer in nucleate boiling of mixtures, *Int. Chem. Eng.;*  
1376 *(United States)*, **23-4** (1983) 589-599
- 1377 46. Thome J.R. and Shakir S., A new correlation for nucleate pool boiling of aqueous  
1378 mixtures, *AIChE Symposium Series*, (1987)
- 1379 47. Fujita Y. and Tsutsui M., Heat Transfer in Nucleate Boiling of Binary Mixtures :  
1380 Development of a Heat Transfer Correlation, *JSME International Journal Series B*  
1381 *Fluids and Thermal Engineering*, **40-1** (1997) 134-141
- 1382 48. Rao G.V. and Balakrishnan A.R., Heat transfer in nucleate pool boiling of  
1383 multicomponent mixtures, *Experimental Thermal and Fluid Science*, **29-1** (2004) 87-  
1384 103
- 1385 49. Inoue T. and Monde M., Prediction of pool boiling heat transfer coefficient in  
1386 ammonia/water mixtures, *Heat Transfer-Asian Research*, **38-2** (2009) 65-72.
- 1387 50. Kandlikar S.G., Boiling Heat Transfer With Binary Mixtures: Part I—A Theoretical  
1388 Model for Pool Boiling, *Journal of Heat Transfer*, **120-2** (1998) 380-387
- 1389 51. Wilke C.R. and Chang P., Correlation of diffusion coefficients in dilute solutions,  
1390 *AIChE Journal*, **1-2** (1955) 264-270
- 1391 52. Kærn M.R., Modi A., Kjær J., Jesper J., Andreasen G. and Haglind F., An assessment  
1392 of in-tube flow boiling correlations for ammonia–water mixtures and their influence  
1393 on heat exchanger size, *Applied Thermal Engineering*, **93** (2016) 623-638
- 1394 53. Inoue T. and Monde M., Nucleate pool boiling heat transfer in binary mixtures,  
1395 *Wärme-und Stoffübertragung*, **29-3** (1994) 171-180
- 1396 54. Shah M.M., A method for predicting heat transfer during boiling of mixtures in plain  
1397 tubes, *Applied Thermal Engineering*, **89** (2015) 812-821
- 1398 55. Scriven L.E., On the dynamics of phase growth, *Chemical Engineering Science*, **10-1**  
1399 (1959) 1-13

- 1400 56. Gogonin I.I., Heat Transfer in Boiling of Binary Mixtures under Free-Convection  
1401 Conditions, *Journal of Engineering Physics and Thermophysics*, **86**-3 (2013) 689-694
- 1402 57. Wu Y.F., Gong M.Q., Ding L., Guo P. and Wu J.F., Nucleate pool boiling heat  
1403 transfer characteristics of tetrafluoromethane and methane binary mixtures, *AIP*  
1404 *Conference Proceedings*, **1434**-1 (2012) 1075-1082
- 1405 58. Nemade R.M. and Khandekar S., Pool boiling heat transfer of ethanol-water mixtures  
1406 at sub-atmospheric pressures, in *Proceedings of the 22th National and 11th*  
1407 *International ISHMT-ASME Heat and Mass Transfer Conference* (2013): IIT  
1408 Kharagpur, India
- 1409 59. Kim J.S., Girard A., Jun S., Lee J. and You S.M., Effect of surface roughness on pool  
1410 boiling heat transfer of water on hydrophobic surfaces, *International Journal of Heat*  
1411 *and Mass Transfer*, **118** (2018) 802-811
- 1412 60. Sarafraz M.M. and Hormozi F., Application of thermodynamic models to estimating  
1413 the convective flow boiling heat transfer coefficient of mixtures, *Experimental*  
1414 *Thermal and Fluid Science*, **53** (2014) 70-85
- 1415 61. Wang S.P. and Chato J.C., Review of Recent Research on Boiling and Condensation  
1416 Heat Transfer With Mixtures, in *Air Conditioning and Refrigeration Center TR-23*,  
1417 1992, *Air Conditioning and Refrigeration Center. College of Engineering*, University  
1418 of Illinois at Urbana-Champaign.: Urbana, IL, USA
- 1419 62. Kandlikar S.G. and Bulut M., An Experimental Investigation on Flow Boiling of  
1420 Ethylene-Glycol/Water Mixtures, *Journal of Heat Transfer*, **125**-2 (2003) 317-325
- 1421 63. He G., Liu F., Cai D. and Jiang J., Experimental investigation on flow boiling heat  
1422 transfer performance of a new near azeotropic refrigerant mixture R290/R32 in  
1423 horizontal tubes, *International Journal of Heat and Mass Transfer*, **102** (2016) 561-  
1424 573
- 1425 64. Wettermann M. and Steiner D., Flow boiling heat transfer characteristics of wide-  
1426 boiling mixtures, *International Journal of Thermal Sciences*, **39**-2 (2000) 225-235
- 1427 65. Kandlikar G., Tian S., Yu J.K. and Koyama S., Further assessment of pool and flow  
1428 boiling heat transfer with binary mixtures, in *2nd, International symposium on two-*  
1429 *phase flow modelling and experimentation* (1999), Pisa, Italy: Edizioni ETS
- 1430 66. Li M., Dang C., and Hihara E., Flow boiling heat transfer of HFO1234yf and R32  
1431 refrigerant mixtures in a smooth horizontal tube: Part I. Experimental investigation,  
1432 *International Journal of Heat and Mass Transfer*, **55**-13 (2012) 3437-3446
- 1433 67. Li M., Dang C., and Hihara E., Flow boiling heat transfer of HFO1234yf and HFC32  
1434 refrigerant mixtures in a smooth horizontal tube: Part II. Prediction method,  
1435 *International Journal of Heat and Mass Transfer*, **64** (2013) 591-608
- 1436 68. Azzolin M., Berto A., Bortolin S. and Col D.D., Flow boiling heat transfer of binary  
1437 and ternary non-azeotropic mixtures inside channels, in *10th International Conference*  
1438 *on Boiling and Condensation Heat Transfer* (2018): Nagasaki, Japan.
- 1439 69. Bertsch S.S., Groll E.A. and Garimella S.V., Effects of heat flux, mass flux, vapor  
1440 quality, and saturation temperature on flow boiling heat transfer in microchannels,  
1441 *International Journal of Multiphase Flow*, **35**-2 (2009) 142-154
- 1442 70. Yu W., France D.M. and Routbort J.L., Pressure drop, heat transfer, critical heat flux,  
1443 and flow stability of two-phase flow boiling of water and ethylene glycol/water  
1444 mixtures - final report for project "Efficient cooling in engines with nucleate boiling",  
1445 2011, Argonne National Lab. (ANL), Argonne, IL (United States). p. Medium: ED.
- 1446 71. Kim S.H., Chu I.C., Choi M.H., Euh D.J., Mechanism study of departure of nucleate  
1447 boiling on forced convective channel flow boiling, *International Journal of Heat and*  
1448 *Mass Transfer*, **126** (2018) 1049-1058

- 1449 72. Peng X.F., Peterson G.P. and Wang B.X., Flow boiling of binary mixtures in  
1450 microchanneled plates, *International Journal of Heat and Mass Transfer*, **39**-6 (1996)  
1451 1257-1264
- 1452 73. Kondou C., BaBa D., Mishima F. and Koyama S., Flow boiling of non-azeotropic  
1453 mixture R32/R1234ze(E) in horizontal microfin tubes, *International Journal of*  
1454 *Refrigeration*, **36**-8 (2013) 2366-2378
- 1455 74. Bamorovat Abadi G., Yun E. and Kim K.C., Flow boiling characteristics of R134a  
1456 and R245fa mixtures in a vertical circular tube, *Experimental Thermal and Fluid*  
1457 *Science* **72** (2016) 112-124
- 1458 75. Vasileiadou P., Flow boiling of ethanol/water binary mixture in a square mini-  
1459 channel, *Applied Thermal Engineering*, **127** (2017) 1617-1627
- 1460 76. Suhas B.G. and Sathyabhama A., Heat transfer and force balance approaches in  
1461 bubble dynamic study during subcooled flow boiling of water-ethanol mixture,  
1462 *Experimental Heat Transfer*, **31**-1 (2018) 1-21
- 1463 77. Azzolin M., Bortolin S. and Col D.D., Flow boiling heat transfer of a zeotropic binary  
1464 mixture of new refrigerants inside a single microchannel, *International Journal of*  
1465 *Thermal Sciences*, **110** (2016) 83-95
- 1466 78. Chen J.C., Correlation for Boiling Heat Transfer to Saturated Fluids in Convective  
1467 Flow, *Industrial & Engineering Chemistry Process Design and Development*, **5**-3  
1468 (1966) 322-329
- 1469 79. Chen W. and Fang X., A note on the Chen correlation of saturated flow boiling heat  
1470 transfer, *International Journal of Refrigeration*, **48** (2014) 100-104
- 1471 80. Kim N.H., Shin T.R. and Lee E.R., Convective flow boiling of refrigerant oil  
1472 mixtures on an enhanced tube bundle, in *Proceedings of Fifth International*  
1473 *Conference on Enhanced, Compact and Ultra-Compact Heat Exchangers: Science,*  
1474 *Engineering and Technology* (2005): Hoboken, NJ, USA
- 1475 81. Yuan D., Chen D., Yan X., Xu J., Lu Q., Huang Y., Bubble behavior and its  
1476 contribution to heat transfer of subcooled flow boiling in a vertical rectangular  
1477 channel, *Annals of Nuclear Energy*, **119** (2018) 191-202
- 1478 82. Sinha G.K., Mahimkar S. and Srivastava A., Schlieren-based simultaneous mapping  
1479 of bubble dynamics and temperature gradients in nucleate flow boiling regime: Effect  
1480 of flow rates and degree of subcooling, *Experimental Thermal and Fluid Science*, **104**  
1481 (2019) 238-257
- 1482 83. Sun Z., Ma X., Ma L., Li W. and Kukulka D.J. , Flow Boiling Heat Transfer  
1483 Characteristics in Horizontal, Three-Dimensional Enhanced Tubes, *Energies*, **12**-5  
1484 (2019) 927
- 1485 84. Kandlikar S.G. and Balasubramanian P., An Extension of the Flow Boiling  
1486 Correlation to Transition, Laminar, and Deep Laminar Flows in Minichannels and  
1487 Microchannels, *Heat Transfer Engineering*, **25**-3 (2004) 86-93
- 1488 85. Trinh V. and Xu J., An Experimental Study on Flow and Heat Transfer  
1489 Characteristics of Ethanol/Polyalphaolefin Nanoemulsion Flowing Through Circular  
1490 Minichannels, *Nanoscale research letters*, **12**-1 (2017) 216-216
- 1491 86. Mahmoud M.M. and Karayiannis T.G., Heat transfer correlation for flow boiling in  
1492 small to micro tubes, *International Journal of Heat and Mass Transfer*, **66** (2013)  
1493 553-574
- 1494 87. Kandlikar S. and Steinke M., Predicting Heat Transfer During Flow Boiling in  
1495 Minichannels and Microchannels, *ASHRAE Transactions*, **109** (2003) 667-676
- 1496 88. Kim S.M. and Mudawar I., Theoretical model for local heat transfer coefficient for  
1497 annular flow boiling in circular mini/micro-channels, *International Journal of Heat*  
1498 *and Mass Transfer*, **73** (2014) 731-742

- 1499 89. Guo C., Wang J., Du X., Yang L., Experimental flow boiling characteristics of  
1500 R134a/R245fa mixture inside smooth horizontal tube, *Applied Thermal Engineering*,  
1501 **103** (2016) 901 - 908
- 1502 90. Grauso S., Mastrullo R., Mauro A.W., Vanoli G.P., CO<sub>2</sub> and propane blends:  
1503 Experiments and assessment of predictive methods for flow boiling in horizontal  
1504 tubes, *International Journal of Refrigeration*, **34-4** (2011) 1028-1039
- 1505 91. Orian G., Jelinek M., and Levy A., Flow boiling of binary solution in horizontal tube,  
1506 *Energy*, **35-1** (2010) 35-44
- 1507 92. Wienecke M., Luke A., Gorenflo D., Span R., Flow boiling of highly viscous fluids in  
1508 a vertical annular tube, *Chemical Engineering Research and Design*, **83-8** (2005)  
1509 1044-1051
- 1510 93. Hu H.T. and Wei W.J., Heat transfer characteristics of R410A-oil mixture flow  
1511 boiling inside a 7 mm straight smooth tube, *Experimental Thermal and Fluid Science*,  
1512 **32** (2008) 857-869
- 1513 94. McAssey E.V. Jr. and Kandlikar S.G., Convective heat transfer of binary mixtures  
1514 under flow boiling conditions, *International Journal of Transport Phenomena*, **3**  
1515 (2001) 51-62
- 1516 95. Barraza R.S., Schwartz F.J., Klein S.A., Nellis G.F. and Reindl D.T., Experimental  
1517 facility to measure heat transfer and pressure drop of boiling zeotropic multi-  
1518 component mixtures in a horizontal tube, *Science and Technology for the Built*  
1519 *Environment*, **22** (2016) 2-14
- 1520 96. Liu J., Ye L. and Liu H., Flow patterns of flow boiling of a highly viscous  
1521 pseudoplastic fluid, *International Communications in Heat and Mass Transfer*, **22-3**  
1522 (1995) 359-367
- 1523 97. Liu D. and Garimella S.V., Flow Boiling Heat Transfer in Microchannels, *Journal of*  
1524 *Heat Transfer*, **129-10** (2006) 1321-1332
- 1525 98. Mishra M.P., Varma H.K. and Sharma C.P., Heat transfer coefficients in forced  
1526 convection evaporation of refrigerants mixtures, *Letters in Heat and Mass Transfer*,  
1527 **8-2** (1981) 127-136.
- 1528 99. Dittus F.W. and Boelter L.M.K., Heat transfer in automobile radiators of the tubular  
1529 type, *University of California Publications of Engineering*, **2** (1930) 443-461
- 1530 100. Lockhart R.W. and Martinell R.C., Proposed Correlation of Data for Isothermal Two-  
1531 Phase, Two-Component Flow in Pipes, *Chemical Engineering Progress*, **45** (1949)  
1532 38-48
- 1533 101. Bennett D. L. and Chen J. C., Forced convective boiling in vertical tubes for saturated  
1534 pure components and binary mixtures, *A.I.Ch.E. J.*, **26-3** (1980) 454-461
- 1535 102. Rammohan T. R., Somalingaswara R.A. and Srinivas N. S., Forced convection heat  
1536 transfer to boiling of binary mixtures, *Can. J. Chem. Engng.*, **59** (1981) 400-402
- 1537 103. Jung D. S., McLinden M., Radermacher R. and Didion D., A study of flow boiling  
1538 heat transfer with refrigerant mixtures, *International Journal of Heat and Mass*  
1539 *Transfer*, **32-9** (1989) 1751-1764
- 1540 104. Sivagnanam P. and Varma Y. B. G., Subcooled boiling of binary mixtures under  
1541 conditions of forced convection, *Experimrntul Thermal Fluid Sci.*, **3** (1990) 515-522
- 1542 105. Granryd E., Heat transfer in flow evaporation of non-azeotropic refrigerant mixtures-  
1543 A theoretical approach, *In: Proc. 18th Int. Congress of Refrigeration, Montreal*, **3**  
1544 (1991) 1330-1334
- 1545 106. Wenzel V. and Steinhagen M., Subcooled flow boiling heat transfer to mixtures,  
1546 *Fourth World Congress of Chem. Engng., Strajres*, **3** (2000) 8-17.
- 1547 107. Little W.A., Heat transfer efficiency of Kleemenko cycle heat exchangers, *in: AIP*  
1548 *Conf. Proc.*, *AIP Publishing*, (2008) 606-613

- 1549 108. Ardhapurkar P.M., Arunkumar S., Atrey M.D., Flow boiling heat transfer coefficients  
1550 at cryogenic temperatures for multi-component refrigerant mixtures of nitrogen–  
1551 hydrocarbons, *Cryogenics*, **59** (2014) 84-92
- 1552 109. Moles F.D. and Shaw J.F.G., Boiling heat transfer to subcooled liquids under  
1553 conditions of forced convection, *Trans. Znsr. Chem. Engng.*, **50** (1972) 76-84
- 1554 110. Forster H.K. and Zuber N., Dynamic of vapour bubbles and boiling heat transfer,  
1555 *A.I.Ch.E. J.*, **1** (1955) 531-535
- 1556 111. Ünal H.C., Prediction of nucleate boiling heat transfer coefficients for binary  
1557 mixtures, *Int. J. Heat Mass Transfer*, **29** (1986) 637-640
- 1558 112. Silver L., Gas cooling with aqueous condensation, *Transactions of the Institution of*  
1559 *Chemical Engineers*, **25** (1947) 30-42
- 1560 113. Bell K.J. and Ghaly M.A., An approximate generalized design method for  
1561 multicomponent/partial condensation, *AIChE Symp.*, **39** (1972) 72-79
- 1562 114. Barraza R., Nellis G., Klein S. and Reindl D., Description and validation of the Little  
1563 correlation for boiling zeotropic in horizontal tubes from cryogenic to room  
1564 temperature, *IOP Conf. Series: Materials Science and Engineering*, **101** (2015)  
1565 012132
- 1566 115. Gungor K.E., Winterton R.H.S., Simplified general correlation for saturated flow  
1567 boiling and comparisons with data, *Chem. Eng. Res. Des.*, **65** (1987) 148-56
- 1568 116. Dang C., Jia L., Zhang X., Huang Q., Xu M., Experimental investigation on flow  
1569 boiling characteristics of zeotropic binary mixtures (R134a/R245fa) in a rectangular  
1570 micro-channel, *International Journal of Heat and Mass Transfer*, **115** (2017) 782-794
- 1571 117. Azzolin M., Bortolin S., Col D.D., Predicting methods for flow boiling heat transfer  
1572 of a non-azeotropic mixture inside a single microchannel, *Heat Transf. Eng.*, **37**  
1573 (2016) 1136-1147
- 1574 118. Buongiorno J., Venerus D.C., Prabhat N., McKrell T., et al., A benchmark study on  
1575 the thermal conductivity of nanofluids, *Journal of Applied Physics*, **106** (2009)  
1576 094312
- 1577 119. Sardesar R.G., Shock A.W. and Butterworth D., Heat and Mass Transfer in  
1578 Multicomponent Condensation and Boiling, *Heat Transfer Engineering*, **3** (1982),  
1579 104-114
- 1580 120. Thome J.R., and Shock A.W., Boiling of Multicomponent Liquid Mixtures, *Advances*  
1581 *in Heat Transfer*, **16** (1984), 59-156
- 1582 121. Celata G. P., Cumo M. and Setaro T., A review of pool and forced convective boiling  
1583 of binary mixtures, *Experimental Thermal and Fluid Science*, **9** (1994), 367-381
- 1584 122. Sarafraz M.M., Nucleate pool boiling of aqueous solution of citric acid on a smoothed  
1585 horizontal cylinder, *Heat Mass Transfer*, **48** (2012), 611–619
- 1586 123. Bajorek S.M., Lloyd J.R., Experimental study of multicomponent pool boiling on  
1587 smooth and finned surfaces, *AIChE Symp. Series*, **85-269** (1989), 54-59
- 1588 124. Sarafraz M.M., Peyghambarzadeh S.M., Influence of thermodynamic models on the  
1589 prediction of pool boiling heat transfer coefficient of dilute binary mixtures,  
1590 *International Communications in Heat and Mass Transfer*, **39** (2012), 1303-1310
- 1591 125. Sarafraz M.M., Experimental Investigation on Pool Boiling Heat Transfer to Formic  
1592 Acid, Propanol and 2-Butanol Pure Liquids under the Atmospheric Pressure, *Journal*  
1593 *of Applied Fluid Mechanics*, **6-1** (2013), 73-79
- 1594 126. Fazel S.A.A., Jamialahmadi M., Safekordi A.A., Experimental Investigation in Pool  
1595 Boiling Heat Transfer of Pure/Binary Mixtures and Heat Transfer Correlations, *Iran.*  
1596 *J. Chem. Chem. Eng.*, **27-3** (2008), 135-150



- 1597 127. Surtaev A. S., Serdyukov V. S., Moiseev M. I., Application of High-Speed IR  
1598 Thermography to Study Boiling of Liquids, *Instruments and Experimental*  
1599 *Techniques*, **59** (2016), 615-620
- 1600 128. Gerardi C., Buongiorno J., Hu L., McKrell T., Infrared thermometry study of  
1601 nanofluid pool boiling phenomena, *Nanoscale Research Letters* **6**:232 (2011)
- 1602 129. Park J. J., and Taya M., Design of Micro-Temperature Sensor Array with Thin Film  
1603 Thermocouples, *Journal of Electronic Packaging*, **127**-3 (2004), 286-289
- 1604 130. Kreider K. G., and Gillen G., High Temperature Materials for Thin-Film  
1605 Thermocouples on Silicon Wafers, *Thin Solid Films*, **376** (1-2) (2000), 32-37
- 1606 131. Sarafraz M.M., Arya H., Saeedi M., Ahmadi D., Flow boiling heat transfer to MgO-  
1607 therminol 66 heat transfer fluid: Experimental assessment and correlation  
1608 development, *Applied Thermal Engineering*, **138** (2018), 552–562
- 1609 132. Sarafraz M.M., Peyghambarzadeh S.M., Vaeli N., Subcooled Flow Boiling Heat  
1610 Transfer of Ethanol Aqueous Solutions in Vertical Annulus Space, *Chemical Industry*  
1611 *& Chemical Engineering Quarterly*, **18** (2) (2012), 315-327
- 1612 133. Tsutsui M., Lim T.W., and Fujita Y., Heat Transfer and Pressure Drop in Flow  
1613 Boiling of Binary Mixtures in a Uniformly Heated Horizontal Tube, *Proceedings of*  
1614 *the 4<sup>th</sup> JSME-KSME Thermal Engineering Conference*, October 1-6, 2000, Kobe,  
1615 Japan
- 1616 134. Zou X., Gong M.Q., Chen G.F. et al., Experimental study on saturated flow boiling  
1617 heat transfer of R170/R290 mixtures in a horizontal tube, *International Journal of*  
1618 *Refrigeration*, **33**-2 (2010), 371-380
- 1619 135. Qiu J.Y., Zhang H., Yu X.M. et al., Experimental investigation of flow boiling heat  
1620 transfer and pressure drops characteristic of R1234ze (E), R600a, and a mixture of  
1621 R1234ze (E)/R32 in a horizontal smooth tube, *Advances in Mechanical Engineering*,  
1622 **7**-9 (2015), 1-12
- 1623 136. Dang C., Jia L., Peng Q. et al., Experimental study on flow boiling heat transfer for  
1624 pure and zeotropic refrigerants in multi-microchannels with segmented  
1625 configurations, *International Journal of Heat and Mass Transfer* **127** (2018), 758-768
- 1626 137. Jige D. et al., Flow boiling heat transfer of zeotropic mixture R1234yf/R32 inside a  
1627 horizontal multiport tube, *International Journal of Refrigeration*, **119** (2020), 390-400
- 1628 138. Guo Q., Li M.X., and Tian X.D., Experimental study on flow boiling heat transfer  
1629 characteristics of R134a, R245fa and R134a/R245fa mixture at high saturation  
1630 temperatures, *International Journal of Thermal Sciences* **150** (2020): 106195
- 1631 139. Qiu J.Y., Fang Y.L., Dai G.L. et al., Investigation of flow boiling heat transfer  
1632 characteristic of mixture refrigerant L-41B in a horizontal smooth tube, *Thermal*  
1633 *Science* **22**-6B (2018), 2835-2846
- 1634 140. Sarafraz M. M. and Peyghambarzadeh S. M., Experimental study on subcooled flow  
1635 boiling heat transfer to water–diethylene glycol mixtures as a coolant inside a vertical  
1636 annulus, *Experimental Thermal and Fluid Science* **50** (2013), 154-162
- 1637 141. Wang Y., Alvarado J.L. and Terrell W.Jr., Thermal and flow characteristics of helical  
1638 coils with reversed loops, *International Journal of Heat and Mass Transfer*, **126**-B  
1639 (2018), 670-680
- 1640 142. Wang Y., Lu T.J., Drögemüller P., Yu Q.H., Ding Y.L., Li Y.L., Enhancing  
1641 deteriorated heat transfer of supercritical nitrogen in a vertical tube with wire matrix  
1642 insert, *International Journal of Heat and Mass Transfer*, **162** (2020), 120358
- 1643 143. Azzolin M., Bortolin S., Condensation and flow boiling heat transfer of a HFO/HFC  
1644 binary mixture inside a minichannel, *International Journal of Thermal Sciences*, **159**  
1645 (2021), 106638

- 1646 144. Jamialahmadi M., Müller-Steinhagen H., Abdollahi H., Shariati A., Experimental and  
 1647 theoretical studies on subcooled flow boiling of pure liquids and multicomponent  
 1648 mixtures, *International Journal of Heat and Mass Transfer*, **51 (9-10)** (2008), 2482-  
 1649 2493
- 1650 145. Moharana M.K., Nemade R.M., Phase-Change Heat Transfer of Ethanol-Water  
 1651 Mixtures: Towards Development of a Distributed Hydrogen Generator, *Proceedings*  
 1652 *of the ASME 2013 Summer Heat Transfer Conference*, July 14-19, 2013, Minneapolis,  
 1653 Minnesota, USA

1654  
 1655 **List of Figures**  
 1656

- Fig. 1 Summary of major effects on pool and flow boiling of (a) pure fluids or (b) binary/multicomponent mixtures
- Fig. 2 Schematic of the pool boiling test apparatus for binary mixtures in Inoue and Monde's study [37]
- Fig. 3 Schematic of the boiling test surface and positions of the embedded thermocouples in Nemade and Khandekar's study [58]
- Fig. 4 (a) Channel wall temperature fluctuation and (b) Local heat transfer coefficient over time of 5% v/v ethanol/water mixture, water and ethanol ( $G = 0.33 \text{ kg/m}^2 \cdot \text{s}$ ,  $q'' = 2.8 \text{ kW/m}^2$ ) [75]
- Fig. 5 (a) Average Nusselt number versus Reynolds number (single phase flow, nano-emulsion and pure PAO)  
 (b) Average heat transfer coefficient with/without phase change versus Reynolds number in laminar flow region [85]
- Fig. 6 Local two-phase heat transfer coefficient conditions of (a) water flow with  $D = 1.73 \text{ mm}$ ,  $G = 100 \text{ kg/m}^2 \cdot \text{s}$ ,  $q_w'' = 8.0 \text{ W/cm}^2$  and  $T_{\text{sat}} = 120 \text{ }^\circ\text{C}$   
 (b) R32 flow with  $D = 2.0 \text{ mm}$ ,  $G = 202 \text{ kg/m}^2 \cdot \text{s}$ ,  $q_w'' = 0.6 \text{ W/cm}^2$  and  $T_{\text{sat}} = 15 \text{ }^\circ\text{C}$  [88]
- Fig. 7 Ranges of Reynolds Number employed in various experimental investigations on flow boiling [84]
- Fig. 8 Experimental suppression factor versus two-phase Reynolds number for flow boiling in small to micro tubes [86]
- Fig. 9 Flow boiling correlation map [87]
- Fig. 10 Flow regimes of flow boiling at  $G = 0.33 \text{ kg/m}^2 \cdot \text{s}$  and  $q = 4.2 \text{ kW/m}^2$  for (a) water, (b) ethanol and (c) 5% v/v ethanol/water mixture and at  $G = 0.66 \text{ kg/m}^2 \cdot \text{s}$  and  $q = 4.2 \text{ kW/m}^2$  for (d) water, (e) ethanol and (f) 5% v/v ethanol/water mixture, and at  $G = 0.66 \text{ kg/m}^2 \cdot \text{s}$  and  $6.1 \text{ kW/m}^2$  for (g) water, (h) ethanol and (i) 5% v/v ethanol/water mixture [75]
- Fig. 11 Nucleation onset positions at different mass and heat fluxes [75]
- Fig. 12 (a) Flow patterns that were observed during flow boiling experiment in a binary mixture: a–c: bubbly, d: bubbly-plug, e–f: plug, g: stratified, h: stratified-wavy, i: wavy, j: wavy-slug (b) Flow pattern map [91]
- Fig. 13 Pressure drop results of R32/R290 mixture and R410A in the experiments conducted by He et al. [64]
- Fig. 14 Pressure drop during transition from single-phase to two-phase flow across the microchannel heat sink,  $G = 324 \text{ kg/m}^2 \cdot \text{s}$ ,  $T_{\text{f, in}} = 66.6 \text{ }^\circ\text{C}$  [95]

1657  
 1658  
 1659 **List of Tables**  
 1660

- Table 1 Existing correlations for pool boiling heat transfer coefficient suppression function  $F$  of binary mixtures

Table 2	Operating conditions of correlations for pool boiling heat transfer coefficient of binary mixtures
Table 3	The effect of fluid composition on pool boiling heat transfer performance of binary mixtures
Table 4	The effect of heat flux on pool boiling heat transfer performance of binary mixtures
Table 5	The effect of pressure on pool boiling heat transfer performance of binary mixtures
Table 6	The effect of surface condition on pool boiling heat transfer performance of binary mixtures
Table 7	Established correlations for flow boiling heat transfer coefficient of binary mixtures
Table 8	Operating conditions for established correlations for flow boiling heat transfer coefficient of binary mixtures
Table 9	The effect of fluid composition on flow boiling heat transfer performance of binary mixtures
Table 10	The effect of heat flux on flow boiling heat transfer performance of binary mixtures
Table 11	The effect of mass flux on flow boiling heat transfer performance of binary mixtures